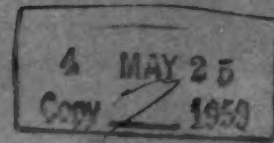


TECHNICAL PROGRESS REVIEWS



REACTOR CORE MATERIALS

Prepared for U. S. ATOMIC ENERGY COMMISSION by BATTELLE MEMORIAL INSTITUTE

MAY 1959

VOLUME 2

NUMBER 2

TECHNICAL PROGRESS REVIEWS

To meet the needs of industry for concise summaries of current atomic developments, the AEC is publishing this series, Technical Progress Reviews. Issued quarterly, each of the reviews digests and evaluates the latest findings in a specific area of nuclear technology and science.

The three journals currently published in this series are:

Power Reactor Technology, Walter H. Zinn and associates, General Nuclear Engineering Corporation

Reactor Fuel Processing, Stephen Lawroski and associates, Chemical Engineering Division, Argonne National Laboratory

Reactor Core Materials (covering solid material developments), R. W. Dayton, E. M. Simons, and associates, Battelle Memorial Institute

Each journal may be purchased (\$2.00 per year for subscription and individual issues \$0.55) from the Superintendent of Documents, U. S. Government Printing Office, Washington 25, D. C. See back cover for remittance instructions and foreign postage requirements.

Availability of Reports Cited in This Review

Unclassified AEC reports are available for inspection at AEC depository libraries and are sold by the Office of Technical Services, Department of Commerce, Washington 25, D. C.

Unclassified reports issued by other Government agencies or private organizations should be requested from the originator.

Unclassified British and Canadian reports may be inspected at AEC depository libraries. British reports are sold by the British Information Service, 30 Rockefeller Plaza, New York, N. Y.; Canadian reports (AECL series) are sold by the Scientific Document Distribution Office, Atomic Energy of Canada, Ltd., Chalk River, Ontario, Canada.

Classified U. S. and foreign reports identified in this journal as Secret or Confidential may be purchased by properly cleared Access Permit Holders from the Technical Information Service Extension, U. S. Atomic Energy Commission, P. O. Box 1001, Oak Ridge, Tenn. Such reports may be inspected at classified AEC depository libraries.

REACTOR CORE MATERIALS

a review of recent developments in
solid materials for reactor cores

prepared by
BATTELLE MEMORIAL INSTITUTE

MAY 1959

VOLUME 2

NUMBER 2



foreword

Each quarter, staff members of Battelle Memorial Institute analyze and evaluate basic research and technological developments pertaining to reactor core materials for which information becomes available during that period. Significant findings and advances are reviewed, correlated by subject area, and published as *Reactor Core Materials*, one of a series of journals supported by the Division of Information Services, U. S. Atomic Energy Commission.

No attempt is made to describe in detail everything that is going on. Rather, emphasis is placed on concrete results. Readers interested in details of work in particular areas are directed to the original references, which are given at the end of each section. On the other hand, persons who wish to keep up with the core-materials field in a general way should find the information presented herein sufficient to meet their needs. Bibliographies, monographs, and survey articles on topics within the scope of this Review are called to the attention of the reader, generally with no attempt to cover them in detail.

Although the Second Geneva Conference was held last year, many of the papers have been slow in becoming available in printed form. Those reviewed in this issue represent pertinent ones from the group which was received at Battelle during the quarter covered by this Review.

R. W. DAYTON

E. M. SIMONS

Battelle Memorial Institute

contents

ii	Foreword
1	I FUEL AND FERTILE MATERIALS
1	Unalloyed Uranium
3	Alpha-Uranium Alloys
5	Gamma-phase Alloys
6	Epsilon-phase Alloys
6	Dilute Uranium Alloys
8	Plutonium Alloys
9	Thorium
11	Dispersion Fuel Materials
11	Refractory Fuel and Fertile Materials
14	Mechanism of Corrosion of Fuel Materials
14	Basic Studies of Radiation Effects in Fuel Materials
20	II MODERATOR MATERIALS
20	Graphite
20	Beryllium Metal and Alloys
22	Solid Hydrides
25	III CONTROL MATERIALS
25	Control-rod Alloys
25	Burnable-poison Dispersions
27	IV CLADDING AND STRUCTURAL MATERIALS
27	Corrosion
32	Radiation Effects in Nonfuel Materials
35	Selected Metallurgical Aspects of Cladding and Structural Materials
39	Selected Mechanical Properties of Cladding and Structural Materials
47	V SPECIAL FABRICATION TECHNIQUES
47	Melting, Casting, Heat-treatment, and Hot Working
48	Cladding
55	Welding and Brazing
55	Nondestructive Testing

RE

U

St
de
un
m
th
ve
th
th
st
dy
cr
dy
(1
fr
ni
de
m
ca
pa
So
pa
de
un
m
at
fo

ra
fo
r
a
w
a
p
y
a
0
a
r

REACTOR CORE MATERIALS

FUEL AND FERTILE MATERIALS

Unalloyed Uranium

Studies in progress at Argonne^{1,2} include the determination of the elastic constants of alpha-uranium single crystals. Table I-1 is a summary of the elastic parameters derived from the fundamental moduli determined in this investigation. The bulk modulus derived from these data is approximately 11 per cent higher than that determined by Bridgman,³ by hydrostatic pressure, in 1931. Other values⁴ for the dynamically determined bulk modulus of polycrystalline uranium are 1.08 and 1.26×10^{12} dynes/cm². In addition, dilation curves in the (100) and (001) directions have been obtained from a pseudo-unit cell single crystal of uranium. The directions were accurate within 0.5 deg. The data obtained from reproduced dilatometric curves are reported in Table I-2. Data calculated from the equation fitted to the lattice parameter measurements reported by Bridge, Schwartz, and Vaughan⁵ are included for comparison. Another determination in progress deals with the self-diffusion coefficient of gamma uranium. Experiments were carried out by measuring the penetration of U²³⁵ into uranium at $952 \pm 2^\circ\text{C}$. The preliminary value of D was found to be between 10^{-8} and 10^{-7} cm²/sec.

Additional mechanical-property tests on irradiated uranium have been conducted by Hanford. Beta heat-treated uranium specimens, irradiated to 0.018, 0.031, and 0.075 at. % burn-up and annealed at high alpha-phase temperatures, were used to determine the degree of recovery as indicated by tensile tests. The results are reported in Fig. 1. Annealing initially reduces the yield strength and increases ductility from the as-irradiated condition. However, at 25 hr, the 0.018 and 0.075 at. % burn-up specimens exhibit a significant increase in yield strength with corresponding change in ductility gains for all ex-

posures and an approach to 10-hr strength values for the 0.075 exposure. Since data are not available for the 0.031 exposure following a 25-hr anneal, the curves are dotted to correspond to the prevailing trend. Since yielding of metals is affected by impurities and the disposition and freedom of dislocations, it is likely that the aging effects shown in Fig. 1 result from interactions between the two. The magnitude of the changes in both strength and ductility suggests that fission products enter into the annealing reactions.

The British⁶ conducted compressive creep tests of alpha uranium under neutron irradiation, and they have concluded that:

1. The secondary creep of alpha uranium at 450°C appears not to differ significantly under identical test conditions of stress and temperature between out-of-pile and in-pile tests.

2. An induced strain, which has the characteristics of primary creep, appears during in-pile tests after each pile start-up. On two occasions when this has been found, the specimen was allowed to cool to room temperature before the creep test was restarted. The effect may therefore be due to thermal cycling. This induced primary creep leads to a significant increase in the creep strain following a pile start-up.

Bridgeport Brass Co.⁷ describes the use of Jominy type end-quench tests in connection with metallography as a means of determining uranium heating history. Geneva Conference papers dealing with uranium are worthy of mention. The British⁸ report on the changes which occur in natural-uranium fuel elements during irradiation in the Windscale or Calder Hall reactors. The growth of perfect crystals of alpha uranium is described by the French.⁹ A book, "Physical Metallurgy of Uranium,"¹⁰ has been issued by the United States in connection with the Geneva Conference. Recent articles^{11,12} on fuel technology

Table I-1 ELASTIC PARAMETERS DERIVED FROM FUNDAMENTAL MODULI FOR ALPHA URANIUM*

Parameter	Value	Definition
$E_{[100]}$	2.038×10^{12} dynes/cm ²	Young's modulus in [1 0 0] direction
$E_{[010]}$	1.484×10^{12} dynes/cm ²	Young's modulus in [0 1 0] direction
$E_{[001]}$	2.084×10^{12} dynes/cm ²	Young's modulus in [0 0 1] direction
C_{44}	1.2444×10^{12} dynes/cm ²	Shear modulus for (0 0 1)[0 1 0] or (0 1 0)[0 0 1]
C_{55}	0.7342×10^{12} dynes/cm ²	Shear modulus for (0 0 1)[1 0 0] or (1 0 0)[0 0 1]
C_{66}	0.7433×10^{12} dynes/cm ²	Shear modulus for (0 1 0)[1 0 0] or (1 0 0)[0 1 0]
$\beta_{[100]}$	0.380×10^{-12} cm ² /dyne	Linear compressibility in [1 0 0]
$\beta_{[010]}$	0.292×10^{-12} cm ² /dyne	Linear compressibility in [0 1 0]
$\beta_{[001]}$	0.225×10^{-12} cm ² /dyne	Linear compressibility in [0 0 1]
β_V	0.897×10^{-12} cm ² /dyne	Volume compressibility
K	1.115×10^{12} dynes/cm ²	Bulk modulus
σ_{12}	+0.243	Poisson's ratio (for stress in i direction):
σ_{21}	+0.177	$\sigma_{ij} = \frac{\text{compressive strain in j direction}}{\text{tensile strain in i direction}}$
σ_{13}	-0.017	
σ_{31}	-0.017	NOTE:
σ_{23}	+0.390	1, 2, and 3 refer to [1 0 0], [0 1 0] and
σ_{32}	+0.548	[0 0 1], respectively.

*Data taken from reference 2.

Table I-2 EXPANSION OF ALPHA URANIUM IN THE [1 0 0] AND [0 0 1] DIRECTIONS*†

Temp., °C	Expansion in the [1 0 0] direction, in./in. $\times 10^4$		Expansion in the [0 0 1] direction, in./in. $\times 10^4$	
	Measured from single crystal	Calculated from equation†	Measured from single crystal	Calculated from equation†
50	4.61	5.87	5.16	4.97
75	10.22	11.91	10.34	10.08
100	15.84	18.14	15.51	15.29
125	22.47	24.59	22.38	20.70
150	29.10	31.24	28.70	26.24
175	37.24	38.13	35.01	32.01
200	44.38	45.26	42.45	38.00
225	52.53	52.66	49.34	44.24
250	59.67	60.34	56.22	50.74
275	66.82	68.30	63.68	57.54
300	74.97	76.55	72.26	64.65
325	84.13	85.13	81.67	72.10
350	93.29	94.03	90.56	79.88
375	102.95	103.28	100.83	88.05
400	113.11	112.88	112.34	96.62
425	123.28	122.86	120.82	105.61
450	133.94	133.22	129.97	115.04
475	144.41	143.99	141.37	124.93
500	155.77	155.15	152.21	135.32
525	167.94	166.75	163.05	146.22
550	179.10	178.78	174.45	157.62
575	190.26	191.27	184.73	169.59
600	203.43	204.23	196.12	182.14
625	221.10	217.66	208.08	195.27
650	235.26	231.60	219.48	209.02

*Data taken from reference 2.

†Based upon 1-in. specimen length at 25°C.

‡The equations for expansion in the [1 0 0] and [0 0 1] directions, as derived from the data of reference 5 are

$$[100] L_T = L_0 \left(1 + 22.50 \times 10^{-6} T + 11.97 \times 10^{-8} T^2 + 14.74 \times 10^{-12} T^3 \right)$$

$$[001] L_T = L_0 \left(1 + 19.37 \times 10^{-6} T + 5.71 \times 10^{-8} T^2 + 23.26 \times 10^{-12} T^3 \right)$$

where L is length and T is expressed in degrees centigrade.

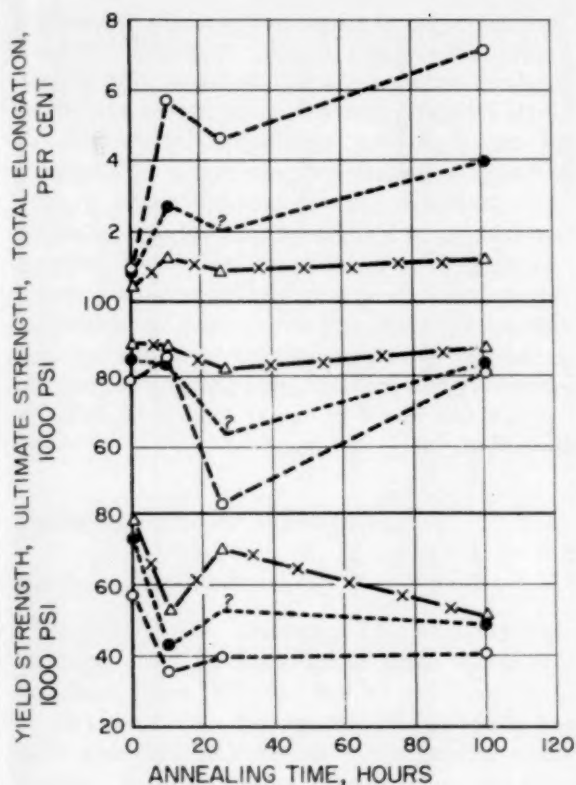


Figure 1—Effect of post-irradiation annealing at 600°C on the tensile properties of uranium. ○—○, 0.018 at.% burn-up; ●—●, 0.031 at.% burn-up; Δ—x—Δ, 0.075 at.% burn-up. Data from Hanford Atomic Products Operation.

give the factors involved in the case of natural uranium versus enriched uranium as a reactor fuel.

(M. S. Farkas)

Alpha-Uranium Alloys

The corrosion behavior of defected fuel elements with a uranium-2 wt.% zirconium core, coextrusion clad with Zircaloy-2, is being studied by Nuclear Metals.¹³ A standard diffusion heat-treatment for 7 hr at 880°C was established to overcome the effect of subtle defects in 15-mil Zircaloy-2 cladding. This heat-treatment has been found to change the nature of failure resulting from gross defects. Corrosion of heat-treated material tends to be more confined to the area around the defect. Quantitative data on the progress of corrosion have been obtained by continuous measurement of hydrogen evolved.

These data, on samples with cylindrical defects tested in water at 530°F (277°C) or 570°F (299°C), have shown that heat-treatment leads to a slower corrosion rate once corrosion has reached the level necessary for detection. In the first runs in 660°F (349°C) water, heat-treatment led to more rapid failure.

The heat-treatment was not found to produce adverse effects on other properties of the Zircaloy-2 cladding. The effectiveness of the heat-treatment can be impaired if the material is cooled too slowly after heat-treatment. In particular, too long a dwell at temperatures in the neighborhood of 600°C should be avoided.

Irradiation studies on uranium-2 wt.% zirconium alloys, coextrusion clad with Zircaloy-2, were conducted by Argonne.² These alloys were diffusion heat-treated prior to irradiation. The cladding was removed from one set of specimens before irradiation. In addition, one specimen was prepared by passing an induction coil so that the alloy was briefly melted and subsequently solidified within the cladding. Four groups of specimens were subjected to burn-ups ranging from 0.051 to 0.16 at.%, at temperatures from 200 to 1250°C. The results of the irradiations are presented in Table I-3.

With regard to the heat-treated specimens, it can be noted that the clad specimens showed generally less growth than the bare specimens. There seems to be little choice in determining the best of the three heat-treatments, since all appeared to be quite effective in stabilizing the material.

The data show that the effect of irradiation temperature outweighed the lesser differences resulting from differences in heat-treatment, with higher temperatures generally tending to lower growth rates. Swelling, however, was much greater in those specimens irradiated at elevated temperatures.

The induction-cast specimen shortened slightly, in contrast to the heat-treated group. Also, it showed a much higher resistance to swelling than the heat-treated specimens. The rate at which the induction-cast specimen increased in volume when irradiated at 1250°C was less than half that displayed by comparable heat-treated specimens irradiated at only 700°C.

A British manual¹⁴ contains a compilation of physical, mechanical, and chemical properties of uranium and its alloys and the effects of irra-

Table I-3 SUMMARY OF IRRADIATION EFFECTS ON SPECIMENS OF EXTRUDED AND HEAT-TREATED URANIUM-2 WT. % ZIRCONIUM ALLOY*
(Data from Argonne National Laboratory²)

Original specimen	Irradiation specimen	Heat-treatment	Cladding thickness, in.	Estimated irradiation temp., °C	Burn-up, at. %	Length change, %	Growth rate, G ₁ †	Diameter change, %	Density decrease, %	Weight change, Mg	Hardness change, RA	Remarks
26-4	CG-22-1	15 min at 800°C, A. C. 1 hr at 500°C, A. C.	None	200	0.051	0.26	5.2	0.61	0.735	-1.5	5.7	
26-4	CG-18-1	15 min at 800°C, A. C. 1 hr at 500°C, A. C.	None	1150	0.13	1.94	15	2.70	5.614	-1.8	0.4	Some melting damage evident
26-4	CG-24-1	15 min at 800°C, A. C. 1 hr at 500°C, A. C.	0.022	400	0.13	0.66	5.1	0.57	1.265	-4.2		
26-4	CG-19-1	15 min at 800°C, A. C. 1 hr at 500°C, A. C.	0.022	700	0.16	1.72	11	0.70	5.188	-4.1		Cladding bulged
	Average						9.1					
26-6	CG-22-2	15 min at 800°C, A. C. 1 hr at 690°C, A. C.	None	200	0.051	1.84	36	-0.17	0.258	-6.3	0.7	
26-6	CG-18-2	15 min at 800°C, A. C. 1 hr at 690°C, A. C.	None	1150	0.13	0.25	1.9	2.68	5.673	-25.3	-7.9	Some melting damage evident
26-6	CG-24-2	15 min at 800°C, A. C. 1 hr at 690°C, A. C.	0.022	400	0.13	0.90	6.9	0.37	1.456	-4.2		
26-6	CG-19-2	15 min at 800°C, A. C. 1 hr at 690°C, A. C.	0.022	700	0.16	1.63	10	0.80	5.899	-4.2		Cladding bulged
	Average						13.7					
26-8	CG-22-3	15 min at 800°C, W. Q. 1 hr at 690°C, W. Q.	None	200	0.051	2.07	42	0.06	0.237	-1.4	9.9	
26-8	CG-18-3	15 min at 800°C, W. Q. 1 hr at 690°C, W. Q.	None	1150	0.13	0.41	3.2	3.63	5.794	-6.9	-5.9	Some melting damage evident
26-8	CG-24-3	15 min at 800°C, W. Q. 1 hr at 690°C, W. Q.	0.022	400	0.13	1.41	11	-0.12	1.886	-4.3		
26-8	CG-19-3	15 min at 800°C, W. Q. 1 hr at 690°C, W. Q.	0.022	700	0.16	1.13	7.1	0.74	7.037	-3.6		Cladding bulged
	Average						15.8					
A-60	CG-18-4	Induction cast in cladding	0.022	1250	0.13	-0.31	-2.4	0.80	2.142	14.6		Cladding slightly bulged

*0.404-in.-diameter rod.

†G₁ = $\mu\text{in.}/(\text{in.})(\text{fission})/10^6$ total atoms).

diation and thermal cycling on these properties. Recently acquired Geneva Conference papers dealing with uranium and alpha-uranium alloys cover: the preparation of uranium and its alloys by the powder-metallurgy process¹⁵ and the atmospheric corrosion of uranium alloys.¹⁶ A French paper¹⁷ discusses the alternatives in choice of reactor fuel for their CO₂ pressurized reactor. The alloys considered were uranium-0.4 wt.% aluminum and uranium-0.5 and 1.0 wt.% molybdenum. A survey of the effects of irradiation on uranium alloys containing chromium, molybdenum, plutonium, silicon, and zirconium is given in a U. S. paper by Kittel and Paine.¹⁸

(M. S. Farkas)

Gamma-phase Alloys

Uranium-Niobium

Battelle¹⁹ has studied a 6 wt.% niobium-uranium alloy by high-temperature X-ray diffraction from 620 to 900°C and has found no evidence of a tetragonal phase, which has been reported as forming in the gamma-phase region. The tetragonal structure is believed to be a transition type structure in the gamma to alpha uranium-plus-gamma₂ transformation which forms on quenching.

Bettis studied the effect of composition on gamma-phase-transformation kinetics at 550°C in uranium-niobium-zirconium alloys. Alloys with compositions ranging from 0 to 15 wt.% zirconium and from 8 to 15 wt.% niobium have been studied. The transformation rate is found to decrease with increasing alloying content; at a constant uranium level, the minimum rate occurs at a particular zirconium to niobium ratio which varies from 0.4 at 86 wt.% uranium to 0.8 at 78 wt.% uranium.

Studies²⁰ of irradiation-induced phase reversal in gamma-phase alloys have continued. Current tests on uranium-niobium and uranium-niobium-zirconium samples indicate a different mechanism is operative than was previously found for uranium-molybdenum alloys. Results on uranium-molybdenum alloys had indicated the reversal occurred as a result of macroscopic diffusion in thermal or displacement spikes.

Uranium-Molybdenum

Bettis²¹ has presented the results of a study in which calorimetric and X-ray spectrometer

measurements were used to verify the existence of an order-disorder reaction in the uranium-molybdenum system.

True stress-true strain curves and modulus of elasticity values for a uranium-10 wt.% molybdenum alloy at room temperature, 250, 500, 750, 1000, and 1250°F are reported²² by the Southern Research Institute. The test results indicate decreased strength and modulus with increasing temperature. Up to 500°F, the true stress values increased with increasing strain from the start of testing until failure. At higher temperatures, the true stress reached a maximum value at an intermediate strain before rupture, probably because the alloy tended to creep at a rate faster than that at which the strain was applied.

Battelle²³ determined the effect of irradiation to 2.1 total at.% burn-up on the modulus of elasticity, ultimate strength, and strain at fracture on the uranium-10 wt.% molybdenum alloy as determined by instrumented bend tests. At a test temperature of 500°C, all of these properties decreased rapidly up to a total burn-up of 0.5 to 1.0 total at.%, with the rate of change decreasing thereafter. An indication that ultimate strength was improved with increasing irradiation temperature to 500°C was noted; this effect probably results from annealing of irradiation-induced damage.

Irradiation test results for the uranium-10 wt.% molybdenum alloy irradiated to between 0.36 and 1.2 total at.% burn-up at temperatures of 250 to 600°C are given in a joint Battelle-Atomic Power Development Associates paper.²⁴ The specimens were hot rolled and cold swaged and then heat-treated to yield either retained, partially transformed, or transformed gamma structures. Average density decreases resulting from irradiation of specimens in the three conditions of heat-treatment were 2.4, 3.3, and 3.9 per cent per at.% burn-up, respectively. Although the retained-gamma structure exhibited the lowest density change, none of the specimens showed severe dimensional changes.

A study²⁵ designed to yield recommended procedures for producing a homogeneous uranium-10 wt.% molybdenum fuel-alloy pin with a uniform cladding is also reported by Battelle. Results obtained with material produced from 4-in.-diameter 25-lb ingots and from small experimental-scale melts are presented. Procedures recommended are: induction melt in a zirconia crucible, pouring from 1850°F after an

alloying time of 1 min into a 4-in.-diameter, 2-in.-wall graphite mold; heat-treat the cast ingot under vacuum for 24 hr at $1050 \pm 25^\circ\text{C}$ and furnace cool; reduce ingot 75 per cent with forging and rolling temperatures of 1850 and 1650°F , respectively; coextrude billets with zirconium and cold swage to size, giving the pins a final heat-treatment of 1 hr at 800°C followed by a rapid cool. The heat-treatments are designed to produce a homogeneous and stress-free pin. Impurity limits of 2000 ppm zirconium, 300 ppm carbon, 225 ppm oxygen, 400 ppm iron and nickel combined, and 400 ppm chromium are also recommended. These limits are recommended on the basis of alloy fabricability, cracking associated with carbide and oxide stringers, and the destabilizing effect of zirconium on the metastable gamma phase.

Complex Alloys

Argonne¹⁸ has been investigating the irradiation behavior of fissium type alloys, which are alloys of uranium containing representative elements of those remaining after pyrometallurgical reprocessing of irradiated uranium. For example, a uranium-5 wt.% fissium alloy contains 95 wt.% uranium, 2.5 wt.% molybdenum, 0.2 wt.% zirconium, 1.5 wt.% ruthenium, 0.3 wt.% rhodium, and 0.5 wt.% palladium. All of these elements are gamma stabilizers, and, when they are present in sufficient amounts, the gamma phase is retained on quenching. A uranium-3.17 wt.% fissium alloy was found to exhibit maximum irradiation stability when heat-treated 24 hr at 650°C , while a 5 wt.% fissium alloy exhibited maximum stability when gamma quenched. The addition of 2.5 and 7.5 wt.% molybdenum to cast uranium-5 wt.% fissium alloys increased surface smoothness and eliminated the dependence of stability on prior heat-treatment. In addition, as-cast samples of uranium-20 wt.% plutonium-5.4 wt.% fissium, uranium-20 wt.% plutonium-10.8 wt.% fissium, and uranium-20 wt.% plutonium-5 wt.% molybdenum have been found to exhibit excellent surface and dimensional stability when irradiated.

(A. A. Bauer)

Epsilon-phase Alloys

Uranium-Zirconium

The X-ray structure of the epsilon phase (hexagonal, partially ordered) is reported by

Argonne.¹ The results confirm earlier structural data. A literature survey summarizing physical-property data on uranium-zirconium alloys published by Knolls²⁶ includes data on density, elastic modulus, thermal conductivity, electrical resistivity, linear coefficient of thermal expansion, thermoelectric characteristics, diffusion coefficients of uranium in zirconium, and damping capacity.

Uranium-Silicon

Argonne reports¹⁸ that cast specimens of U_3Si exhibited excellent surface smoothness and dimensional stability on irradiation. Extruded specimens also exhibited excellent surface stability but elongated markedly when irradiated. A single-cast specimen of those irradiated developed a central void when irradiated at a calculated temperature near 600°C . While the unirradiated alloy exhibits excellent corrosion resistance, the irradiated alloy eventually fails in 315°C water by a process of mechanical disintegration rather than chemical dissolution.

Chalk River also reports²⁷ on the irradiation of U_3Si samples. Samples of 3.89 wt.% silicon, 0.3 in. in diameter, clad by coextrusion with Zircaloy-2, were irradiated in the epsilonized and de-epsilonized conditions in 275°C water to 250 and 500 Mwd/metric ton. The samples showed no length change and only a 0.001 in. change in diameter.

(A. A. Bauer)

Dilute Uranium Alloys

Aluminum-Uranium Alloys

As a result of continued interest in aluminum-uranium alloys, Oak Ridge²⁸ reports the determination of deformation textures for alloys containing up to 13 wt.% uranium fabricated by extrusion and cold rolling. These textures were determined by the quantitative X-ray spectrometer technique, employing spherical diffraction specimens and a special goniometer. The data were obtained as "inverse" pole figures or axis distribution charts. The two major conclusions reached as a result of this study were (1) alloys containing increasing amounts of dispersed UAl_4 exhibit an increasing tendency toward random orientation as would be expected, and (2) cold-rolled stock has a texture similar to a fibered texture, caused by alignment of the dispersed phase during initial passes.

By using a special device which provides for concentric turning of a centrifugal mold, Battelle^{29,30} has produced 26-in.-long extrusion-blank castings with wall thicknesses which are as consistent as those produced by static casting techniques. By centrifugal casting, sound ingots of aluminum-uranium alloy containing 35 wt.% uranium have been produced in air. Additions of 3 wt.% of germanium, magnesium, palladium, silicon, and zirconium appear to improve the fabricability of the basic aluminum-uranium alloy, and they contain UAl_3 as the predominant compound after fabrication.

Zirconium-Uranium Alloys

The effect of transients and longer time anneals on irradiated zirconium-uranium alloys is under continuing study by Knolls³¹. Alloys containing 7 and 8 wt.% uranium with burn-ups between 0.4 and 1.4 total at.% were heated isothermally for 500 hr at 510, 540, and 620°C. The structure of the alloys prior to irradiation was delta dispersed in epsilon. In all cases, saturation in swelling occurred after about 200 hr at temperature. Although the alloys with the highest burn-up swelled most rapidly on initial heating, there were cases where other alloys had swelled more by the time saturation had occurred. As a result of the isothermal anneals, only a fraction of the theoretical amount of fission gas was released and the rate of release was not proportional to the square root of time.

Electron microscopy showed the formation of gas bubbles 0.1μ or smaller in the epsilon phase, with no noticeable change in over-all density. At higher burn-up more bubbles were noted, some of which had increased in size.

In transient heating tests it was obvious that swelling is dependent on the amount of burn-up. Specimens having only 0.2 at.% burn-up swelled within acceptable levels up to 1800°F (top test temperature). Higher burn-ups resulted in unacceptable swelling at lower temperatures. The alloy phase transformation at 620°C is no doubt responsible for large amounts of swelling above this temperature, and increasing burn-up lowers this transformation temperature.

Saturation of swelling as a result of high flux irradiation could be explained as follows: Because of the low diffusion rate of gas in metal, supersaturation is easily produced. The higher the degree of supersaturation the smaller the

critical nucleus size; therefore small bubbles are produced. Atoms that are produced will either form new bubbles or diffuse only a very short distance to an existing bubble. Consequently, the bubbles remain small, and their surface tension is such that it restrains swelling.

Postirradiation heating to or below the irradiation temperature will cause no additional swelling. Postheating above that temperature will cause swelling when pressure-volume-temperature relations overcome the surface tension and the creep resistance of the matrix. Surface tension decreases but so does internal pressure until, for a certain temperature, equilibrium is reached and saturation of swelling occurs.

Bettis³² reports that a plate type specimen of zirconium-12 wt.% uranium alloy having a burn-up of 1 total at.% increased in thickness over 400 mils as a result of an 87-min heat-treatment at 760°C. Such a specimen must contain a large void volume. On the basis of the theory proposed in the preceding paragraph, an explanation of this excessive swelling must be that, because of the large size of the fission bubbles initially produced or because of voids present in the structure prior to irradiation, the restraining effect of surface tension was negligible at the temperature of heat-treatment.

Postirradiation corrosion tests in 680°F water, performed by Bettis on alloys containing 5 to 6 wt.% uranium, indicate that the corrosion rate varies directly with burn-up. The higher the burn-up, the more severe the corrosion. In the use of fuel alloys containing boron as a burnable poison, the amount of contained boron has a pronounced effect on the postirradiation corrosion rate. As an example, bare edge-corrosion specimens of 5.5 wt.% uranium alloy containing 0.113 and 0.02 wt.% boron were tested in 650°F water. The alloy containing 0.113 wt.% received a burn-up of 1.6 total at.% and was irradiated at 900 to 1035°F. It failed by cladding rupture within 1 hr. On the other hand the alloy containing 0.02 wt.% was irradiated to identical burn-up at temperatures of 860 to 1055°F and corrosion tested in the same manner. This material did not fail until after 24 hr.

In an effort to develop zirconium-base fuel alloys which have good tensile properties at 650°C, alloy compositions of zirconium-5 wt.% uranium-5 wt.% niobium, zirconium-15 wt.% uranium-15 wt.% niobium, zirconium-5 wt.% uranium-15 wt.% niobium, and zirconium-15 wt.%

uranium-20 wt.% niobium have been studied. The zirconium-15 wt.% uranium-20 wt.% niobium alloy was the only one of the four which exhibited reasonable strength at 650°C (47,000 psi yield strength). The next best alloy was zirconium-5 wt.% uranium-15 wt.% niobium. This material had a yield strength of 31,600 psi at 650°C.

The constitution, transformation kinetics, physical properties, and irradiation behavior of zirconium-uranium alloys were reviewed in a paper by Bauer et al.,³³ presented at the Second Geneva Conference.

Niobium-Uranium Alloys

Battelle^{19,30} has been concentrating effort on the binary alloys in the range between 10 and 60 wt.% uranium. Tests show that there is very little softening of any of these alloys at temperatures to 900°C. The niobium-60 wt.% uranium alloy has a hardness of 176 DPHN at 900°C, whereas the niobium-10 wt.% uranium alloy has a hardness of 95.1 DPHN. The alloys containing 10 to 20 wt.% uranium will hot roll at 2400°F without cracking. On the other hand, recent tests indicate that temperatures of at least 2700°F will be required to break down the cast structure of the other compositions by rolling or forging. Extrusion temperatures may be lower. Indications are that if initial breakdown of the cast structure can be accomplished, all alloys can be cold rolled.

Miscellaneous Alloys

As a result of work on the uranium-zinc alloy system, Ames³⁴ reports the following solubilities of uranium in zinc.

Temperature, °C	Solubility of uranium, wt. %
475	0.005
550	0.083
625	0.38
700	1.06
800	4.83

The Bureau of Standards³⁵ reports that the solubility of uranium in platinum is about 4 at.% at room temperature and increases to about 4.5 at.% at the eutectic temperature (1345°C). The system is characterized by two eutectics: the first at 1005°C at 12 at.% platinum; and the second at 1345°C and 87.5 at.% platinum. There

are four intermetallic compounds in the system. Three of these compounds form peritectically: 50 at.% platinum (UPt) at 961°C; 66.7 at.% platinum (UPt₂) at 1370°C; and 83.3 at.% platinum (UPt₃) at 1460°C. One forms by melting congruently: 75 at.% platinum (UPt₃) at 1700°C.

(R. F. Dickerson)

Plutonium Alloys

Plutonium Metal

Tensile properties of as-cast and delta-annealed plutonium have been redetermined by Hanford.³⁶ The average tensile properties of as-cast plutonium of 99.50 per cent purity, 19.50 g/cm³ density, and 220 DPH hardness are: ultimate strength, 62,000 psi; 0.02 per cent offset yield strength, 37,000 psi; modulus of elasticity, 13.8×10^6 psi; and modulus of resilience, 12.7 to 26.1 in.-lb/cu in. No significant differences in tensile properties were noted for delta-annealed plutonium.

Sandenaw and Gibney³⁷ have determined the electrical resistivity and thermal conductivity of high-purity plutonium. Resistivity values are

Table I-4 RESISTIVITY VALUES OF PLUTONIUM SPECIMENS*

Temp., °K	Resistivity, $\mu\text{ohm-cm}$	
	Specimen 1 (99.95 wt.% Pu)	Specimen 2 (99.96 wt.% Pu)
25.8		68.5
27.2	61.1	
50	128.0	128.0
100	157.0 \pm 0.10	156.8 \pm 0.06
150	153.5	153.5
273.15	146.3 \pm 0.25	146.6 \pm 0.04
380	141.0	141.8
420	107.5	109.5
475	107.0	110.0
505	106.2	109.5
590	105.0	109.3
625	97.7	103.0
725	98.5	104.0
735	99.4	104.8
774	107.1	114.0
787		114.1

*Data taken from reference 37.

listed in Table I-4 and thermal conductivity values are shown in Fig. 2. Phase transformation temperatures as indicated by electrical resistivity data are presented in Table I-5.

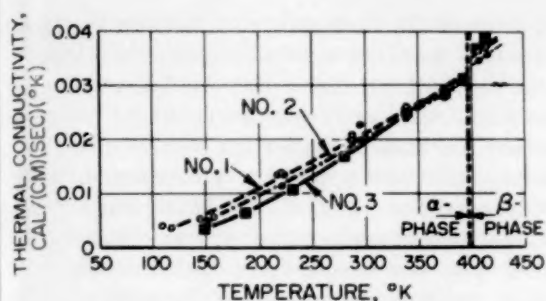


Figure 2—Thermal conductivity of high-purity plutonium as a function of absolute temperature. Data taken from reference 37.

Table I-5 PHASE-CHANGE TEMPERATURES AS INDICATED BY RESISTANCE MEASUREMENTS*

Phase change	Temp., °K	
	Specimen 1	Specimen 2
$\alpha \rightarrow \beta$	397.0 ± 0.2	396.4 ± 0.1
$\beta \rightarrow \gamma$	$478.6 - 499.2$	474.7 ± 0.2
$\gamma \rightarrow \delta$	592.7 ± 0.5	590.1 ± 0.5
$\delta \rightarrow \delta'$	$727.5 - 731.7$	729.2 ± 1.0
$\delta' \rightarrow \epsilon$	$753.7 - 759.9$	$753.2 - 760.6$

*Data taken from reference 37.

depth of 1.5 mils in 30 days, whereas a slow-cooled (large PuAl_4 particles) alloy corroded to 20 mils in 15 days.

Data on corrosion of plutonium and some plutonium alloys in air have been reported by Los Alamos.¹⁶ The corrosion rate of unalloyed plutonium in air of 50 per cent relative humidity is approximately 65 times greater than in dry air at the same temperature. Considerable improvement in corrosion rates in moist air can be

Table I-6 CORROSION RATES OF PLUTONIUM AND PLUTONIUM ALLOYS IN AIR OF 20 PER CENT RELATIVE HUMIDITY AT 35°C*

Composition	Weight increase, mg/cm ² , at time indicated	
	900 hr	8730 hr
Pu-7.5 at.% Zr	0.044	0.12
Pu-10.0 at.% Zr	0.044	0.14
Pu-8.0 at.% Al	0.05	0.55
Unalloyed Pu	0.96	28.1

*Data taken from reference 16.

gained by alloying with zirconium. Table I-6 lists the effects of zirconium and aluminum additions on corrosion properties.

The zirconium-containing alloys were also examined in air of 50 per cent relative humidity at 55°C. After 5600 hr of exposure, duplicate unalloyed alpha-plutonium specimens had gained 68 and 85 mg/cm², whereas the zirconium alloy specimens had gained less than 0.5 mg/cm².

(V. W. Storhok)

Thorium

Two new books on thorium and its alloys have been published recently.^{39,40} The first, "Thorium Production Technology," contains data on the mechanical and physical properties of thorium, fabrication of thorium, and metallography of thorium and identification of inclusions, plus other subjects. The second, "The Metal Thorium," contains data on the mechanical properties of thorium and thorium alloys, recrystallization of thorium, fabrication and cladding of thorium metal, corrosion of thorium and its alloys, metallography, effects of irradiation upon thorium, and constitution of thorium alloys.

The British have announced some revisions to the thorium-aluminum constitution diagram.⁴¹ The solubility of aluminum in thorium is given

Plutonium-Uranium Alloys

Argonne³⁸ has irradiated small pinspecimens of chill-cast, nickel-plated uranium-10 wt.% plutonium and uranium-15 wt.% plutonium alloys to $\frac{1}{2}$ at.% burn-up. The 15 wt.% plutonium alloy showed excellent dimensional stability. It is uncertain whether improvement over bare cast uranium is due primarily to intrinsic characteristics of the alloy or to restraint imposed by nickel coating. Uranium-10 wt.% plutonium appeared somewhat inferior, behaving as would be expected for coarse-grained uranium enclosed in a strong can.

Plutonium-Aluminum and -Zirconium Alloys

Chalk River²⁷ has corrosion tested 0.25-in.-diameter by 0.375-in.-long specimens of aluminum-5, -10, -15, and -20 wt.% plutonium alloys in 340°C water. The 5 and 10 wt.% plutonium alloys corroded to a depth of 3 mils, and the 15 wt.% plutonium alloy corroded to 1.5 mils in 30 days. The particle size of PuAl_4 was found to have an appreciable effect on the corrosion rates of the 20 wt.% plutonium alloy. A chill-cast (small PuAl_4 particles) alloy corroded to a

as 0.85 at.% at 1300°C and 0.4 at.% at 1000°C. The eutectic at 20 at.% aluminum is at 1243°C, and Th_2Al melts at 1307°C. The eutectic at 38 at.% aluminum is at 1296°C, and Th_3Al melts at 1301°C. The eutectic at 43 at.% aluminum is at 1290°C; ThAl forms peritectically at 1318°C; a compound near Th_2Al_3 forms peritectically at 1394°C; and ThAl_2 melts above 1520°C. ThAl_3 forms peritectically at 1120°C, and the eutectic at 97 at.% aluminum is at 630°C. The solubility of thorium in aluminum at 630°C is less than 0.1 at.%.

Donagala, Elliott, and Rostoker⁴² of Armour Research Foundation report that the solubility of thorium in mercury is negligible at -32°C but is about 2 wt.% at 200°C and about 5 wt.% at 300°C. The compound Hg_3Th is stable in a pressurized system to at least 700°C, and HgTh is stable to at least 1000°C.

Ames Laboratory indicates that preliminary data suggest that the solidus in the thorium-yttrium system is a continuous curve extending between the melting points of the pure metals.³⁴ Extensive terminal solid solutions are to be expected in this system. The solubility of hydrogen in thorium is shown to be 25 at.% at 800°C, 9 at.% at 600°C, and 1 at.% at 300°C. The first thorium-hydrogen compound is ThH_2 . The thorium-tantalum system is a simple eutectic type, with the eutectic occurring at about 20 wt.% tantalum and 1700°C between thorium-3 wt.% tantalum solid solution and tantalum-5 wt.% thorium solid solution. Terminal solubilities become negligible in the tantalum-thorium system at room temperature.

Ivanov and Badayeva⁴³ have summarized the results of several investigations of thorium systems in the USSR. New data reported include statements to the effect that the solubility of lead in thorium does not exceed 0.7 at.% between 1000 and 1400°C and that the solubility of tin in thorium is about 0.2 at.% at 1300°C. As a result of language difficulties and attempts to be brief, much has been lost in a description of the important thorium-uranium-zirconium ternary system, but it appears that the addition of uranium to the thorium-zirconium system at high temperatures causes the solid miscibility gap to expand, resulting in two body-centered cubic phases, a zirconium-rich phase containing most of the uranium, and a thorium-rich phase containing only a little zirconium and uranium. The major features of the ternary diagram de-

rive from the insolubility of thorium in gamma uranium and the low solubility of uranium in thorium. All extensive high-temperature solid solutions can be regarded as being based on zirconium and, at high-alloy contents, two such solid solutions appear: a zirconium-uranium body-centered cubic solid solution and a zirconium-thorium body-centered cubic solid solution. The low-temperature transformations of these two solid solutions are the same as those occurring in the binary systems. The two solid solutions dissolve in one another, forming one solid solution at 1000°C only at compositions containing more than 70 at.% zirconium.

The reactions of thorium monocarbide are reported also.⁴³ Thorium metal apparently displaces uranium from uranium monocarbide producing a uranium-thorium monocarbide plus uranium metal. The thorium monocarbide-zirconium monocarbide system appears to be unusual in that thorium monocarbide will dissolve only 6 mole % zirconium monocarbide, and zirconium monocarbide dissolves no thorium monocarbide. In the ternary thorium-zirconium-uranium monocarbide system, uranium monocarbide acts as the solvent and complete solubility is found only in compositions over 70 mole % uranium monocarbide. The compounds ThBe_{13} and UBe_{13} were found to be completely soluble in one another.

Nuclear Metals, Inc., has prepared a review of the metallography of thorium.⁴⁴ Techniques are described, and 32 photomicrographs of thorium and thorium alloys are shown. It is clear that the metallography of thorium and its alloys has not yet been reduced to a routine operation.

Kantan, Raghavan, and Tendolkar⁴⁵ of Trombay, India, report success in preparing a thorium-metal compact with a density of 96 per cent of theoretical from calcium-reduced thorium-metal powder. Minus 325-mesh powder was compacted at 40 tsi and sintered in a vacuum for 1 hr at 1300°C.

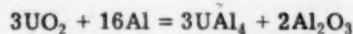
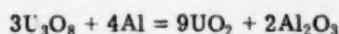
Battelle has provided additional details on the results of irradiations of as-swaged specimens of thorium-11 wt.% uranium alloy.²⁹ Twelve specimens were irradiated in two NaK-filled capsules to burn-ups ranging from 0.57 to 1.5 total at.%. Maximum specimen temperatures ranged around 1200°F (650°C). All specimens were $\frac{3}{8}$ in. in diameter and $1\frac{3}{8}$ in. long and contained 93 per cent enriched uranium. Of the

twelve specimens, six showed no gross swelling or cracking. Density decreases of 2.6 to 4.9 per cent were measured on these specimens. Rates of density decrease in one capsule ranged from 2.4 to 3.8 per cent per total at.% burn-up, whereas rates in the other capsule ranged from 4.9 to 7.8 per cent per total at.% burn-up. Burn-up data suggest that the second capsule operated at temperatures averaging 100°F higher than the first, and the faster rate of density decrease is attributed to the higher temperature of the specimens. The behavior of the other six specimens which showed gross cracks and other defects in the irradiated condition was attributed to incomplete coverage of the specimens by NaK and to other external causes. (W. Chubb)

Dispersion Fuel Materials

Two recent reports deal with the development of fabrication techniques, preparation of specifications, and manufacture of stainless-steel- UO_2 dispersion elements for the Army Package Power Reactor (APPR). One report by Oak Ridge and Alco Products, Inc.,⁴⁶ describes the step-by-step fabrication procedure which has been developed and will be adopted for the second APPR core. A second report by Sylvania-Corning⁴⁷ is of similar nature, describing additional development studies which have preceded the manufacture of the APPR Core II fuel elements.

Compatibility and growth studies on dispersions of U_3O_8 in aluminum have continued at Oak Ridge. The U_3O_8 appears to react with aluminum at 600°C in the following manner:



The reaction of UO_2 with aluminum is the same as the second step of the U_3O_8 -Al reaction; however, the ultimate growth of U_3O_8 -Al fuel plates after 3000 hr at 600°C is only 4 per cent, whereas a growth of 20 to 36 per cent has been observed in UO_2 -Al fuel plates after only 24 hr at 600°C.

Sylvania-Corning⁴⁸ describes the preparation of UN and U_3Si_2 fuel materials and the compatibility of these dispersants with several metallic matrices. A series of specimens containing 30 vol.% UN in molybdenum, niobium, Nichrome V, 40 wt.% titanium-niobium alloy, and

vanadium were cold compacted at 50 tsi, vacuum sintered at 1200°C, and then hot forged and vacuum annealed at 1200°C. The densities of these specimens ranged between 90 and 100 per cent of theoretical. It is reported that no reaction occurred between UN and either molybdenum or niobium, a slight reaction between UN and vanadium, and a very definite reaction between UN and both Nichrome V and the titanium-niobium alloy.

Specimens of 30 vol.% U_3Si dispersed in the same metal matrices were prepared in a similar manner. It was observed that some reaction occurred between all combinations of materials.

Recent Battelle reports (references 19, 29, 30, and 49) describe progress on the development of cermet fuel bodies. These studies include an investigation of fabrication techniques and the measurement of pertinent mechanical and physical properties of UO_2 and UN bodies containing from 10 to 40 vol.% of various metal additives (stainless steel, niobium, and molybdenum). Dense bodies, 90 to 95 per cent of theoretical, have been obtained by press forging, swaging, and hydrostatic pressing. The cermets containing a stainless-steel matrix have been clad successfully with stainless steel by swaging and pressure bonding. Electrical resistivity measurements have been made on several of the specimens, and these values are being related to thermal-conductivity measurements.

The modulus of rupture of 80 vol.% UO_2 -molybdenum having a density of 94 per cent of theoretical is reported to be 22,200 psi. This compares to measured values of 8850 and 7000 psi for 100 per cent UO_2 having densities of 95 and 93 per cent of theoretical, respectively.

Dispersion fuel specimens of 24 wt.% UN and 24 wt.% UC in stainless steel are being irradiated by Battelle⁴⁹ in a three-capsule program. The first series of four specimens which operated at core temperatures of from 1500 to 1750°F to burn-ups ranging from approximately 5 to 10 of the U^{235} are presently undergoing hot-cell evaluation. (D. L. Keller)

Refractory Fuel and

Fertile Materials

Fabrication of UO_2 -containing Ceramics

Uranium oxides having compositions ranging from UO_2 to U_3O_8 were sintered in argon, nitro-

gen, carbon dioxide, or hydrogen atmospheres at Harwell.⁵⁰ It was found that an increase in the oxygen content of the starting powder from $\text{UO}_{2.00}$ to $\text{UO}_{2.02}$ resulted in a major increase in sintered density. Further increase in the oxygen content of the starting powder had only a minor effect on the sintered density. Sintered densities of pellets fired in argon, nitrogen, carbon dioxide, or vacuum were considerably higher than those of pellets fired in dry hydrogen. This is in good agreement with data reported earlier by the Canadian Bureau of Mines.⁵¹ Specimens fired in partially dried atmospheres were denser than those fired in dry hydrogen, but not so dense as those fired in the other atmospheres studied.

Sylvania-Corning has been investigating the hot isostatic pressing of clad UO_2 elements. Fired pellets, with densities of 92 to 94 per cent of theoretical, were placed in stainless-steel tubing and pressed at 1250°C , using argon at a pressure of 13,000 psi as the pressing medium. The cladding did not pleat, although small circular ridges between pellets were reported. The cladding adhered strongly to the UO_2 when an element was sectioned. Further experiments using unfired pellets are planned.

(H. D. Sheets)

Properties and Behavior

of Uranium Oxides

During the period covered by this Review, a substantial number of papers have appeared, summarizing various aspects of UO_2 technology.⁵²⁻⁵⁶

The uranium-oxygen system is being investigated by several laboratories. Plastic deformation of UO_2 , important in the sintering and pressing behavior of this fuel, has been studied by the British.⁵⁷ The flow behavior of sintered UO_{2+x} was studied as a function of temperature and stress. Sintered $\text{UO}_{2.06}$ and $\text{UO}_{2.16}$ having theoretical densities greater than 95 per cent deformed plastically above 800°C . $\text{UO}_{2.00}$ becomes plastic only above 1600°C . The UO_2 - $\text{UO}_{2.20}$ system has been studied⁵⁸ by an electrochemical technique in the temperature range 1150 to 1350°K . In this Bettis study, equations relating thermodynamic quantities to the degree of non-stoichiometry have been developed on the assumption that the UO_{2+x} region can be treated as an interstitial solution of oxygen ions in the UO_2 fluorite lattice.

Miscellaneous studies of the uranium-oxygen system include electrical properties,⁵⁹ melting point and emissivity of UO_2 ,⁶⁰ U_3O_8 - UO_3 ,⁶¹ and U_3O_8 ,⁶²⁻⁶³ structures, and the phase diagrams⁶ of UO_2 systems containing Al_2O_3 , BeO , and MgO additives.

Bettis²¹ has studied the oxidation of Mallinckrodt UO_2 powder in oxygenated water at 87 to 177°C . In water containing 25 cc of oxygen per kilogram of water, a new phase, $\text{UO}_3 \cdot 0.8\text{H}_2\text{O}$, is reported. The oxidation proceeds in a different manner from that characteristic of the oxidation of the powder in air or oxygen at the same oxygen pressure (500 mm Hg). Degassed water does not hydrate or oxidize UO_2 powder at these temperatures.

Battelle^{19,30,49} has measured the thermal conductivity of unirradiated UO_2 in preparation for measurements on irradiated specimens of the oxide. Sintered UO_2 slugs, 3 in. long by $\frac{1}{4}$ in. in outside diameter, were tested in a steady-state heat-flow apparatus. Interpolated values for three specimens are reported in Table I-7.

Table I-7 UO_2 THERMAL CONDUCTIVITY*

Temp., $^\circ\text{C}$	Thermal conductivity, watts/(cm)($^\circ\text{C}$), at indicated density, % of theoretical		
	87.4	93.7	95.3
100	0.069	0.075	0.079
200	0.056	0.060	0.065
300	0.047	0.050	0.056
400	0.040	0.043	0.048
500	0.035	0.038	0.043
600	0.032	0.035	0.038
700	0.031	0.033	
800	0.030	0.031	

*Data taken from references 19, 30, and 49.

In the PWR Core II fuel-evaluation program, Bettis is irradiating compartmented UO_2 plates for the blanket. The plate thickness is 80 mils. Fission-gas release data⁶⁵ are reported in Table I-8. Information on diffusion coefficients and activation energies for Kr^{85} release is given in the section on Radiation Effects in Ceramic Fuels, pp. 14-15.

Hanford is studying the irradiation performance of UO_2 fuel elements consisting of loose powder enclosed in a can. If successful, this type

of element would certainly permit significant reductions in fuel fabrication cost.

(W. S. Diethorn)

Table I-8 FISSION-GAS RELEASE FROM COMPARTMENTED UO_2 *

Burn-up, Mwd/ton UO_2	Initial heat flux, Btu/(hr)(ft ²)	Kr ⁸⁵ released, per cent of theoretical amount formed
7,300	574,000	0.13
10,250	702,000	0.23
9,650	650,000	0.24

*Data taken from reference 65.

Fabrication of Uranium Carbides

and Nitrides

Studies of the fabrication of uranium carbides and mixtures of uranium carbides with other compounds are continuing at various laboratories. Murray and Williams⁵⁴ prepared UC by various methods including reacting UO_2 with carbon, reacting UH_3 with hydrocarbons, and reacting uranium powder with carbon powder. In the latter method, the powders were compacted initially to a high density by hot pressing or hot extrusion at 650 to 800°C. The hot-pressed compacts were sintered at 1050°C. The hot-pressing dies were fabricated from Stellite alloys or bonded titanium carbide. Temperatures of 1800 to 2000°C were required in sintering compacts pressed from UC made by reacting UO_2 with carbon or from the hydride. Houyvet et al.⁶⁶ obtained densities of 95 per cent of theoretical by hot pressing mixed powders of uranium and carbon at 900 to 1000°C in graphite dies.

Sound, homogeneous cylindrical castings of UC of near stoichiometric composition were consistently produced at Battelle⁶⁷ by a special arc-melting technique. UC buttons, previously prepared by arc-melting the elements in a helium atmosphere, are placed over the opening of a graphite mold in a helium-atmosphere arc furnace. The molten carbide is dropped by gravity into the mold and is cooled in place. The resultant casting has a density of 98 per cent of theoretical, and could be readily machine ground using a water-base cutting fluid. The formation of a thin layer of UC_2 on the outer surface of the

UC casting (by reaction with the mold) apparently improves room-temperature stability by protecting against atmospheric oxidation.

In studies of the UC-UN system at Harwell,⁶⁸ mixtures of the two compounds were cold pressed and then melted in an arc furnace under an argon atmosphere. Extensive decomposition of UN occurred during melting, even in an atmosphere of 66 per cent nitrogen.

Sylvania-Corning has prepared graphite fuel elements by mixing UC with graphite flour and Bakelite binder. The UC was stabilized with 30 wt. % MoC to permit handling. Vacuum appeared to be preferable to argon atmosphere in a 750°C bake. Samples were later heat-treated to 1900°C. A maximum of 29.6 wt. % UC in graphite was used.

(M. J. Snyder)

Properties of Refractory Fuels

Other Than Uranium Oxides

The mechanical and physical properties of uranium monocarbide have received considerable attention because of the attractiveness of this compound as a reactor fuel, owing to its high uranium density and high melting point. The properties of sintered bodies with densities of 10.2 to 10.4 (75 per cent of theoretical) by German investigators⁶⁹ are given as: Vickers hardness ranging from 550 to 700 kg/mm²; specific heat at 125°C of 0.048 cal/(g)(°C), increasing to 0.055 cal/(g)(°C) at 250°C; thermal conductivity at 60°C of 0.080 cal/(cm)(sec)(°C), decreasing to 0.050 cal/(cm)(sec)(°C) at 265°C; and electrical conductivity of 1×10^{-4} ohm-cm. The dimensional stability and resistance to shock were reported to be very good over the temperature range 1000°C to room temperature. British investigators⁵⁴ found the bend strength to be about three times that of UO_2 . These latter investigators reported that UC reacts with CO_2 more rapidly than does metallic uranium at 500°C but less rapidly at 700°C. In hydrogen, UC reacts rapidly at 300°C but is very stable at temperatures above 600°C. UC was reported to have good compatibility with beryllium or zirconium canning materials, and no reaction was observed between liquid sodium and UC. After irradiation of 3000 Mwd/ton at 650°C, sintered bodies of UC (density = 10.5) were reported to crack and to release approximately 10 per cent of the total fission gases. This amount of fission-gas release is considerably greater than that observed at Battelle²⁹ in the case of arc-melted

high-density UC specimens. Battelle calculations, based upon Kr⁸⁵ release to capsules containing UC, which had a burn-up of 700 Mwd/ton at 600 to 660°C, indicate that the only mechanism of gas release was by recoil. In postirradiation heat-treatment methods of evaluating gas release, Battelle³⁰ found that only 0.09 per cent of the total Xe¹³³ was released in 120 hr at 1800°F after an effective irradiation of 3.12×10^{13} nvt.

Nichols⁵² has compiled the physical, mechanical, and chemical properties of several ceramic fuels, such as, UO₂, UC, U₃Si, ThC, and ThO₂. Some of the properties of these materials have been reported previously.

The crystallographic, chemical, magnetic, and electrical properties, and methods of preparation of the various compounds in the uranium-sulfur system were reported by Picon and Flahaut.⁷⁰ Six compounds were prepared, and three crystalline modifications of US₂ were established. Powder X-ray diffraction data for these compounds are presented along with those of the oxysulfide, UOS. (D. A. Vaughan)

Mechanism of Corrosion of Fuel Materials

Uranium Oxide - Carbon Monoxide

The decomposition of carbon monoxide on urania has recently been studied by Roberts et al. at Harwell.⁷¹ It was found that the rate of decomposition depended upon sample size and was independent of temperature in the range of 500 to 900°C. Decomposition stopped at carbon dioxide levels of about 1 per cent. As carbon was deposited, the chemisorptive capacity of urania for oxygen was decreased and oxygen was lost from the solid oxide; the latter was based on the observation that more carbon dioxide was formed than could be accounted for from $2\text{CO} \rightarrow \text{C} + \text{CO}_2$. When CO-CO₂ mixtures were circulated over the carbon deposits of urania, some carbon dioxide was lost. The Harwell personnel believe that oxygen from the carbon dioxide replaced that in the urania which was lost during carbon deposition. The readsorption of this small amount of oxygen inhibited further deposition of carbon, the decomposition then being controlled by an equilibrium involving oxygen, not carbon. Re-exposing the oxide to pure carbon monoxide resulted in reduction of the oxide again.

Zirconium-Uranium-H₂O

The role of microstructure in determining the corrosion behavior of equilibrium zirconium-uranium alloys in high-temperature water has been investigated at Battelle.⁷² In alloys containing less than 25 wt.% uranium, it was found that alpha zirconium was the major phase and determined corrosion behavior; alloys containing more than 60 wt.% uranium were predominantly alpha uranium and oxidized rapidly, while the corrosion rate of alloys containing 25 to 55 wt.% uranium correlated with the penetration rate of epsilon, the major phase in these alloys. The corrosion rates of the latter were found to fall within limits as calculated from the penetration rates of alloys representing the extremes in epsilon composition (45 and 55 wt.% uranium). Anomalies in corrosion rates were correlated with segregation, usually at grain boundaries, of one of the alloy phases. Corrosion behavior in these alloys depended upon the relative corrosion resistance of the segregated phase. (W. E. Berry)

Basic Studies of Radiation Effects in Fuel Materials

Radiation Effects in Ceramic Fuels

A technique which offers possibilities for more definitive studies of the microstructure of irradiated specimens is described in a recent Hanford report.⁷³ Metallographic examination of fracture surfaces is accomplished by preparation of replicas for electron microscopy. To minimize deformation of the surfaces during fracturing, low temperatures are used. At -198 and -78°C, excellent surfaces were obtained with unirradiated uranium and plutonium. Fracture of these materials at 25°C produced a definite smearing of the surfaces. Good fracture surfaces were obtained in UO₂ at 25°C. Work is in progress toward applying this technique to irradiated plutonium, uranium, and uranium dioxide. No detailed results on irradiated materials are reported to date.

A recent British report⁷⁴ presents several interesting papers on X-ray diffraction techniques for irradiated specimens. Equipment for X-ray measurements on high-activity specimens using a combination of shielding and a quartz monochromator, applications of small-angle scatter-

ing techniques, and single-crystal techniques for high specific activity are discussed.

The measurement of fission-product release by delayed-neutron and gross gamma-activity measurements on fueled MgO and graphite was reported by Cowan and Osth.⁷⁵ Studies were made at temperatures up to 2600°C. It was found that fission products which form volatile oxides (molybdenum, arsenic) diffuse more rapidly in the MgO than in the graphite matrix. Those which form refractory oxides (cadmium, silver, tin, and strontium) diffuse at a lower rate in MgO than in graphite. Palladium, tellurium, iodine, and barium behave similarly in both matrices.

Further work on fission-gas release in UO₂ is reported by Bettis.²⁰ Post-irradiation annealing experiments conducted over the temperature range 1000 to 1300°C on a material of 93.7 per cent theoretical density yielded an activation energy for Kr⁸⁵ release of 60 kcal/mole. Three samples of different particle size were irradiated to very low burn-up (0.003 at. % U²³⁵) and then annealed in the temperature range 900 to 1500°F. The activation energy for Kr⁸⁵ release was 34.3, 37.0, and 36.0 kcal/mole for particle sizes, expressed in terms of specific surface area, of 1.3, 0.1, and 0.05 m²/g, respectively. For the fine and coarse particles, the diffusion coefficient varied from 2×10^{-18} cm²/sec at 900°C to 3×10^{-16} cm²/sec at 1500°C. The diffusion coefficient for the intermediate-size particles was reported to be an order of magnitude higher.

Work is also in progress on the use of natural radioactive-decay-product additions to UO₂ to study the diffusion on thoron. Measurements are made by flowing helium carrier gas over heated specimens spiked with thorium and detecting the release of the naturally radioactive rare-gas daughter, thorium, by α -scintillation counting. Work is in progress to determine the effect of particle size on thoron release. For coarse (5 to 10 μ) UO₂ particles, preliminary data at temperatures up to 1500°C indicate an activation energy of 96 kcal/mole and diffusion coefficients of 9.6×10^{-14} cm²/sec at 1093°C and 1.1×10^{-10} cm²/sec at 1482°C. (P. Schall)

Radiation Effects in Metallic Fuels

The literature for this period concerning fundamental effects of irradiation on metallic fuels is largely devoted to an understanding of

the formation and growth of bubbles or voids and to the diffusion and release of fission gases in uranium fuels. In one case, swelling studies, based upon formation of hydrogen and helium in lithium, are included because of the analogy to swelling of uranium fuels.

Additional reports on physical effects of irradiation and on studies of irradiation-related phenomena in uranium are reviewed. A colloquium on X-ray diffraction techniques in irradiated materials is also reviewed.

1. *Swelling and Fission-gas Diffusion.* A paper reviewing various aspects of British technology on swelling and inert-gas diffusion in irradiated uranium was presented at the Geneva Conference.⁷⁶ Included in this paper are discussions of swelling during irradiation, swelling during out-of-pile heating, emission of rare gases during and after irradiation, and a calculational analysis of swelling in uranium.

Various studies of void formation and void growth during swelling of irradiated uranium are in progress at Hanford. Results of electron and optical microscopy of voids are being interpreted in terms of a mechanical model involving the creep resistance of uranium. A fundamental study of swelling in uranium has also been started. As a first step in this study, it is planned to determine the surface tension of uranium using fine wires of high-purity metal. Studies of bubbles formed by irradiation and the effects of postirradiation heating upon these bubbles are also in progress.

An experiment to study the mechanism of swelling of fuels is in progress at Bettis. Several zirconium binary alloys containing uranium or boron are being irradiated to produce varied concentrations of fission gas or helium which are sufficient to cause yield-point behavior during mechanical testing. The activation energy for diffusion of fission-gas atoms will be calculated by measuring the yield point recovery as a function of time and temperature.

At the General Electric Research Laboratory, a study of the effects of He⁴ and H³ produced by (n, α) reaction with lithium in magnesium-lithium alloys has been reported.⁷⁷ In this study, effects analogous to those occurring in uranium and uranium-base alloys due to fission and accompanying rare gases are analyzed. It was not possible to distinguish clearly between a proposed growth mechanism where swelling is due to gas pressure in voids and one in which swell-

ing due to generation and diffusion of vacancies to gas atoms, causing annihilation of the vacancies and agglomeration of the gases. There was some evidence supporting both mechanisms. In this study, irradiations were performed on magnesium, magnesium-4 wt.% lithium, and magnesium-13 wt.% lithium alloys to integrated neutron fluxes of 10^{12} to 10^{18} nvt. Dimensional changes, electrical resistance effects, lattice parameters changes, mechanical properties, and microstructure are the bases of the study.

In connection with swelling of irradiated uranium, Hanford is studying the diffusion of xenon through uranium. Laboratory apparatus for this purpose has been built which depends upon a glow discharge to introduce xenon into one side of a uranium disk.

2. Other Effects of Irradiation and Related Studies. In an experiment at Argonne,⁷⁸ the effects of irradiation on single-crystal dimensional changes have been quantitatively evaluated giving growth values for different crystallographic directions. The deformation rates were: $G(1\ 0\ 0) = 420 \pm 20$, $G(0\ 1\ 0) = 420 \pm 20$, and $G(0\ 0\ 1) = 0 \pm 20$, where G is the logarithmic increment divided by the fission ratio. Lineage or pseudo crystals deformed in the $(0\ 1\ 0)$ direction at appreciably higher rates than did the single crystals. These data represent burn-ups of 0.1 to 0.4 total at.% and irradiation temperatures probably much lower than 150°C .

Barss, Basinski, and Nabarro⁷⁹ discuss the possible mechanisms of formation of filamentary growths observed projecting upward from the lower piece of fractured NRX uranium fuel slugs. These filaments are believed to grow rather than being drawn out by tension. The authors favor a mechanism of whisker growth involving a dislocation source which acts as a pump driven by alternating thermal stresses in the metal. Dominant factors in the mechanism are the rates of emission and diffusion of vacancies.

At Hanford, X-ray diffraction line-broadening studies are being made on uranium irradiated at 50°C . Changes in the diffraction pattern are being interpreted in terms of stacking faults in the lattice.

The problem of thermal cycling growth has been studied in Japan.⁵⁵ It was found, from internal friction measurements at low temperatures, that dislocations are formed when a uranium specimen is thermally cycled. The activation energy is around 0.5 ev. A mechanism of

unidirectional growth is proposed consisting essentially of $(1\ 3\ 0)$ $(3\ 1\ 0)$ twinning and $(0\ 1\ 0)$ $(1\ 0\ 0)$ slip in the twinned regions.

In British research⁸⁰ on uranium, the kinetics of the creep process, which become important when the temperature is raised in thermal cycling, are derived from thermal-cycling data obtained by Argonne. Further experiments to determine the internal-stress cycle and the modes of deformation during a typical cycle are described, and a quantitative account is presented of the internal strains and resulting external growth. This analysis includes a description of the processes leading to a change in growth per cycle when the heating and cooling rates are changed. The behavior of polycrystalline aggregates is interpreted also in terms of the behavior of bicrystals.

A report of a colloquium primarily on methods and techniques of X-ray diffraction analysis for various research problems associated with radiation effects has been issued by the British.⁷⁴ Several papers are included in the report. An interesting discussion of self-damage by the alpha-emitting heavy elements is included in this report.

(F. A. Rough)

References

1. Metallurgy Division Quarterly Report for April, May, and June, 1957, ANL-5790, July 1958. (Unclassified AEC report.)
2. Metallurgy Division Quarterly Report for July, August, and September, 1957, ANL-5797, October 1958. (Unclassified AEC report.)
3. P. W. Bridgman, "The Physics of High Pressures," Macmillan Company, New York, 1931, p. 161.
4. H. L. Laquer, W. E. McGee, and M. F. Kilpatrick, Elastic Constants of Uranium, *Transactions of the American Society for Metals*, 2: 771-782 (1950).
5. J. R. Bridge, C. M. Schwartz, and D. A. Vaughan, X-Ray Diffraction Determination of the Coefficients of Expansion of Alpha-Uranium, *Transactions of the American Institute of Mining and Metallurgical Engineers*, 206: 1282 (1956).
6. H. C. Rose, A Compressive Creep Test of Alpha-Uranium under Neutron Irradiation, *Journal of the Institute of Metals*, 86: 122-128 (November 1957).
7. L. Lewis, Contribution of the Jominy-Type End Quench to Metallographic Phase Identification, BRB-44, Dec. 8, 1958. (Unclassified AEC report.)

- 8.* V. W. Eldred, G. B. Greenough, and P. Leach, Fuel Element Behavior under Irradiation, A/CONF./15/P/50.
- 9.* P. Larcombe and D. Calois, Growth of Perfect Crystals in Alpha-Uranium, A/CONF./15/P/1258.
10. A. M. Holden, "Physical Metallurgy of Uranium," Addison-Wesley Publishing Company, Inc., Reading, Mass., 1958.
11. Chauncy Starr, The Case for Enriched Uranium, *Nucleonics*, 16(8): 86-90 (August 1958).
12. J. R. Menke, The Case for Natural Uranium, *Nucleonics*, 16(8): 86-90 (August 1958).
13. S. Isserow, Corrosion Behavior of Defected Fuel Elements with Uranium-2 Wt.% Zirconium Core Clad with Zircaloy-2, NMI-4364, July 1958. (Unclassified AEC report.)
14. E. L. Francis, comp., Uranium Data Manual, IGR-R/R 287, May 1958. (Unclassified British report.)
- 15.* H. Lloyd and J. Williams, The Powder Metallurgy of Uranium, A/CONF./15/P/1470.
- 16.* J. T. Waber, The Corrosion of Plutonium and Uranium, A/CONF./15/P/699.
- 17.* J. A. Stohr, M. Englander, and M. Gauthron, Fuel Elements for Pressurized Gas Reactors, A/CONF./15/P/1157.
- 18.* J. H. Kittel and S. H. Paine, Effect of Irradiation of Fuel Materials, A/CONF./15/P/1890.
19. R. W. Dayton and C. R. Tipton, Jr., Progress Relating to Civilian Applications During October, 1958, BMI-1301, Nov. 1, 1958. (Confidential AEC report.)
20. Technical Progress Report—Pressurized Water Reactor (PWR) Project for the Period August 24, 1958, to October 23, 1958, WAPD-MRP-76. (Unclassified AEC report.)
21. Bettis Technical Review, WAPD-BT-10, October 1958. (Unclassified AEC report.)
22. Bryan McPherson, The Determination of True Stress-True Strain Curves and Modulus of Elasticity of Uranium-10 Wt.% Molybdenum Alloy at Elevated Temperatures, AECU-3801, Mar. 28, 1958. (Unclassified AEC report.)
23. J. E. Gates et al., Stress-Strain Properties of Irradiated Uranium-10 Wt.% Molybdenum, BMI-APDA-638, Jan. 6, 1958. (Unclassified AEC report.)
24. G. D. Calkins et al., Symposium on Radiation Effects on Materials. Vol. 2. Effect of Heat Treatment and Burn-up on Radiation Stability of 10 Per Cent by Weight Molybdenum-Uranium Fuel Alloys, ASTM Special Technical Publication No. 220, pp. 70-83, 1958.
25. J. B. Fox et al., Studies of the Preparation of Zirconium-Clad Uranium-10 Wt.% Molybdenum Fuel Pins, BMI-APDA-644, Oct. 27, 1958. (Unclassified AEC report.)
26. C. A. Kindness, A Literature Survey of the Physical Properties of Uranium-Zirconium Alloys, KAPL-M-CAK-1, July 30, 1958. (Confidential AEC report.)
27. Atomic Energy of Canada, Ltd., 1958. (Unpublished.)
28. W. C. Thurber, Deformation Textures in Uranium-Aluminum Alloys, ORNL-2635, Nov. 20, 1958. (Unclassified AEC report.)
29. R. W. Dayton and C. R. Tipton, Jr., Progress Relating to Civilian Applications During November, 1958, BMI-1304, Dec. 1, 1958. (Unclassified AEC report.)
30. R. W. Dayton and C. R. Tipton, Jr., Progress Relating to Civilian Applications During December, 1958, BMI-1307, Jan. 1, 1959. (Confidential AEC report.)
31. W. V. Johnston, The Effect of Transients and Longer Time Anneals on Irradiated Platinum-Zirconium Alloys, KAPL-1965, Oct. 3, 1958. (Unclassified AEC report.)
32. Technical Progress Report—Pressurized Water Reactor (PWR) Project for the Period June 24, 1958 to August 23, 1958, WAPD-MRP-75. (Unclassified AEC report.)
- 33.* A. A. Bauer, S. Koss, and K. Goldman, Physical Metallurgy and Properties of Zirconium-Uranium Alloys, A/CONF./15/P/1785.
34. Semi-Annual Summary Research Report in Metallurgy for July-December, 1957, ISC-977. (Unclassified AEC report.)
35. J. J. Park and D. P. Fickle, The Uranium-Platinum System, NBS-5946, June 19, 1958. (Unclassified AEC report.)
36. H. R. Gardner and J. M. Jeffus, The Tensile Properties of Pure Plutonium, HW-57130, Aug. 6, 1958. (Unclassified AEC report.)
37. T. A. Sandenaw and R. B. Gibney, The Electrical Resistivity and Thermal Conductivity of Plutonium Metal, *Physics and Chemistry of Solids*, 8: 81-88 (July 1958).
38. S. H. Paine and F. L. Brown, "Pin-Cushion" Irradiation of Cast Uranium-Plutonium Alloy Specimens, ANL-5795, October 1958. (Unclassified AEC report.)
39. F. L. Cuthbert, "Thorium Production Technology," Addison-Wesley Publishing Company, Reading, Mass., 1958, 303 pp.
40. H. A. Wilhelm, editor, "The Metal Thorium," American Society for Metals, Cleveland, Ohio, 1958, 397 pp.
41. J. R. Murray, The Thorium-Aluminum System, AERE-M/R-2665, September 1958. (Unclassified British report.)
42. R. F. Donagala, R. P. Elliott, and W. Rostoker, The System Mercury-Thorium, *Transactions of the American Institute of Mining and Metallurgical Engineers*, 212: 393 (June 1958).

- 43.* O. Ivanov and T. Badayeva, Phase Diagrams of Certain Uranium and Thorium Systems, A/CONF./15/P/2043.
44. H. P. Roth, Metallography of Thorium, NMI-1193, June 17, 1958. (Unclassified AEC report.)
- 45.* S. K. Kantan, R. V. Raghavan, and G. S. Tendolkar, Sintering of Thorium and Thorium Oxide, A/CONF./15/P/1705.
46. J. E. Cunningham, R. J. Beaver, and R. D. Robertson, Specifications and Fabrication Procedures for APPR-1 Core II Stationary Fuel Elements, CF-58-7-72, July 15, 1958. (Unclassified AEC report.)
47. W. Weinberger, Development of Fabrication Techniques and Manufacturing Specifications for APPR Fuel Elements, SCNC-262, April 1958. (Unclassified AEC report.)
48. I. Sheinhart and J. L. Zambrow, Dispersion-Type Materials for Fuel Elements. Part I. Uranium Mononitride and Uranium Silicide Dispersion Materials, SCNC-266, June 1958. (Confidential AEC report.)
49. R. W. Dayton and C. R. Tipton, Jr., Progress Relating to Civilian Applications During September, 1958, BMI-1294, October 1958. (Unclassified AEC report.)
50. J. Williams et al., Sintering of Uranium Oxides of Composition UO_2 to U_3O_8 in Various Atmospheres, AERE-M/R-2653, August 1958. (Unclassified British report.)
51. A. H. Webster and N. F. H. Bright, The Effects of Furnace Atmospheres on the Sintering Behavior of Uranium Dioxide, April 4, 1958. Department of Mines and Technical Surveys, Ottawa, Canada.
52. Ceramic Fuels—Properties and Technology, *Nuclear Engineering*, 3(29): 327 (August 1958).
- 53.* J. Gatter et al., The Manufacture of PWR Blanket Fuel Elements Containing High-density Uranium Dioxide, A/CONF./15/P/2380.
- 54.* P. Murray and J. Williams, Ceramic and Cermet Fuels, A/CONF./15/P/318.
- 55.* R. R. Hasiguti, Fundamental Researches on Physical Metallurgy of Nuclear Fuels in Japan, A/CONF./15/P/1324.
56. J. C. Danko, Uranium Oxide Experience, *Nucleonics*, 16(8): 90 (August 1958).
57. A. R. Hall, R. Scott, and J. Williams, The Plastic Deformation of Uranium Oxides Above 800°C, AERE-M/R-2648, August 1958. (Unclassified British report.)
58. S. Aronson and J. Belle, Nonstoichiometry in Uranium Dioxide, *Journal of Chemical Physics*, 29: 151 (July 1958).
- 59.* J. M. Brabers, Electrical Properties of Uranium Oxides, A/CONF./15/P/1474.
60. T. C. Ehlert and J. L. Margrave, Melting Point and Spectral Emissivity of Uranium Dioxide, *Journal of American Ceramic Society*, 41(8): 330 (August 1958).
- 61.* H. R. Hoesksta and S. Siegel, The Uranium-Oxygen System: U_3O_8 - UO_3 , A/CONF./15/P/1548.
62. A. F. Andresen, The Structure of U_3O_8 Determined by Neutron Diffraction, *Acta Crystallographica*, 11(9): 612 (1958).
- 63.* B. Chodura and J. Maly, A Contribution to the Study of the Structure of U_3O_8 , A/CONF./15/P/2099.
- 64.* P. P. Budnikov, S. G. Tresvyaksky, and V. I. Kushakovsky, Binary Phase Diagrams: UO_2 - Al_2O_3 , UO_2 - BeO , UO_2 - MgO , A/CONF./15/P/2193.
65. Technical Progress Report—Pressurized Water Reactor (PWR) Project for the Period October 24, 1958, to December 23, 1958, WAPD-MRP-77. (Unclassified AEC report.)
- 66.* A. Houyvet et al., Hot Pressing of U-UC Cermets and Stoichiometric UC, A/CONF./15/P/1162.
67. A. C. Secrest, Jr., E. L. Foster, and R. F. Dickerson, Preparation and Properties of Uranium Monocarbide Castings, BMI-1309, Jan. 2, 1959. (Unclassified AEC report.)
68. R. A. J. Sambell and J. Williams, The Uranium Monocarbide/Uranium Mononitride System, AERE-M/R 2654, September 1958. (Unclassified British report.)
- 69.* A. Boettcher and G. Schneider, About Some Qualities of Uranium Monocarbide, A/CONF./15/P/964.
70. Marius Picon and Jean Flahaut, The Sulfides of Uranium, *Bulletin de la société chimique de France*, 6: 772-780 (June 1958).
71. L. E. J. Roberts, A. J. Walker, and V. J. Wheeler, The Oxides of Uranium, Part IX. The Decomposition of Carbon Monoxide on Uranium and Thorium Dioxides, *Journal of Chemical Society*, 2472-2481 (July 1958).
72. Warren E. Berry and Robert S. Peoples, The Corrosion Behavior of Zirconium-Uranium Alloys in High-temperature Water, *Corrosion*, 14(9): 414t-418t (September 1958).
73. T. K. Bierlein and B. Mastel, Fractography of Some Reactor Fuel Materials, HW-57207, Aug. 15, 1958. (Unclassified AEC report.)
74. J. Thewlis, Irradiation Damage Papers Presented at the First Colloquium of the UKAEA Diffraction Analysis Conference held at AWRE, AERE M&C/R 2751, November 1958. (Unclassified British report.)
- 75.* George A. Cowan and Charles J. Osth, Diffusion of Fission Products at High Temperatures from Refractory Materials, A/CONF./15/P/613.

76. R. S. Barnes et al., Swelling and Inert Gas Diffusion in Irradiated Uranium, A/CONF./15/P/81.
- 77.* D. W. Lillie, Effects of Pseudo Fission Gases in Metallic Lattices, A/CONF./15/P/1866.
78. S. H. Paine and J. H. Kittel, Preliminary Analysis of Fission-Induced Dimensional Changes in Single Crystals of Uranium, ANL-5676, October 1958. (Unclassified AEC report.)
79. W. M. Barss, Z. S. Basinski, and F. R. N. Nabarro, Filamentary Growth in Irradiated Uranium, *Canadian Journal of Physics*, 36: 980-983 (1958).
80. S. F. Pugh, The Mechanism of Growth of Uranium on Thermal Cycling in the Alpha Range, *Journal of the Institute of Metals*, 86: 497-503 (August 1958).

*Second United Nations International Conference on the Peaceful Uses of Atomic Energy, Geneva, September 1958. (Individual papers available from the Office of Technical Services, Dept. of Commerce, Washington 25, D. C. Bound volumes of papers will be available from United Nations, Office of Public Information, New York.)

Graphite

British investigators¹ have reported dimensional changes and fission-product release from graphite fuel elements containing fuel in the form of metallic uranium, UO_2 , and UC_2 . The fueled bodies were tubes 0.4 in. long and 0.45 in. in outside diameter, with 0.125-in.-thick walls. Each sample contained 6 g of fully enriched uranium uniformly dispersed in the graphite. Average particle size of the fuel was 20 to 30 μ . These samples were irradiated to a burn-up of 0.5 per cent of the uranium atoms present.

Measurements of dimensional changes indicated a decrease in outside diameter of 0.6 per cent and an increase in length up to 1.1 per cent for samples containing metallic uranium or uranium dicarbide fuel. For samples containing uranium oxide fuel, an average diameter decrease of 1.9 per cent and length increase of 3.7 per cent were observed.

The release of fission-product gas, expressed as a percentage of that formed, was 4 to 5 per cent for UC_2 samples and 8 to 12 per cent for samples containing uranium metal. Data on samples containing UO_2 were not obtained. Measurements of the release of cesium and strontium indicated that less than 1 per cent of the total amount formed escaped from the fuel cores.

Studies have been conducted at Los Alamos on diffusion of fission products from fueled graphite.² Delayed neutron precursor elements diffuse at rates consistent with measured rates of bromine and iodine. Where stable carbides are known to be formed, the fission products do not diffuse (e.g., zirconium and molybdenum). Rapid diffusion of elements having low melting and boiling points, such as cadmium and tin, has been noted. Very rapid diffusion of silver from graphite may be related to its low melting point plus its small atomic radius.

The British³ report studies of the compatibility of liquid sodium with graphite. It was concluded that these materials are not compatible because of sodium penetration into the pores of the graphite at temperatures above 260°C and because of chemical interaction at temperatures above

120°C. The chemical reaction results in a lamellar compound of the ideal formula C_{64}Na . The compound formation involves a 5 per cent increase in the average interplanar spacing of the graphite crystallites. This, in turn, results in dilation and, frequently, severe cracking of the graphite body. The magnitude of the dilation may be predicted from the thermal expansion of the graphite. A similar treatment of the interactions between sodium and graphite was presented by Brookhaven⁴ at the French-American Conference on Graphite Reactors held Nov. 12 to 15, 1957. (W. C. Riley)

Beryllium Metal and Alloys

A Lockheed report⁵ describes preliminary results of electron bombardment, melting, and casting of 3-in.-diameter beryllium ingots. On the basis of data obtained for fifteen ingots, beryllium melted by electron bombardment shows finer grain size in the cast structure and better machinability than induction-melted, vacuum-cast material. However, no improvement in tensile strength or elongation was noted, although a slight decrease in oxygen content was effected.

Russian work on the centrifugal casting of beryllium tubular shapes is discussed in a Geneva Conference paper.⁶ Melting was done in a vacuum of 2 μ , but an argon atmosphere was introduced before casting. The mold materials were graphite and steel coated with BeO . Rotation speed was not given, but wall thicknesses of 3 mm were obtained. The density of the cast material was 1.84 g/cm³. The mechanical properties in the direction of the tube axis were given as follows:

	Tensile strength, psi	Elongation, %
As cast	22,800	0.3
As cast and extruded*	37,200	3.3-9.8

*The extrusion conditions were as follows: temperature, 500°C; reduction, 70 to 80 per cent; pressure, 8 tons/cm²; lubricant, colloidal graphite.

Other Russian workers⁷ claim to have produced 99.98 per cent pure beryllium metal by vacuum distillation. The authors state that it is necessary to maintain the condensation surface at a rather high temperature in order to achieve success. Earlier attempts at purification of beryllium by distillation have been consistently disappointing.

The pressureless sintering of beryllium powder is described in a British paper⁸ presented at the Geneva Conference. Loose powders (bulk density, $\approx 0.90 \text{ g/cm}^3$) can be sintered into solid or hollow shapes with a density of 1.76 to 1.81 g/cm^3 by a 6-hr sintering treatment at 1200 to 1220°C in vacuum. Graphite molds are used. Powder size is -200 mesh, and, in order to obtain successful sintering, a critical particle-size distribution is required. The product is reported to have random orientation, fine-grain size, good machinability, and good mechanical properties and is fusion-weldable with an argon shielded arc. The process shows promise for fabrication of fuel cans.

Workers at Nuclear Metals⁹ have redetermined the solid solubilities of iron and nickel in beryllium using X-ray absorption measurements on beryllium-beryllium alloy diffusion couples. The results of their determinations are shown in Fig. 3 for the beryllium-iron system and in Fig. 4 for the beryllium-nickel system. Their results for the beryllium-nickel system are at considerable variance with previous work. The eutectoid reaction at 1065°C and 36 wt. % nickel was not detected by earlier investigators.

A fundamental investigation of fracture in beryllium¹⁰ is also being conducted. An attempt will be made to determine the interaction of dislocation and impurity networks and their effect on the critical stresses for slip and fracture of both high-purity Pechiney flake beryllium and of a lower purity grade. Techniques to be employed are automicroradiography, microradiography, fractography, etch-pit studies, electrical-resistivity measurements, and resolved-shear-stress measurements. Initial microradiography experiments show impurity networks clearly in less pure material. These networks were absent in the Pechiney beryllium.

The texture of hot- and warm-extruded beryllium rods and tubes has been studied by British workers.¹¹ The extrusion temperature was found to have little effect on the texture, but the extrusion reduction governed which of two textures was developed. For low reductions (<12:1) basal

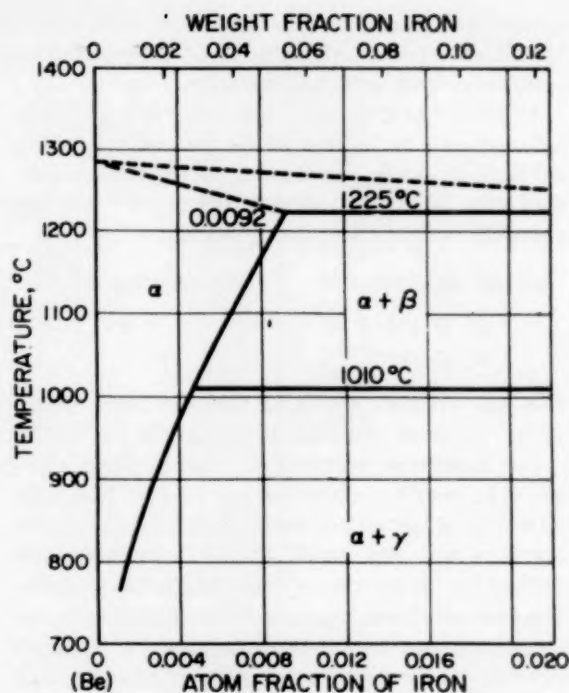


Figure 3—Solid solubility of iron in beryllium. Data taken from reference 9.

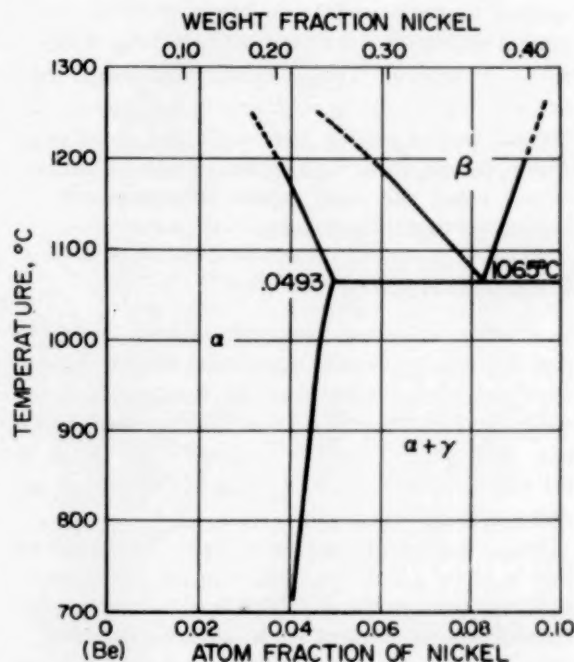


Figure 4—Portion of the beryllium-nickel equilibrium diagram. Data taken from reference 9.

planes are parallel to the surface of the tube; for greater reductions, the same is true, but the planes are concentrated radially.

Work at Chalk River¹² indicates that neutron-induced gas formation in beryllium will not be serious, at least up to 600°C. Beryllium, irradiated with an integrated fast flux of 10^{22} nvt, was annealed with the following results:

Annealing treatment	Density decrease, %
1 hr at 600°C	0.8
1 hr at 995°C	20

The gas formation was 23 cm³ per cubic centimeter of beryllium and consisted chiefly of He⁴.

The following referenced Geneva papers relating to beryllium are worthy of note. The compatibility of beryllium with other metals used in reactors was discussed by the British;¹³ a new method for determining analytically small quantities of beryllium using 8-hydroxyquinoline as a reagent was reported by Japanese workers;¹⁴ and the fabrication technology of beryllia and beryllium at Harwell has been described in another British paper.¹⁵ (A. J. Griest)

Solid Hydrides

Although research is continuing on the hydrides of pure metals, a large portion of the recent effort is concerned with the properties of alloy hydrides. These latter materials give promise of providing solutions to many problems encountered with the pure hydrides. A bibliography compiled at Oak Ridge¹⁶ lists 517 references from the AEC report literature on the subject of metal hydrides.

Zirconium Hydride

A linear relation between changes in length and specific volume of zirconium with hydrogen absorption was observed by Espagno and his associates.¹⁷ They found that $\Delta L/L_0$ reached 4.4 per cent at 150 cm³ of hydrogen per gram of zirconium and that $\Delta V/V_0$ was 12 per cent at the same hydrogen content.

Irradiation experiments at Bettis¹⁸ have shown that normal Zircaloy-2 picks up only 44 ppm of hydrogen compared with 2900 ppm for the nickel-diffusion-bonded alloy (total neutron flux 6.53×10^{20} nvt). Increasing the nickel content was found to increase the hydrogen absorption, whereas an oxide film on the zirconium decreased it. Beta-

quenched samples took up less hydrogen than alpha-annealed specimens. A study of the redistribution of hydrogen in an isothermal tensile stress gradient has shown a significant concentration increase at the point of maximum stress.

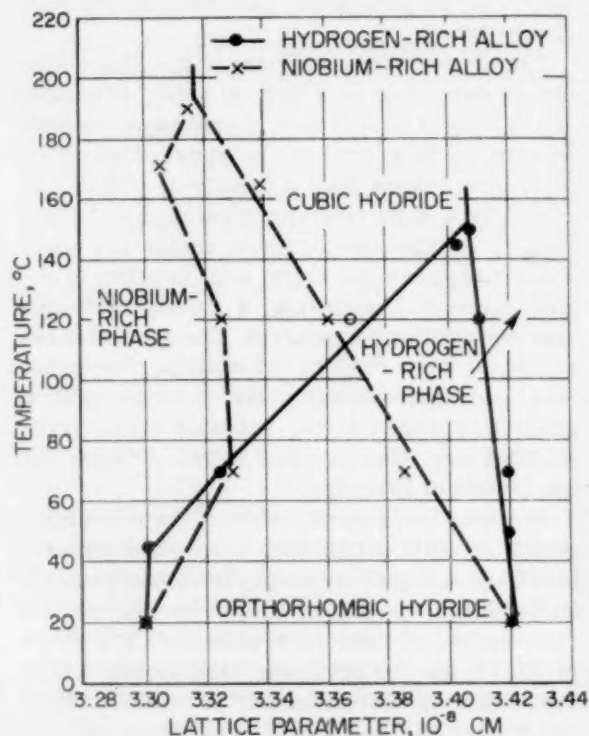


Figure 5—Variations of lattice parameters in two-phase field of the niobium-hydrogen system. Data taken from reference 20.

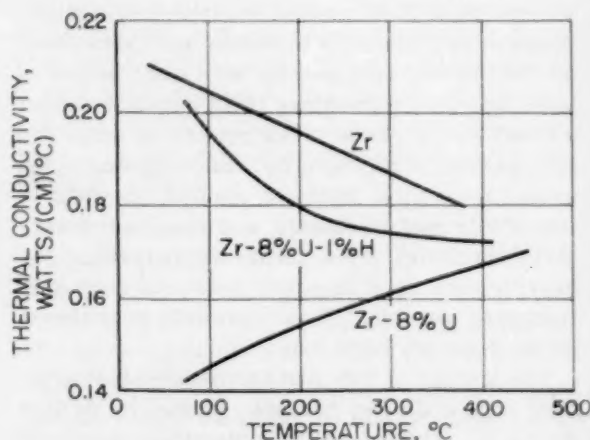


Figure 6—Thermal conductivities of zirconium alloys. Data taken from reference 21.

Table II-1 PHASE BOUNDARIES IN THE ZIRCONIUM-25 WT.% URANIUM ALLOY HYDRIDE SYSTEM*

Temperature, °C	Phase boundaries							
	1		2		3		4	
	Hydrogen absorption, cm ³ /g	Pressure, cm of Hg	Hydrogen absorption, cm ³ /g	Pressure, cm of Hg	Hydrogen absorption, cm ³ /g	Pressure, cm of Hg	Hydrogen absorption, cm ³ /g	Pressure, cm of Hg
601†	30.0	0.059	None	None	None	None	123.2	0.059
627	31.2	0.103	55.9	0.103	65.0	0.122	123.8	0.127
650	31.0	0.161	57.7	0.164	72.6	0.235	127.3	0.250
676	31.6	0.273	57.5	0.301	73.5	0.475	128.4	0.510
690	35.0	0.395	58.8	0.398	77.3	0.670	127.9	0.695
710	39.6	0.55	62.7	0.59	86.1	1.24	128.8	1.30
716	34.3	0.634	56.1	0.634	84.5	1.48	129.6	1.52
730	33.9	0.84	53.7	0.84	84.3	2.19	129.6	2.26
748	36.7	1.06	57.4	1.20	87.2	3.37	129.2	3.50
776	36.2	1.84	50.8	1.84	88.3	6.70	129.8	6.75
803	36.4	2.90	46.9	2.90	89.8	12.9	130.2	13.25

*Data taken from references 22 through 24.

†Only two phase boundaries detected at this temperature.

Cerium Hydride

The hydriding of cerium up to a composition of $\text{CeH}_{3.15}$ has been reported by Mikheyva and Kost.¹⁹

Niobium Hydride

The X-ray diffraction patterns of the niobium-hydrogen system in the temperature range 50 to 250°C were observed by Wainwright.²⁰ He found that (1) the single-phase orthorhombic structure at room temperature changes to a cubic structure above 100°C, (2) alloys in the two-phase field at room temperature show both structures, and (3) beyond about 250°C there is a continuous body-centered cubic phase across the niobium-hydrogen system. Figure 5 shows the variation of lattice parameters with temperature in the two-phase field.

Alloy Hydrides

Various properties of a zirconium-8 wt.% uranium alloy were examined at General Atomics.²¹ Difficulties were encountered with cracking and with concentration of the uranium in beads on the surface. After the zirconium-8 wt.% alloy was hydrided to 1 wt.% hydrogen, its electrical resistivity was found to be 53 $\mu\text{ohm-cm}$, Young's modulus was 14×10^6 psi, and ultimate tensile strength was about 30,000 psi. No physical deterioration or loss of hydrogen was noted after irradiation at 10^{13} neutrons/cm² sec to uranium atom burn-ups of 1.5 and

2.5 per cent. The thermal conductivity was determined as a function of temperature; a comparison with the alloy before hydriding and with pure zirconium is given in Fig. 6.

Hydrogen-absorption isotherms have been determined at Battelle²²⁻²⁴ for the zirconium-25 wt.% uranium alloy system. The values corresponding to the various phase boundaries are given in Table II-1. (H. H. Krause)

References

1. J. B. Sayers et al., Atomic Energy Research Establishment, October 1957. (Unpublished.)
2. G. A. Cowan and C. J. Orth, Diffusion of Fission Products at High Temperatures from Refractory Matrices, A/CONF./15/P/613.
3. R. C. Asher, The Chemical and Physical Interaction of Sodium and Graphite, AERE-CE/R-2618, August 1958. (Unclassified British report.)
4. S. C. Carniglia, Interactions of Graphite with Liquid Sodium, BNL-489, September 1958. (Unclassified AEC report.)
5. T. Sumsion and C. O. Matthews, Electron Bombardment Melting and Casting of Beryllium, LMSD-48330, Nov. 7, 1958. (Unclassified.)
6. V. M. Shmeley, Melting and Casting of Beryllium, A/CONF./15/P/2048.
7. K. D. Sinelkov et al., Refining Beryllium and Other Metals by Condensation on Heated Surfaces, A/CONF./15/P/2051.
8. T. Barrett, G. C. Ellis, and R. A. Knight, Pressureless Sintered Beryllium Powder, A/CONF./15/P/320.
9. S. H. Gelles, R. E. Ogilvie, and A. R. Kaufmann, The Solid Solubilities of Iron and Nickel in Beryl-

- lium, NMI-1207, July 29, 1958. (Unclassified AEC report.)
10. S. H. Gelles and E. J. Rapperport, Quarterly Progress Report to the AEC Research Division for the Period July 1, 1958, through September 30, 1958, NMI-1209, Nov. 14, 1958. (Unclassified AEC report.)
 11. N. A. Hill and J. Williams, Textures in Hot- and Warm-extruded Rods and Tubes, AERE-M/R-2652, September 1958. (Unclassified British report.)
 12. C. E. Ells, The Swelling of Beryllium from Neutron Induced Gases, GRMet-809, November 1958. (Unclassified Canadian report.)
 - 13.* G. A. Beach, A. G. Knapton, and K. B. C. West, Compatibility of Beryllium with Other Metals Used in Reactors, A/CONF./15/P/24.
 - 14.* Kenji Motojima, New Analytical Methods of Beryllium, A/CONF./15/P/1325.
 - 15.* D. T. Livey and J. Williams, Fabrication Technology of Beryllia and Beryllium, A/CONF./15/P/319.
 16. W. E. Bost, U. S. Atomic Energy Commission, October 1958. (Unpublished.)
 17. Lucien Espagno, Pierre Azou, and Paul Bastien, Variations in Length and Density Accompanying the Hydriding of Zirconium, *Comptes rendus*, 247: 83-86 (July 7, 1958).
 18. Technical Progress Report — Pressurized Water Reactor (PWR) Project, for Period June 24, 1958, to August 23, 1958, WAPD-MRP-75, Aug. 23, 1958. (Unclassified AEC report.)
 19. V. I. Mikheyva and M. Ye. Kost, Hydrides of Cerium, *Zhurnal Neorganicheskoi Khimii*, 3: 260-268 (February 1958).
 20. C. Wainwright, The Niobium-Hydrogen System, *Journal of the Institute of Metals*, 86: 68-69 (July 1958).
 - 21.* U. Merten et al., The Preparation and Properties of Zr-U-H Alloys, A/CONF./15/P/789.
 22. R. W. Dayton and C. R. Tipton, Jr., Progress Relating to Civilian Applications During October 1958, BMI-1301, Nov. 1, 1958. (Confidential AEC report.)
 23. R. W. Dayton and C. R. Tipton, Jr., Progress Relating to Civilian Applications During November 1958, BMI-1304, Dec. 1, 1958. (Unclassified AEC report.)
 24. R. W. Dayton and C. R. Tipton, Jr., Progress Relating to Civilian Applications During December 1958, BMI-1307, Jan. 1, 1959. (Confidential AEC report.)

*Second United Nations International Conference on the Peaceful Uses of Atomic Energy, Geneva, September 1958. (Individual papers available from the Office of Technical Services, Dept. of Commerce, Washington 25, D. C. Bound volumes of papers will be available from United Nations, Office of Public Information, New York.)

Control-rod Alloys

Rare-earth Alloys

The Bureau of Mines¹ has been investigating zirconium-dysprosium and zirconium-erbium alloys. Alloys containing up to 11 wt.% dysprosium have been cold worked extensively. Between 11 and 37 wt.% dysprosium, ductility decreased, and the alloys had to be annealed between cold reductions. Above 37 wt.% dysprosium, the alloys had to be sheathed in stainless-steel tubing and hot rolled at 850 to 875°C. Zirconium-erbium alloys containing up to 5 wt.% erbium could be extensively cold worked, while those with up to 50 wt.% erbium had to be hot rolled in stainless-steel sheaths at 850 to 875°C. No attempts to fabricate higher-erbium alloys have been made. A zirconium-1 wt.% dysprosium alloy, corrosion tested in 680°F water, had a weight gain of 10 mg/cm² after 14 days of exposure. Specimens with more dysprosium exhibited severe white oxide surfaces. In 750°F steam, all specimens disintegrated before 7 days of test. Zirconium-2 and -4 wt.% erbium alloys had weight gains of 63 mg/dm² and 266 mg/dm², respectively, after 14 days in 680°F water. Specimens with 6, 8, and 9 wt.% erbium had a loose, flaky coating of white oxide.

Other Alloys

Flash butt welding of wrought silver-15 wt.% indium-5 wt.% cadmium alloy to Zircaloy-2 control-rod extensions results in clean, sound joints with the strength of the wrought material.² However, the same type joints with a powder alloy showed low ultimate strength at 550°F and failed by distinctly brittle fracture. Attempts are being made to improve these joints.

(V. W. Storhok)

Burnable-poison Dispersions

Bettis is investigating methods for fabricating lumped-burnable-poison elements.^{3,4} Satisfac-

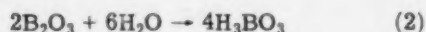
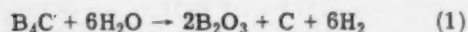
tory dispersions of Fe₂B¹⁰ in iron have been fabricated with Fe₂B¹⁰ particle-size ranges of 50 to 75, 75 to 100, 100 to 150, and 150 to 250 μ. Up to 2 wt.%, B¹⁰ was incorporated in the iron matrix, which was clad with Zircaloy-2. Little or no interaction could be detected between the boride and matrix. Dispersions could not be fabricated when either ferritic or austenitic stainless steel was used as a matrix. Corrosion data indicated that best results could be obtained with the small particle size. For example, the 150 to 250-μ dispersion gained 5.0 mg/cm², compared with a weight gain of 0.2 mg/cm² after 49 days of exposure to 680°F water for the finer-particle-size dispersions. Only the 50 to 75-μ particle-size dispersion is being considered for irradiation testing.

Burnable-poison plates containing compartmented B₄C pellets have been clad with Zircaloy-2 by copper diffusion bonding. It was necessary to spray coat the B₄C pellets with graphite to prevent a Cu-Zr-B₄C reaction during bonding. Defected compartments showed no swelling after 49 days of exposure to 680°F water. A third type of burnable-poison element containing alloys of 1 or 2 wt.% B¹⁰ in iron, ferritic stainless, or austenitic stainless steels has been roll clad with Zircaloy-2 and core-cladding barrier materials at 1550°F, using a 6 to 1 reduction ratio.

Postirradiation corrosion data have been obtained⁵ for specimens of 5 wt.% B₄C in Zircaloy-2, 23 and 30 wt.% B₄C in Al₂O₃, and B₄C irradiated to approximately 60 at.% B¹⁰ depletion. After 24 hr in 650°F deionized, deoxygenated water, the ceramic specimens disintegrated, whereas the B₄C-Zircaloy-2 specimens retained their integrity. No dimensional change was noted in the B₄C-Zircaloy-2 specimens, but there was some weight loss in irradiated specimens and some weight gain in unirradiated control specimens. Postirradiation annealing of similar specimens is in progress at temperatures from 450 to 750°C.

Because B₄C is sometimes used as a burnable-poison or control material in systems which are water cooled, Knolls is conducting a study of the

chemical reaction of B_4C and water.⁶ A strong affinity has been found to exist, and it was found difficult to fabricate materials containing B_4C and obtain a finished product free of water. The reaction is represented by the following equations:



The free energy of reaction for reaction (1) varies from -233.1 at $25^\circ C$ to -199.9 at $727^\circ C$. The units are not stated but are probably in calories per mole B_4C . Additional data are reported, but the rate equation has not been definitely established.

Annealing studies⁷ were conducted at Knolls on two specimens: (1) 0.35 wt.% B^{10} dispersed in zirconium, irradiated to 37 at.% B^{10} burn-up, and (2) 1.2 wt.% natural boron dispersed in zirconium, irradiated to 99 at.% B^{10} burn-up. These studies show changes in resistivity, volume, and thermal conductivity. Specimens were annealed 24 hr at $50^\circ C$ intervals up to a maximum of $750^\circ C$. Thermal-conductivity measurements showed an 18.1 per cent decrease for Specimen (1) and a 14 per cent decrease for Specimen (2) after irradiation. Specimen (1) recovered to show a 15.1 per cent decrease after 24 hr at $400^\circ C$ but showed a decrease of 24.7 per cent after 24 hr at $750^\circ C$. Specimen (2) recovered to show a 10.8 per cent decrease after 24 hr at $350^\circ C$ but had a decrease of 25.5 per cent after 24 hr at $750^\circ C$. A minimum was shown in the data for electrical resistivity, with values increasing from approximately $70 \mu\text{ohm-cm}$ after annealing at $400^\circ C$ to 80 to $85 \mu\text{ohm-cm}$ after annealing at $750^\circ C$. Volume changes of up to 3 per cent increase for Specimen (1) and 1 per cent decrease for Specimen (2) were reported for samples annealed at $750^\circ C$.

At Oak Ridge, methods of incorporating boron in APPR fuel elements have included a study of

B_4C , BN, ZrB_2 , and 0.25 at.% boron master-alloy additions to a stainless-steel matrix. Compacts containing approximately 0.11 wt.% boron were sintered in hydrogen, roll clad at 1100, 1150, and $1200^\circ C$ and annealed 1, 2, and 3 hr at their respective fabrication temperatures. The B_4C completely reacted with the matrix to form complex carbides and borides after two 1-hr anneals at $1150^\circ C$. A reaction precipitate randomly distributed in the stainless-steel matrix was noted for all three compounds. An increase in temperature and time appears to increase migration of the precipitate. No precipitate was noted during fabrication of the plates containing the master alloy, but large boron losses occurred during sintering in hydrogen. It is suggested that boron losses can be minimized by sintering either *in vacuo* or in an inert atmosphere. (G. W. Cunningham)

References

1. H. Kato, R. A. Beall, H. P. Holmes, and G. C. Ware, U. S. Bureau of Mines, Oct. 15, 1958. (Unpublished.)
2. I. Cohen, Rod Material Program—PWR Alternate Control, WAPD-PWR-PMM-2756, Sept. 15, 1958. (Unclassified AEC report.)
3. Technical Progress Report—Pressurized Water Reactor (PWR) Project for the Period August 24, 1958, to October 23, 1958, WAPD-MRP-76. (Unclassified AEC report.)
4. Technical Progress Report—Pressurized Water Reactor (PWR) Project for the Period June 24, 1958, to August 23, 1958, WAPD-MRP-75. (Unclassified AEC report.)
5. Reactor Technology Report Number 6, October 1958, KAPL-2000-3, Oct. 20, 1958. (Unclassified AEC report.)
6. J. L. Jellison, Statistical Method for Particle Size and Distribution Measurement of Boron Carbide Particles Dispersed in Zircaloy, KAPL-M-JLJ-1, Sept. 9, 1958. (Unclassified AEC report.)
7. W. V. Johnston and J. E. Noonan, Annealing of Irradiated Boron-Containing Alloys and Dispersions, KAPL-M-WVJ-4, May 12, 1958. (Unclassified AEC report.)

Corrosion

Zirconium

The occurrence of stringer type corrosion in zirconium alloys has been responsible for the intensified effort to develop a postfabrication heat-treatment which will improve the corrosion behavior of Zircaloy-2 and -3. It has been demonstrated that one of the controlling factors in the corrosion resistance of Zircaloy-2 is the distribution of the alloy and impurity elements. Partitioning of the various elements can occur during heating in the alpha-plus-beta phase region because of the differential solubility of the elements in alpha and beta zirconium.

Studies at Bettis¹ have indicated that, in order to maintain good corrosion resistance in Zircaloy-2, any heat-treatment in the beta or alpha-plus-beta region must be followed by a rapid cooling rate of, e. g., 90°F per minute or higher.

Work at Knolls² has dealt with the corrosion films produced on Zircaloy-2 during exposure to high-temperature water. It has been postulated that the corrosion film formed on Zircaloy-2 is initially continuous and that at "breakaway" the film ruptures. Capacitance measurements of the oxide film, however, indicate that the film is porous during all stages of corrosion in high-temperature water. In an effort to determine the nature of the porosity, samples of Zircaloy-2 that had been corroded for 30, 90, 179, and 429 days in 680°F water were examined under an electron microscope. Cracks were detected in the oxide films of all specimens. Furthermore, no correlation was found between the pattern or frequency of cracks and exposure time. This evidence suggests that further studies are needed to pin down the mechanism of attack in high-temperature water.

Work at Case Institute of Technology³ on the scaling of zirconium at elevated temperatures has indicated that the growth mechanism is different in air and in oxygen. In air, the growth appears to be associated with the presence of

ZrN at the metal surface. It is believed that the conversion of the ZrN to ZrO₂ at elevated temperatures gives rise to stresses which distort the metal surface. Metallographic studies reveal that, when growth begins in pure oxygen, the metal-oxide interface becomes jagged and irregular. The implication is that growth takes place by a finger type penetration of the oxide, which results in increased dimensions. Experiments are presently under way to check this theory.

The behavior of zirconium and its alloys in CO₂ atmospheres at elevated temperatures has been the subject of investigation both in the United Kingdom⁴ and at Hanford.⁵ The findings are in reasonably good agreement. Scaling rates for zirconium in CO₂ at 500°C are of the order of 0.38 mil for 1500 hr of exposure. Binary and ternary additions of molybdenum, tungsten, and copper result in some improvement. It is concluded, however, that outstanding improvement is not likely and that there is little or no hope for zirconium in CO₂ at temperatures in excess of 500°C.

The effect of various pickling procedures on the corrosion behavior of Zircaloy has been investigated at Bettis.⁶ Rinsing Zircaloy in a HNO₃ solution after etching in the standard HNO₃-HF bath was found to be beneficial. On the other hand, rinsing as-pickled Zircaloy in H₂SO₄ solutions produced deleterious effects on corrosion behavior.

Work at Knolls⁷ has dealt with the effect of HNO₃-HF pickling solution retained in a crevice. In general, it was found that the amount of corrosion of Zircaloy in high-temperature water and steam was proportional to the amount of fluoride ion retained in the crevice. In each case, however, a protective film formed under the white corrosion product, and rates returned to normal after two to four weeks of exposure.

(W. K. Boyd)

Aluminum

Jet-impingement corrosion of aluminum is being studied at Hanford to determine whether

the X-8001 aluminum alloy is more susceptible to erosion corrosion than the 1245 alloy. Experiments were run using a 0.009-in.-diameter nozzle. Specimens were placed $\frac{1}{4}$ in. in front of the nozzle outlet. When the jet velocity was 222 fps, both materials exhibited equally high penetration rates. However, at a 122-fps jet velocity in tap water, penetration rates for the X-8001 alloy were twice those of the 1245 material, namely, 4.75 and 2.05 mils/4 hr, respectively. With a further reduction in jet velocity to 89 fps, the 1245 alloy was only roughened, whereas the X-8001 alloy still evinced well-defined areas of penetration. No significant differences in penetration attributable to velocity were observed in distilled water.

(W. K. Boyd)

The French⁸ have studied a series of aluminum-0.4 to 2.2 wt.% iron-0.2 to 2.2 wt.% nickel alloys and found several alloys with adequate corrosion resistance for service for 3000 hr in 660°F water. They also observed that prior cold working appeared to diminish the magnitude of corrosion in aluminum-base alloys.

Chalk River⁹ workers, in continued efforts to understand the corrosion behavior of aluminum alloys in simulated reactor environments, completed investigations of the behavior in conjunction with the use of what might be considered sacrificial anode protection. With this scheme, a plate of aluminum alloy is placed upstream from the specimen under investigation. This sacrificial plate is attacked first, resulting in a solution which is saturated with corrosion product by the time it reaches the specimen. The resulting inhibition is effective. Corrosion rates on specimens investigated in 500°F water flowing at 20 fps are about 8 mils/yr. Pretreating the specimen in static 570°F water appears promising, but complete data are not yet available. An electroless nickel plate, 0.2 mil thick, has afforded protection to aluminum specimens for 500 hr in a loop test.

(E. S. Bartlett)

Magnesium-base Alloys

For service in air, magnesium is limited to temperatures below about 660°F. However, the French¹⁰ have found that, in the presence of small amounts of fluoride ion, inhibition of oxidation is appreciable, and maximum operating temperatures may be increased to about 930°F. It was also noted that the addition of a few per cent of water vapor to CO₂ atmospheres does not cause the medium to be particularly corrosive to mag-

nesium. This suggests a possible method of increasing the power yield in CO₂-cooled reactors through the use of moisture-laden cooling atmospheres. French workers have also observed decreased corrosion rates in magnesium alloys containing about 0.7 per cent zirconium.

Although magnesium and its alloys are generally considered unsuited for use as cladding materials in aqueous reactors, the desirable metallurgical and nuclear properties have warranted continued investigation of alloys toward this end. Argonne¹¹ workers, aiming at a maximum permissible corrosion rate of 1.5 mils/day in 300°F water, found no commercial or experimental alloys to be acceptable. However, inhibition with 50 to 100 ppm of PbF₂ reduces the corrosion rates of selected alloys to about 0.5 mil/day. Work is continuing to define the characteristics of inhibited systems.

The importance of cold-water corrosion resistance of magnesium has been pointed out by McIntosh.¹² Spent magnesium-clad fuel elements from the Calder Hall reactors are cooled in a pool of water. In this environment, failure by pitting is a hazard, as contamination would result. It has been observed that raising the pH of the pool to a minimum of 11 by the addition of caustic soda retards pitting corrosion.

Work at Hanford has indicated another potential maleffect which may be attributable to water corrosion. Magnesium-clad fuel rods exposed to monoisopropylbiphenyl (MIPB) at 1000 psi and 680 to 790°F for 175 and 24 hr, respectively, resulted in 14 and 29 ppm hydrogen pickup in the uranium core. Calculated hydrogen pressures for permeation of the cladding in the amounts observed are excessively high, and not probable if the environment is pure MIPB. On the other hand, if traces of water were present in the environment, it was calculated that the release and permeation of atomic hydrogen resulting from water corrosion to the extent of 1 mg/cm² of the magnesium cladding would account for the hydrogen pickups observed in the core material.

(E. S. Bartlett)

High-temperature Alloys

Studies at Knolls on the resistance of Inconel to hydrogenated, aerated, and ammoniated water at 600°F have been summarized² after eight-week exposure periods. Steady-state corrosion rates of about 0.04 mil/yr in these media are reported. A preexposure heat-treatment of 1200°F

appears to result in improved resistance to corrosion, although reasons for this behavior were not postulated. The corrosion product formed is loose and may result in contamination of the environment. Under the application of stress in aerated water (600°F), pitting was observed, with pit depths of 1 to 2 mils being attained in four weeks. No stress-corrosion cracking was reported.

The first year's work at the Bureau of Standards on evaluating the oxidation behavior, under stress, of 10 alloys has been summarized.¹³ The compositions of the alloys studied, along with activation energies and rate constants for the oxidation process, are presented in Table IV-1.

stainless-steel alloys. Diffusion voids, resulting from preferential oxidation of baser constituents at the surface, were observed generally, and their formation was accelerated by increasing the temperature and stress levels. Internal grain-boundary cracking was observed only in the Nichrome V type alloys at 1800 and 2000°F but not at the 2100 to 2000°F stressed exposures.

Thermal cycling under stress is very detrimental to the mechanical endurance of Inco 702, R235, and the iron-chromium-aluminum alloys. In general, the effect of thermal cycling on oxidation penetration was minor.

In work at Battelle¹⁴ on the oxidation resistance of iron-chromium-aluminum alloys, the

Table IV-1 OXIDATION KINETICS FOR SELECTED HIGH-TEMPERATURE ALLOYS*

Alloy	Approximate composition, wt. %								Temp. range investigated, °F	Kinetic constants		
										At max temp.		
										A, (mg/cm ²) ²	K, (mg/cm ²) ² hr	C, kcal/mole
Al-modified Nichrome V	76	20		4					1800-2200	0.35	0.008	67.6
Nb modified Nichrome V	79	20						1	1800-2200	4.6	0.143	72.6
	80	20							1800-2200	3.6	0.013	57.5
Fe-Cr-Al		25	70	5					1800-2200	1.3	0.039	52.3
Inco 702	80	15	0.5	3	0.5				1600-1800	0.26	0.0065	49.3
Hastelloy R235	62	16	11	1.5	2	7			1500-1800	0.26	0.056	58.9
Hastelloy W	67	5	8			20			1300-1800	4.5	0.43	57.2
Type 316 stainless	12	17	66			2.5	2		1450-1600	4.3	0.004	28.5
Inconel X	74	15	7	1	2.5				1450-1600	0.01	0.001	56.9
Inconel	76	15	8						1450-1600	0.02	0.0005	72.3

*Data taken from reference 13.

These data were obtained from weight-change data. Metallographic study showed apparent stress dependency of oxidation rate above stress levels sufficient to cause 1 per cent strain in 100 hr. This was concluded to be real, but wide scatter in the data and neglecting Poisson contraction effects detract from the significance of the assumed relationships in many cases. An interesting effect, which substantiates prior findings, concerns the decrease in depth of oxide penetration over the unstressed condition when specimens were lightly stressed. This is explained as resulting from decreasing the compressive stress in the characteristic oxide by applying small tensile strains, which implies isotropic behavior of the complex oxides (a rather unlikely situation). Slight intergranular oxidation was observed in niobium-modified Nichrome V, R235, Inconel X, and type 316

effects of water vapor and CO₂ contaminants in air upon the oxidation resistance of a 24 wt.% chromium-6 wt.% aluminum alloy were investigated. The results of this work are summarized in Table IV-2. Ratings for a nickel-chromium-niobium alloy, determined simultaneously, are included for comparison. Water vapor apparently exhibits a beneficial effect, whereas CO₂ is slightly detrimental in the ranges investigated.

Selective oxidation at the surface of the nickel-chromium-niobium alloy was observed to some extent in all cases. This behavior is surprising, because (1) the temperature ranges investigated were above the range where selective oxidation (known as green rot) normally occurs, (2) the addition of niobium tends to minimize selective oxidation in nickel-chromium alloys, and (3) the atmospheres used should not have been conducive to selective oxidation. The oxidation behavior of

Table IV-2 PERFORMANCE RATINGS OF
IRON-23.7 WT.% CHROMIUM-6 WT.% ALUMINUM
AND NICKEL-20 WT.% CHROMIUM-1.1 WT.%
NIOBIUM ALLOYS IN VARIOUS GAS ATMOSPHERES
AT 1900 AND 2100°F*

Atmosphere	Oxide penetration rating†			
	Fe-Cr-Al		Ni-Cr-Nb	
	1900°F	2100°F	1900°F	2100°F
Normal air (0.76 vol.% H ₂ O)	A	A	B	C
Dry air (0.005 vol.% H ₂ O)	B	B	C	D
Air + 2.5 vol.% H ₂ O	A	A	A	B
Air + 5.0 vol.% H ₂ O	A	A	B	D
Air + 2.5 vol.% H ₂ O + 2.5 vol.% CO ₂	B	B	B	D
Air + 5.0 vol.% H ₂ O + 5.0 vol.% CO ₂	B	B	B	C
Dry air + 5.0 vol.% CO ₂	B	B	D	D
N ₂ + 9 vol.% H ₂ O + 6 vol.% CO ₂ + 8 vol.% O ₂		A	B	

*Data taken from reference 14.

†Maximum oxide penetration ratings (mils per 100-hr test) are as follows: A, 0.45 to 1.10; B, 1.11 to 1.76; C, 1.77 to 2.42; D, 2.43 to 2.99.

nickel-chromium type alloys is sensitive to trace elements and specific melting practices; since the source of the nickel-chromium-niobium alloy was not specified, it is doubtful whether this alloy was representative of similar material available commercially.

Selective attack at the surface of the iron-chromium-aluminum alloy was observed only in the atmosphere containing 2.5 vol.% each of H₂O and CO₂. (E. S. Bartlett)

Niobium

The protection of niobium from oxidation by coatings has been studied at Horizons, Inc., and Oak Ridge. Horizons¹⁵ reports that flame spraying with chromium-34 wt.% silicon-20 wt.% aluminum, Fecral, CrSi₂-20 wt.% aluminum, or TiSi₂-25 wt.% aluminum affords some protection at 2500°F, but porosity in the coatings is a major problem. Aluminum dipping after flame spraying provided no improvement. Electroplating with nickel containing occluded SiO₂, Al₂O₃, and ThO₂, followed by aluminum dipping, did not improve oxidation resistance. It was concluded that coatings may protect unalloyed niobium for 4 to 6 hr at 2500°F, but coating reliability is poor at present.

Oak Ridge has studied flame-sprayed coatings of Wall Colmonoy, Microbraz, and Coast Metals Nos. 52 and 53 on niobium. The coated samples had satisfactory 1700°F oxidation resistance, but the coatings were nonuniform and subject to cracking.

Water and steam corrosion of niobium are under study at Bettis and Battelle. Workers concluded, from a metallographic study of corroded samples, that the scale consists of a thin adherent layer which remains at constant thickness and an overlying layer which increases in thickness with time. This behavior is similar to that observed by Cathcart et al.¹⁶ in oxygen at 500°C (930°F). Bettis also observed platelets in the metal just under the adherent scale after long-time corrosion, e.g., 100 days at 750°F. These are believed to be hydride.

Battelle is studying the effects of alloying on corrosion resistance in 680°F water. Binary alloys containing 45 at.% (44.5 wt.%) zirconium, 25 at.% (15.5 wt.%) vanadium, and 35 at.% (21.7 wt.%) titanium had dark iridescent scales and low weight gains (0.2 mg/cm²) after 42 days of exposure. Unalloyed niobium exhibited a weight loss of 2 mg/(cm²)(day). Ternary alloys containing titanium-vanadium, titanium-molybdenum, and titanium-chromium also exhibited excellent corrosion resistance. (W. D. Klopp)

Tantalum

Initial results of a Battelle study¹⁷ indicate that binary additions of titanium, zirconium, hafnium, and tungsten improve the 1200°C oxidation resistance of tantalum. The degree of improvement ranged from twofold (tungsten) to fivefold (titanium). Titanium, zirconium, and hafnium also reduced the amount of contamination hardening in the metal by reacting with the inward-diffusing oxygen to form internal scales. (W. D. Klopp)

Molybdenum

Results of coating work at the Bureau of Standards¹⁸ have shown that the oxidation resistance of chromium-nickel plated molybdenum can be improved by overplating with aluminum. The molybdenum is plated successively with 1 mil of chromium, 7 mils of nickel, and 2 mils of aluminum. The aluminum is plated slowly from a cryolite bath at 1000°C, so that alloying with the nickel occurs. Molybdenum panels plated in this manner exhibit a weight gain of 5 mg/cm²

after 400 hr at 1100°C, compared with 40 mg/cm² for straight chromium-nickel plated panels.

(W. D. Klopp)

Corrosion by Liquid Metals and Fused Salts

Atomics International has been investigating ferritic steels for sodium containment at the 1050°F level. In isothermal and polythermal pumping-loop experiments¹⁹ ferritic steel specimens were exposed to sodium flowing in type 304 stainless-steel loops; in the polythermal case, the fluid thermal cycle was 500°F. In all cases, corrosion rates were negligible, the main effect being carburization or decarburization. General findings are shown in Figs. 7 and 8; in the latter, carbon loss represents most of the weight loss. It may be seen that the tendency for migration of carbon in these high austenitic-to-ferritic ratio systems is appreciable; it is thought to be controlled by the diffusion of carbon in the ferritic steels. However, it is pointed out that carbon will tend to migrate until system carbon activities are equalized. Thus, if carbon migration is to be avoided, original carbon activities throughout dissimilar metal systems must be balanced through the tailoring of materials compositions. However, appropriate carbon-activity data must first be obtained.

Corrosion and mass transfer incurred with molten bismuth-uranium alloy has been the subject of extensive investigation at Brookhaven. A great number of long-duration thermal-convective and low-velocity pumping-loop experiments have been conducted and have demonstrated that corrosion is virtually nonexistent when small amounts of zirconium and magnesium are present as inhibitors. The operation and performance of two typical pumping loop systems are described in a recent progress report.²⁰ The first loop was constructed of 1¼ chromium-½ molybdenum steel (¾ in. Schedule 40 pipe); a bismuth alloy containing 1000 ppm uranium, 250 ppm zirconium, and 350 ppm magnesium was circulated between temperatures of 520°C and about 445°C. After 4600 hr of operation, radiographic inspections indicated that there was no hot-zone corrosion, although some cold-zone deposition was noted after 1400 hr of operation. The second system was fabricated of 2¼ chromium-1 molybdenum steel; here the fluid charge which circulated between the above temperature limits contained 340 ppm zirconium and 350 ppm magnesium. Corrosion was first de-

tected after 4500 hr, and mass transfer was not detected until 2600 hr of operation.

Past reports have covered, in some detail, activity in the Molten Salt Reactor Program which is directed toward evaluating the corrosion resistance of Inconel and INOR-8 to fluoride

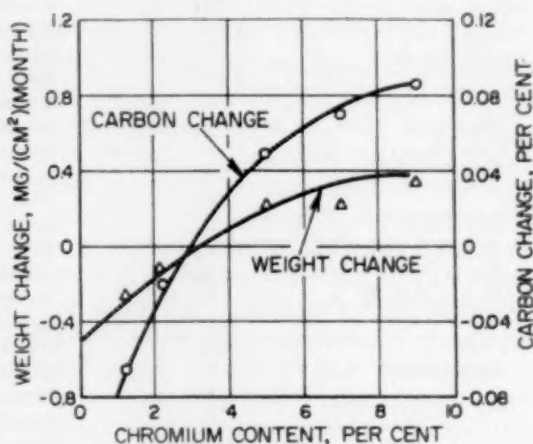


Figure 7—Chromium content versus loss in weight and loss of carbon of specimens exposed in high-velocity isothermal pump loop. Exposure temperature, 1025°F; exposure time, 943 hr; oxygen content, 36 to 80 ppm; carbon content, ≈40 to 60 ppm. Data taken from reference 19.

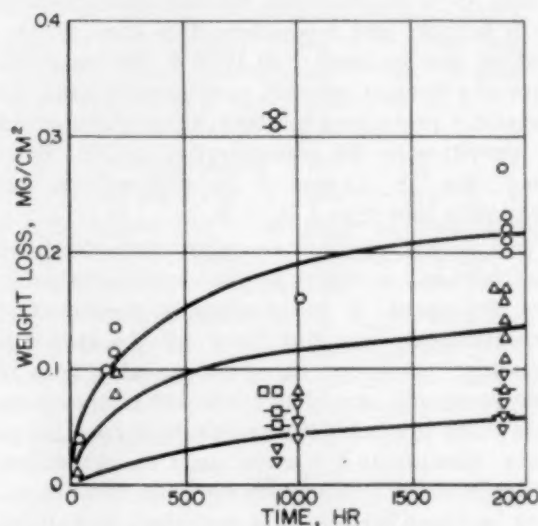


Figure 8—Loss in weight versus exposure time for specimens exposed in low-velocity anisothermal pump loop. —○—, 1¼ Cr-½ Mo; —□—, 2¼ Cr-1 Mo; —△—, 5 Cr-½ Mo; —▽—, 5 Cr-½ Mo-Ti; —◇—, 7 Cr-½ Mo; —◻—, 9 Cr-1 Mo; —△—, type 304 stainless steel; —▽—, Inco A. Temperature, 1050°F; ΔT, 500°F, velocity, 0.13 fps; oxygen, 10 ppm. Data taken from reference 19.

Table IV-3 SUMMARY OF CORROSION DATA OBTAINED IN THERMAL-CONVECTION AND FORCED-CIRCULATION LOOP TESTS OF INCONEL AND INOR-8 EXPOSED TO VARIOUS CIRCULATING SALT MIXTURES*

Constituents of base salts	UF ₄ or ThF ₄ content, mole %	Loop material	Maximum salt temp., °F	Time of operation, hr	Depth of subsurface void formation at hottest part of loop, in.
NaF-ZrF ₄	1 UF ₄	Inconel	1250	1000	<0.001
	1 UF ₄	Inconel	1270	6300	0-0.0025
	4 UF ₄	Inconel	1250	1000	0.002
	4 UF ₄	Inconel	1500	1000	0.007-0.010
	4 UF ₄	INOR-8	1500	1000	0.002-0.003
	0	Inconel	1500	1000	0.002-0.003
NaF-BeF ₂	1 UF ₄	Inconel	1250	1000	0.001
	0	Inconel	1500	500	0.004-0.010
	3 UF ₄	Inconel	1500	500	0.008-0.014
	1 UF ₄	INOR-8	1250	6300	0.00075
LiF-BeF ₂	1 UF ₄	Inconel	1250	1000	0.001-0.002
	3 UF ₄	Inconel	1500	500	0.012-0.020
	1 UF ₄	INOR-8	1250	1000	0
NaF-LiF-BeF ₂	0	Inconel	1125	1000	0.002
	0	Inconel	1500	500	0.003-0.005
	3 UF ₄	Inconel	1500	500	0.008-0.013
NaF-LiF-KF	0	Inconel	1125	1000	0.001
	2.5 UF ₄	Inconel	1500	500	0.017
	0	INOR-8	1250	1340	0
	2.5 UF ₄	INOR-8	1500	1000	0.001-0.003
LiF	29 ThF ₄	Inconel	1250	1000	0-0.0015
NaF-BeF ₂	7 ThF ₄	INOR-8	1250	1000	0

*Data from Oak Ridge National Laboratory.²¹

fuel-bearing salts in flow-loop experiments. Table IV-3 summarizes the information (from both forced- and free-convection loop experiments) now on hand.²¹ At 1250°F, the temperature of principal interest, both materials display excellent resistance to attack, although the attack is sensitive to the concentration of UF₄. However, the UF₄ content of the fuel will be low, nominally less than 1 mole %.

In a British paper,²² a number of mechanisms that govern corrosion in liquid-metal systems are discussed. A compilation is presented of experimental data that bear out the fact that practical corrosion rates are greater both in magnitude and rate of increase with temperature than those predicted from theoretical considerations. Comments are made about the protective action of oxide films on steels in decreasing attack by liquid metals. It is suggested that effective protection demands high and low limits on the oxygen concentration; a high concentration would reduce the adherence of the film, whereas a low concentration would prevent its formation. By this thesis, ultracleanliness in a flow system could lead to aggravated corrosion.

(J. H. Stang)

Radiation Effects in Nonfuel Materials

Basic Studies

Diffusion can be the rate-controlling process in many reactions, particularly at lower temperatures. Dienes and Damask²³ have developed the theory of radiation-enhanced diffusion for the steady-state condition of defect concentration in excess of the thermal concentration. The self-diffusion coefficients are related by vacancy and interstitial processes. The annealing of defects is assumed to be by migration to dislocations and surfaces, or by recombination. The first process gives a linear dependence upon the rate of defect production, and the enhanced diffusion is independent of temperature. The second process imposes a square-root dependence on the rate of defect production, and the enhanced diffusion is an exponential function of 1/T. The ordering of alpha brass was used for an experimental measurement of enhanced diffusion during neutron irradiation. The rate of ordering during irradiation was found to be constant from 0 to 150°C, and at 190°C it approached the thermal rate.

Oak Ridge²⁴ has reported that the electrical resistivity of copper-aluminum alloy decreases during neutron irradiation at room temperature, the magnitude being dependent upon aluminum concentration. The effect was not observed at -120°C , which indicates a diffusion-controlled process enhanced by radiation. Simnad and co-workers²⁵ have shown that proton irradiation accelerates the reduction of NiO at lower temperature. They interpret the controlling process to be diffusion. At 250°C the induction period is decreased by a factor of 4, and the rate of reduction is increased about twofold for proton-irradiated NiO. No effect was observed at 400°C .

Prior work on irradiation of metals at low temperature was reviewed.²⁶ At liquid-helium temperatures there is no apparent migration of defects. Above 15°K there is some interstitial movement and vacancy annihilation, and at higher temperatures there may be movement of more dispersed interstitials and possibly clusters. Oak Ridge²⁴ has measured resistivity changes in metals irradiated by fast neutrons at 4.17°K . The resistivity change in ohm-centimeters per neutron was as follows:

	$d\rho/dn$
Copper annealed crystal	0.95×10^{-26}
Copper cold-worked crystal	1.29×10^{-26}
Silver	1.42×10^{-26}
Gold	1.34×10^{-26}
Zinc	8.48×10^{-26}
Platinum	2.58×10^{-26}

Values for copper are comparable to prior data. Workers at the University of Illinois²⁷ have carried out studies of low-temperature (25°K) deuteron irradiation of germanium, measuring resistivity and expansion. The germanium became p type, with a large increase in resistivity which decreased irreversibly by a factor of 10^6 on heating between 65 and 300°K . The linear expansion was $(1.5 \pm 0.3) \times 10^{-21}$ per deuteron/ cm^2 . Recovery took place only gradually above 200°K , becoming 85 per cent complete at 360°K . It is suggested that, at a liquid-nitrogen temperature (85°K), there are separate clusters of interstitials and vacancies to explain expansion effects and the observation of low-angle X-ray scattering, together with early annealing of resistivity effects. Fujita and Ganser²⁸ have measured low-angle X-ray scattering from germanium irradiated at -180°C with 5×10^{16} 8-Mev deuterons/ cm^2 . They estimate the scattering

regions to have a radius of 35 Å or to contain about 9×10^3 atoms. Annealing at room temperature decreased the concentration of scattering centers to 20 per cent of its initial value.

Ring, O'Keefe, and Bray²⁹ report finding free fluorine in neutron-irradiated LiF, by nuclear magnetic resonance. For 1×10^{19} nvt, they estimate 7 per cent free fluorine and also detect free Li⁷. Spaepen³⁰ has measured the density decrease in LiF neutron irradiated at 80°C . The decrease saturates at 23 per cent at 1.2×10^{18} nvt, and the crystals break up.

Data on the lattice expansion and annealing of irradiated molybdenum are summarized in a Hanford report.³¹ The expansion amounts to 6.041 per cent at 2.3×10^{19} nvt at 35°C and anneals by different processes in three ranges: at 100 to 200°C , at about 400°C , and fully at 500 to 800°C . The X-ray broadening of molybdenum irradiated to 6×10^{19} and 1.2×10^{20} nvt has been analyzed. A particle size of 500 to 600 Å and strains which are several times greater in the $[2\ 1\ 1]$ direction than in $[2\ 0\ 0]$ direction were found.

Damask³² has found that the hardness of neutron-irradiated diamond, as measured by wear, decreases about 75 per cent for 5×10^{20} nvt, with a corresponding density decrease of 4 per cent.

Primak³³ has summarized the information on fast-neutron effects in quartz and vitreous silica. There are three stages in the metamictization of quartz: (1) local strain occurs with retention of long-range order, for irradiation up to 5×10^{19} nvt; (2) the quartz loses symmetry, becoming crystocrySTALLINE with disordered regions; and (3) the structure becomes disordered and approaches the same state as irradiated vitreous silica. This third state anneals to vitreous silica. The irradiation of vitreous silica at 5×10^{19} nvt produces local deformation and reorientation of the silica tetrahedra with a 2.9 per cent density increase. (A. E. Austin)

Effects of Irradiation

on Mechanical Properties

Harwell is continuing to investigate the effect of neutron irradiation on the properties of pure metals, which now include niobium,³⁴ copper,³⁵ and nickel.³⁵ After being irradiated at an integrated flux of about 10^{20} neutrons/ cm^2 at 16°C , niobium showed a moderate increase in yield strength and ultimate tensile strength, as indicated in Table IV-4. Further increases occurred

Table IV-4 THE EFFECT OF NEUTRON IRRADIATION ON THE ROOM-TEMPERATURE TENSILE PROPERTIES OF NIOBIUM*

Treatment	Yield strength (0.2% offset), 1000 psi	Ultimate tensile strength, 1000 psi	Per cent total elongation to fracture	Reduction of area, %
Unirradiated	57.8	68.6	21.5	87
	57.6	70.0	19.8	79
	60.3	75.2	19.0	
	61.1	72.2	21.4	83
	60.3	73.8	21.5	
As irradiated (10^{20} neutrons/cm ² at 16°C)	77.2	80.4	8.0	48
	74.1	74.4	6.4	
	74.4	77.0	6.5	55
Irradiated and annealed at 200°C for 60 min	92.2	92.8	6.8	47
	92.2	92.7	7.7	68
	91.2	91.7	4.2	

*Data taken from reference 34.

on annealing at 200°C, but the yield strength dropped sharply at the start of deformation. The most serious effect was the large reduction, from 17 to less than 2 per cent, in uniform elongation before fracture. This behavior was a consequence of a lack of work-hardening capacity in the irradiated metal. Recovery of ductility by postirradiation annealing started at 350°C and was complete after 1 hr at 600°C. The effect of neutron irradiation of 5×10^{19} neutrons/cm² at 100°C on the mechanical properties of polycrystalline copper and nickel has been studied in the range of -195 to 200°C. The yield strength of both metals was increased reversibly by the irradiation, and, as indicated in Table IV-5, this increase was markedly temperature dependent, being much greater at the low temperatures than at the high. The rate of work hardening was greatly reduced by irradiation, especially at low strains. In addition, the ultimate tensile strength and brittleness were increased by the irradiation. The results for the three metals were discussed in terms of possible interstitial-vacancy mechanisms of irradiation hardening.

At Oak Ridge specimens of titanium and zirconium alloys were exposed to a 250 to 280°C uranyl sulfate fuel solution. Tests for tensile and impact behavior in in-pile loops were then made. After air exposure of 10^{18} to 10^{19} fast neutrons/cm², the impact curves of Zircaloy-2, Zircaloy-3A, and crystal-bar zirconium remained essentially unchanged, whereas elongation decreased slightly. After the same exposure, the yield strength and ultimate tensile strength at 25 and 315°C of Ti A-55, Ti A110AT, and Ti C130AM increased somewhat, with corresponding de-

creases in ductility. Exposures of 2.5 to 5.0×10^{18} fast neutrons/cm² for Ti A-55 and Ti A110AT and 4.9 to 9.5×10^{19} fast neutrons/cm²

Table IV-5 EFFECT OF NEUTRON IRRADIATION OF 5×10^{19} NEUTRONS/CM² ON THE MECHANICAL PROPERTIES OF COPPER AND NICKEL*

Test temp., °C	Condition	Yield strength, 1000 psi	Ultimate tensile strength, 1000 psi	Elongation, %
Copper				
-195	Irradiated	41.0	53.0	21.6
	Unirradiated	10.7	45.8	40.7
-78	Irradiated	33.6	39.5	21.2
	Unirradiated	11.2	33.6	38.4
20	Irradiated	30.3	34.3	27.5
	Unirradiated	8.4	27.1	42.2
200	Irradiated	23.1	24.0	15.9
	Unirradiated	7.9	22.5	30.9
Nickel				
-195	Irradiated	90.8	104.5	15.0
	Unirradiated	37.9	87.7	31.6
-78	Irradiated	74.8	78.3	23.8
	Unirradiated	37.5	69.7	40.6
20	Irradiated	61.5	62.9	23.4
	Unirradiated	36.2	58.6	34.4
200	Irradiated	53.8	58.6	18.5
	Unirradiated	33.5	51.0	27.0

*Data taken from reference 35.

for Ti A-40 produced no measurable changes in impact energies.

Irradiation effects on a variety of alloys suitable for use in high-pressure reactor equipment have been determined through the cooperation of

Table IV-6 EFFECT OF NEUTRON IRRADIATION ON THE ROOM-TEMPERATURE TENSILE PROPERTIES OF SOME ALLOYS*

Alloy	Integrated neutron flux, nvt (> 1 Mev)	Rockwell hardness	Tensile strength, psi		Total elongation, %	Uniform elongation, %
			Ultimate	Yield (0.2% offset)		
16-1 Croloy	0	B-83	76,500	57,800	36	
	4.9×10^{19}	B-96	116,600	116,600		
	7.8×10^{19}	B-95	108,600	108,600	14	
	4.7×10^{20}	B-94	112,800	112,800	14	4
Hastelloy-X	0	B-87	112,500	49,400	52	
	5.0×10^{19}	B-96	129,300	100,200	50	
	1.8×10^{20}	B-99	130,700	104,000	43	
	2.5×10^{20}	B-100	131,000	106,300	42	
	3.6×10^{20}	B-71	135,900	116,000	39	23
Inconel-702	0	B-82	94,900	42,600	67	
	5.0×10^{19}	B-96	113,100	101,100	50	
	1.8×10^{20}	B-100	121,500	120,300	41	
	2.9×10^{20}	B-101	130,000	128,800	36	
Inconel-X (double aged)	0	C-27	170,100	103,200	28	
	0.8×10^{19}	C-30	165,100	143,300	22	
	1.6×10^{20}	C-30	161,300	158,600	14	
	2.9×10^{20}	C-28	165,000	163,200	10	2
	0	C-32	184,300	120,300	23	
Inconel-X (single aged)	0.8×10^{19}	C-34	172,600	154,500	18	
	1.6×10^{20}	C-34	174,000	170,800	13	
	2.9×10^{20}	C-31	172,200	171,500	12	2
	0	C-28	163,400	132,400	22	
K-Monel	4.9×10^{19}	C-29	168,700	167,600	12	
	7.6×10^{19}	C-26	167,600	166,500	11	
	4.7×10^{20}	C-27	159,000	159,000	9.6	1
	1.2×10^{19}	C-36	225,000	175,500	17	5
Type 410 stainless steel (Westinghouse material)	1.5×10^{20}	C-41	233,000	198,000	11	1
Zircaloy-2	0		81,500	52,900	29	
	3.6×10^{20}	C-65	96,000	90,200	18	7
Type 414 stainless steel	6.4×10^{19}	C-44	240,000	206,000	15	3
AM-350 stainless steel	0	C-38	195,400	162,400	23	
	1.2×10^{19}	C-40	215,000	190,000	17	2
	1.5×10^{20}	C-42	222,000	199,000	15	1

*Data taken from reference 36.

Oak Ridge and Phillips Petroleum Co.³⁶ As was found previously, most of the alloys increase in strength and brittleness with increasing irradiation time. Results of tensile tests conducted on various alloys after exposure to severe neutron irradiation are presented in Table IV-6. Data for subsize Izod impact specimens irradiated between 1×10^{19} and $3 \times 10^{20} > 1$ Mev neutrons/cm² are summarized in Table IV-7. Since all the specimens were cooled, irradiation temperatures were probably close to 100°F.

Three review articles discuss neutron-irradiation effects above an exposure of 5×10^{18} fast neutrons/cm² and are concerned with iron and nickel alloys³⁷ and nonfuel metals in general.^{38,39}

(B. C. Allen)

Selected Metallurgical Aspects of Cladding and Structural Materials

Recrystallization of Niobium

Westinghouse⁴⁰ is carrying out recrystallization studies on niobium and niobium alloys. The onset of recrystallization in alloys containing tungsten (0.25 to 5.0 wt.%), nickel (0.25 to 1.0 wt.%), cobalt (0.25 wt.%), iron (0.25 to 1.0 wt.%), and rhenium (5.0 and 10.0 wt.%) is reported to be only about 150°C higher than the onset in unalloyed niobium. Recrystallization is just beginning at 1000°C, with the exception of the alloy containing 0.25 wt.% nickel, which is 40 per cent recrystallized. Recrystallization is

Table IV-7 EFFECT OF NEUTRON IRRADIATION ON THE IMPACT PROPERTIES OF SOME ALLOYS IN THE FORM OF SUBSIZE IZOD SPECIMENS³⁶

Alloy	Neutron exposure	Test temperature ^a	Fracture energy ^{a,b}	Fracture appearance	Brittle facets or highlights	Shear lip	Fracture, % ^c
16-1 Croloy	Unirradiated	Low	Low	Brittle	Many	None to slight	> 95
		High	High	Ductile	Few	Moderate to heavy	40-95
	Irradiated	Low	Low	Brittle	Many	None to slight	> 95
		High	High	Ductile	Few	Moderate to heavy	40-95
Hastelloy-X	Unirradiated	Low	High	Ductile	Few	Slight	> 75
		High	High	Ductile	Few	Moderate to heavy	50-75
	Irradiated	Low	High	Ductile	Few	Slight	> 75
		High	High	Ductile	Few	Moderate to heavy	50-75
Inconel-702	Unirradiated	Low	High	Ductile	Few	Slight	> 75
		High	High	Ductile	Few	Moderate to heavy	50-75
	Irradiated	Low	High	Ductile	Few ^d	Slight	> 75
		High	High	Ductile	Few	Moderate to heavy	50-75
Inconel-X	Unirradiated	Low	Low	Ductile	Few	Slight	80-95
		High	Low	Ductile	Few	Moderate	80-95
	Irradiated	Low	Low	Ductile	Few	Slight	80-95
		High	Low	Ductile	Few	Moderate	80-95
Inconel-X	Unirradiated	Low	Low	Brittle	Few	Slight	> 95
		High	Low	Brittle	Few	Moderate	> 95
	Irradiated	Low	Low	Ductile ^e	Few	Slight	> 70
		High	Low	Ductile	Few	Moderate	> 70
K-Monel	Unirradiated	Low	Low	Ductile	None	Heavy	> 95
		High	Low	Ductile	None	Heavy	> 95
	Irradiated	Low	Low	Ductile	None	Heavy	> 90
		High	Low	Ductile	None	Heavy	> 80
Zircaloy-2	Unirradiated	Low	Low	Brittle	None	None	> 80
		High	High	Brittle	Very few	Moderate	50-80
	Irradiated	Low	Low	Brittle	None	None	> 80
		High	High	Brittle ^f	Very few	Moderate	50-80
Type 410 stainless steel	Unirradiated	Low	Low	Brittle	Many	None	> 95
		High	High	Ductile	Very few	Moderate	60-95
	Irradiated	Low	Low	Brittle	Many	None	> 95
		High	High	Ductile	Very few	Moderate	60-95
Type 410 stainless steel (Westinghouse material)	Unirradiated	Low	Low	Brittle	Many	None	> 95
		High	High	Ductile	Very few	Moderate	60-95
	Irradiated	Low	Low	Brittle	Many	None	> 95
		High	High	Ductile	Very few	Moderate	60-95
Type 414 stainless steel	Unirradiated	Low	Low	Brittle	Few	None	> 99
		High	High	Brittle	Few	Heavy	> 98
	Irradiated	Low	Low	Brittle	Few	None	> 95
		High	High	Brittle ^g	Few ^h	Heavy	> 90
AM-350	Unirradiated	Low	Low	Ductile	None	Slight	> 95
		High	High	Ductile	Few	Moderate	> 95
	Irradiated	Low	Low	Ductile	None	Slight	> 95
		High	High	Ductile	Few	Moderate	> 95

^aHigh or low test temperature and fracture energy refer to the relative values of the individual materials.^bThere was no great change in the fracture energy level if each group is listed as all high or all low.^cThe per cent fracture is the amount of fracture caused by the initial blow of the hammer.^dMore bright facets were seen on these specimens than on the other specimens of this group.^eOne specimen tested at -200°F was completely brittle.^fOne specimen irradiated at the high dose and tested at 500°F was ductile.^gA specimen tested at 300°F was ductile.^hNo bright facets were observed on the specimen referred to in footnote g.

completed in all the above-mentioned alloys after 1 hr at 1400°C. (J. A. DeMastry)

Phase Studies

Ames,⁴¹ working with the aluminum-vanadium system, has shown changes in the system from previously reported data. It is stated that (1) the alpha phase does not occur at Al_{11} but varies between Al_{10} and V_2Al_{21} ; (2) the beta phase occurs at V_4Al_{23} , rather than Al_6 ; and (3) an additional phase, alpha prime, has been located between the alpha and beta phases. This compound is monoclinic with the following parameters: $a = 25.4$ Å, $b = 7.59$ Å, $c = 11.0$ Å, and $\beta = 127$ deg; the tentative formula is V_7Al_{45} . All three of the phases, alpha, alpha prime, and beta, form by peritectic reaction.

In the zirconium-tantalum phase diagram, the termination of the eutectoid horizontal on the tantalum-rich section of the diagram was established to be 96 ± 1 per cent.⁴¹ The solubility of zirconium in tantalum at room temperature was found by X-ray to be 2 wt.%. The eutectoid in the range of 0.5 to 20 wt.% tantalum is placed at about 10 wt.% tantalum. The solubility limits of tantalum in alpha zirconium are between 1.5 and 20 wt.%, determined metallographically.

(J. A. DeMastry)

Recrystallization of Inconel

Oak Ridge⁴² has made a study of the recrystallization and grain growth of Inconel. It has been found that deformations of less than 20 per cent do not appreciably refine the grain structure. The shape of the deformed coarse grain remains outlined by the carbide precipitates after recrystallization occurs. The effect of this pseudo grain structure on mechanical properties is not known, but it is not likely to be beneficial. Although cold work in the range of 50 to 80 per cent results in a fine grain size after 2 hr at 1800°F, this is probably not a stable grain size, and a further increase in size approaching that of metal given 5 to 10 per cent cold work seems likely. This will occur as the carbide particles begin to coalesce and dissolve with time, thus unblocking the boundaries and allowing further grain growth to occur. At 1900°F, no significant difference in final grain size is obtained regardless of the previous amount of deformation. The grain size reached in 30 min is essentially the same as that resulting from a 2-hr anneal.

Temperatures of 1700°F will produce recrystallization of all worked structures regardless of severity, but the resulting final grain size, at least for short exposure, will depend on the degree of prior cold work. On the other hand, the grain size resulting from a 1900°F anneal appears to be independent of the original grain size or the amount of prior cold work. When the material has a coarse grain size prior to deformation, a somewhat higher temperature is required for recrystallization. The carbides in the grain boundaries of the worked coarse-grained material remain fixed when recrystallization occurs, so that the new grains do not receive the usual contribution to their creep resistance from such particles. The mixed structure is still found in some cases after 2 hr at 1800°F, but it is removed at 1900°F.

(J. A. DeMastry)

Diffusion Studies

Diffusion is being studied in the uranium/nickel/X-8001 (aluminum alloy), uranium/zirconium, and (uranium-zirconium) alloy/aluminum systems at Hanford. Diffusion couples were used in the diffusion studies of the uranium/nickel/X-8001 system. Migration of uranium was traced by means of high-resolution autoradiography. It was shown by this method that no uranium diffused into or beyond the visible AlNi compounds. In order to gain a reasonable understanding of diffusion in this system, it had to be considered in at least two parts: (1) diffusion of aluminum through the nickel prior to contact between Ni_2Al_3 and uranium, and (2) diffusion of uranium and AlNi compounds toward the outer surface of the X-8001 after this contact. However, the studies on both parts were run concurrently. Data from the uranium/nickel/X-8001 diffusion studies are given in Table IV-8. The ratios of the penetrations of nickel into X-8001 to those of aluminum into the nickel, as determined from these data, are listed in Table IV-9.

Russian investigators⁴³ have studied the diffusion of boron and carbon in titanium, zirconium, niobium, tantalum, molybdenum, and tungsten. On the basis of microscopic investigations and of the results of chemical and X-ray analyses, the calculations of activation heat in the diffusion of boron and carbon in these metals were carried out, and the equations for the temperature dependence of the diffusion coefficient were derived.

Table IV-8 DIFFUSION IN URANIUM/NICKEL/X-8001 COUPLES

(Data from Hanford Atomic Products Operation)

Data point number	Temp., °C	Time, days	Original metal-metal interface penetration, mils				Thickness of X-8001/nickel compounds, mils	Original nickel barrier thickness, mils
			Aluminum into nickel	Nickel into X-8001	Uranium toward X-8001 surface	Aluminum-nickel-uranium compounds into uranium		
11411	350	28			0	0	0.19	0.65
11511	348	41			0	0	0.31	0.75
10711	404	14	0.29	0.75	0	0	0.99	1.13
10721	404	14	0.24	1.12	0	0	1.36	0.76
11111	403	27	0.40	1.40	0	0	1.80	0.80
11121	403	27	0.70	1.10	0	0	1.80	0.80
11112	403	27	0.45	1.37	0	0	1.82	0.83
11611	411	27	*	0.82	0.13	2.74	0.88	0.33
11211	403	41	0.44	0.70	0	0	1.14	0.88
11221	403	41	0.60	0.60	0	0	1.12	0.88
11212	403	41	0.62	1.63	0	0	2.25	0.81
11222	403	41	0.26	1.50	0	0	1.76	0.86
10811	459	14	1.10	2.00	0	0	3.10	1.06
10821	459	14	0.79	2.40	0.06	0.12	3.19	0.85
13711	450	14	1.23†	3.13†	0	0	4.36	1.23— 1.58†
13721	450	14	†	3.02†	<1.0†	9.15	3.96	0.65— 1.25†
13211	450	14	†	3.84†	2.4	9.76	1.84	0.58— 0.81
10911	448	27	*	3.00*	0.50	5.00	3.30	0.80
10912	448	27	*	3.22*	0.50	9.00	3.33	0.80
10922	448	27	*	2.80*	0.69	8.6	2.90	0.80
10931	448	27	*	3.10*	0.92	10.5	3.15	0.97
11011	446	41	*	3.98*	2.60	12.3	2.29	0.88
11021	446	41	*	4.45*	2.50	11.3	2.82	0.87
11012	446	41	*	4.61*	2.53	8.8	2.85	0.77

*AlNi compound layer had moved toward the outer surface of the X-8001 causing the apparent position of the original Al-Ni interface to move toward the uranium.

†Nickel was electroplated directly on the uranium; nonuniform nickel thickness made these values impossible to determine accurately.

At the Second Geneva Conference, the French⁴⁴ presented results of diffusion of uranium with various transitional metals. Diffusion couples consisted of uranium strips plus one of the following metals: zirconium, niobium, molybdenum, or titanium. The depths of penetration were measured by means of micrography, microhardness, and autoradiography, and by point analysis using the Castaing "microsonde" apparatus. Concentration-penetration curves plotted by point analyses were used to compute the coefficients of diffusion and to study their variation with concentration. In the "gamma" phase (body-centered cubic), a very clear Kirkendall effect was demonstrated. Comparison of the diffusion coefficients reveals that the mobility of molybdenum is greater than that of zirconium. Although the comparisons for the other diffusion constants are somewhat qualitative, the penetra-

tions measured in the uranium-niobium couples were considerably weaker than in the other couples.

Studies of the diffusion of uranium into the cladding have been performed at Brookhaven²⁰ on the BNL enriched-uranium fuel-element plates. Six plates were examined, of which one plate was not heat-treated. The five other plates were heat-treated at temperatures of 350, 400, and 500°C for between 20,000 and 24,000 hr. Milled samples from the flats of the plates were analyzed for uranium contents. The results indicated that little or no diffusion took place in any of the plates examined, except for one surface of one heat-treated plate. This latter result has not been explained. In addition to chemical analyses, microscopic examination revealed no diffusion.

Table IV-9 RATIO OF THE PENETRATION OF NICKEL INTO X-8001 TO THAT OF ALUMINUM INTO THE NICKEL FROM THE ORIGINAL X-8001/NICKEL INTERFACE

(Data from Hanford Atomic Products Operation)

Data point number	Temp. of anneal, °C	Time of anneal, days	Penetration from original metal-metal interface, mils		Nickel/X-8001 Al/Ni
			Aluminum into nickel	Nickel into X-8001	
10711	404	14	0.29	0.75	2.58
10721	404	14	0.24	1.12	4.68*
11111	403	27	0.40	1.40	3.50
11121	403	27	0.70	1.10	1.57
11112	403	27	0.45	1.37	3.04
11211	403	41	0.44	0.70	1.59
11221	403	41	0.60	0.60	1.00*
11212	403	41	0.62	1.63	2.53
11222	403	41	0.26	1.50	5.77*
10811	459	14	1.10	2.00	1.82
10821	459	14	0.79	2.40	3.04
10311	529	2	0.87	2.24	2.60†

*This ratio is undoubtedly pressure sensitive. A difference between local pressure at each point and the average pressure in the couple may have caused the wide variation in the ratio at these points. Values of the ratio at these points were therefore discarded from the average. Average after discarding points marked a = 2.47.

†This data point is beyond the range of temperatures of interest in this study. It was included to indicate the comparison between the penetration ratio at highest temperatures and those at lower temperatures.

Nuclear Metals⁴⁵ has conducted metallographic studies of interdiffusion behavior between uranium-10 wt.% molybdenum fuel alloy

Table IV-10 DIFFUSION LAYER THICKNESS VERSUS HEAT-TREATMENT*

Heat-treatment temp., °F	Time at temp., °F	Width of diffusion zone, in.
As extruded at 1600°F		
950		0.00006
	1	0.00006
	8	0.00008
	168	0.00012
1100	744	0.00020
	1	0.00006
	8	0.00010
	168	0.00016
1300	744	0.00028
	1	0.00028
	8	0.00052
	168	0.00052
1500	1	0.00064
	8	0.00140
	48	0.00220
	1	0.00160
1650	1	0.00160

*Data taken from reference 45.

and zirconium cladding at temperatures ranging from 950 to 1650°F. Specimens cut from a reference fuel-element pin, produced by coextrusion and followed by cold swaging, were subjected to heat-treatment at specified times and tempera-

tures, as given in Table IV-10. The finished rod, extruded at 1600°F, consisted of a 0.150-in.-diameter core clad with 0.004 in. of zirconium. The results and conclusions obtained are as follows:

1. The visible growth of the interface layer is predominantly outward, so that the uranium diffuses into the zirconium.

2. If all of the diffusion were into the zirconium, extrapolation of a plot of interface thickness versus time ($t^{1/2}$) for the 950°C treatment indicates that a period of 5.9×10^5 hr would be required for the visible interface to penetrate completely the 0.004-in.-thick cladding.

3. The work suggests that a discontinuity in diffusion mechanism does exist for the interdiffusion of uranium-molybdenum and zirconium cladding.

(M. A. Gedwill, Jr.)

Selected Mechanical Properties of Cladding and Structural Materials

The British Industrial Group has published an extensive annotated bibliography⁴⁶ relating to the choice and properties of nonfuel reactor materials. The references were selected with the interests of reactor design engineers in mind, and

cover the period from 1934 to mid-1958. They are grouped according to materials, ranging from aluminum through zirconium.

A detailed set of specifications for certain reactor materials, their welding, and their inspection for acceptability has been set forth⁴⁷ by ORNL. These materials include stainless steels, Hastelloys, and Inconel. The stated purpose of the specifications is to ensure "adequate standards for a high-temperature, highly stressed, experimental nuclear reactor in which reliability of operation is a prime consideration."

Zirconium and Zirconium Alloys

The tensile properties of an age-hardenable zirconium alloy, zirconium-5 wt.% molybdenum-2 wt.% tin, were determined at room temperature by Nuclear Metals. Two heat-treated conditions were investigated: (1) solution treated 1 hr at 1400°F, water quenched, aged at 932°F for 1½ hr; (2) solution treated for 1 hr at 1400°F, water quenched, aged at 1112°F for 96 hr. Results are shown in Table IV-11.

Table IV-11 ROOM-TEMPERATURE TENSILE STRENGTH OF A ZIRCONIUM-5 WT.% MOLYBDENUM-2 WT.% TIN ALLOY*

Aging treatment	Hardness, Rockwell C	Ultimate tensile strength, psi	Yield strength (0.2 per cent offset), psi	Elongation in 1 in., %	Elastic modulus, 10 ⁶ psi
96 hr at 1112°F	26	127,000	110,000	8.70	15.0
1½ hr at 932°F	40	201,500	184,000	6.88	16.0

*Data from Nuclear Metals.

Unalloyed uranium rod was clad with 40 mils of this alloy by extrusion. The rod was solution treated at 1400°F and water quenched. It was swaged from 0.420 in. in diameter to 0.375 in. The cladding was approximately 0.035 in. thick after swaging, and showed no evidence of rupture. The clad rod was aged for 24 hr at 1112°F and water quenched to room temperature. Metallographic examination of the bond area indicates a good bond between cladding and core.

A binary zirconium-base alloy containing 15 wt.% niobium prepared by Oak Ridge was water quenched from the beta phase and aged at 400 and 500°C. The ultimate tensile strength at room temperature after aging at 400°C for 24 hr was 200,000 psi, and the material showed a total elongation of 1 per cent. Aging the same alloy at 500°C for 14 days gave a room-temperature

tensile strength of 150,000 psi, a yield strength of 135,000 psi, and an elongation of 10 per cent. The tensile properties at 300°C of this alloy aged at 500°C are: tensile strength, 105,000 psi; yield strength, 90,000 psi; and elongation, 16 per cent.

The effects of heat-treatment on the grain size and tensile properties of Zircaloy-2 have been studied at Knolls. Specimens of Zircaloy-2 were heat-treated at several different temperatures to obtain different grain sizes. The tensile properties at room temperature were determined at strain rates of 0.02, 1.2, and 20 in. per inch per minute. Tests conducted at 600°F were made at the lowest strain rate. The test data indicate that (1) the observed reduction of area changes less than 5 per cent over the range of strain rates covered for specimens of all grain sizes, (2) changes of less than 20 per cent were noted in the uniform and total elongation for the same range of strain rates, and (3) the ultimate tensile strength was increased by approximately 10 per cent when the strain rate was increased from 0.02 to 20 in. per inch per minute.

The effect of grain size on tensile properties was only slight. The small grain-size material was slightly stronger than that having larger grain sizes. The α -phase material showed a significantly smaller reduction of area than the $\alpha + \beta$ and β -treated materials. The influence of grain size observed during room-temperature testing was less noticeable at 600°F.

Mechanical tests were made at Oak Ridge to evaluate the sensitivity of the tests to the anisotropic behavior of hexagonal metals. Table IV-12 shows the results of tensile testing Zircaloy-2 at room temperature and 300°C. The fabrication variables are noted at the bottom of the table. Impact properties were measured, and they were found to vary with sample selection and notch orientation. Some Zircaloy-2 samples having identical tensile properties in the longitudinal

Table IV-12 TENSILE PROPERTIES OF ZIRCALLOY-2*

(Data from Oak Ridge National Laboratory)

Plate†	Specimen orientation in plate	Ultimate tensile strength, psi	Yield strength (0.2% offset), psi	Elongation in 1 in., %	Reduction, %			
					Area	Longitudinal or transverse direction‡	Normal direction§	Isotropic ratio of reduction
Broken at room temperature								
1	Longitudinal	64,900	54,800	31.1	47.7	45.5	4.4	10.4
	Transverse	69,000	58,300	25.8	43.3	40.6	3.3	13.7
2	Longitudinal	73,200	63,300	31.0	46.4	35.5	16.7	2.1
	Transverse	75,200	59,400	29.1	44.0	28.4	21.6	1.3
3	Longitudinal	73,800	66,400	32.2	46.0	37.2	14.4	2.6
	Transverse	74,200	58,400	32.7	44.3	25.5	25.5	1.0
4	Longitudinal	61,400	52,300	30.7	60.6	56.6	10.0	5.7
	Transverse	63,300	59,000	24.5	62.1	57.8	10.0	5.8
Broken at 300°C								
1	Longitudinal	32,600	25,500	35.5	43.5	38.4	7.8	4.9
	Transverse	29,300	21,200	29.3	68.4	65.5	13.3	4.9
2	Longitudinal	38,600	31,400	30.4	64.5	52.2	24.4	2.1
	Transverse	37,600	29,000	31.3	61.5	43.8	31.6	1.4
3	Longitudinal	32,800	27,800	32.9	76.5	63.3	35.5	1.8
	Transverse	35,000	25,100	32.1	68.7	48.3	39.4	1.2
4	Longitudinal	28,400	22,200	38.8	77.6	68.9	27.2	2.5
	Transverse	32,200	29,600	27.9	76.2	71.1	17.8	4.0

*Strain rate, 0.05 in. per inch per minute.

†Plate 1, hot worked commercially in alpha-plus-beta field without any cross rolling; Plate 2, fabricated experimentally according to new fabrication schedule, except inert-gas melted; Plate 3, same material as used for Plate 2 and fabricated to same schedule in laboratory; Plate 4, core tank scrap material from HRE-2, hot worked commercially in alpha plus beta; cross rolled.

‡Minor axis of elliptical fractured face.

§Major axis of elliptical fractured face.

and transverse direction showed different properties in the thickness direction, as indicated by impact tests or by shapes of the fracture of the tested tensile specimens. Fractures in the tensile specimens were elliptical in shape rather than round. The isotropic ratio of reduction shown in Table IV-12 appears to be a rather sensitive index of anisotropy. Long-time creep tests are in progress on Zircaloy-2 under loads approximately equivalent to the 0.2 per cent offset yield strength. Of particular interest is the transition from second- to third-stage creep.

Additional creep data on Zircaloy-2 are being obtained by the Canadians⁴⁶ and Battelle.⁴⁸ Table IV-13 shows creep data from Canada for the various heat-treated conditions. Some creep tests at Battelle on 15 per cent cold-worked Zircaloy-2 have been in progress approximately 10,000 hr. Of particular interest is the deformation associated with the initiation of third-stage creep and the time necessary to start third-

stage creep. The temperature range covered by this investigation is 450 to 750°F.

The tensile properties of vacuum-melted Zircaloy-2 heat-treated at 1010°C for 1 hr were

Table IV-13 CREEP DATA FROM ZIRCALLOY-2*

Heat-treated condition	Test temp., °F	Test load, 1000 psi	Creep strain	Hours on test
Annealed†	550	8	0.037	1938
Annealed‡	550	13.5	0.07	1889
12.1% C.W.	550	13.5	0.075	1220
25.5 C.W. + anneal†	550	13.5	0.028	550
25.5 C.W. + anneal‡	550	13.5	0.035	864

*Data taken from reference 9.

†Annealed 425°C in vacuum at Chalk River.

‡Annealed 450°C in air at Ottawa.

determined at room temperature, 500, and 700°F by Bettis. The results are shown in Table IV-14.

(F. R. Shober)

Table IV-14 TENSILE PROPERTIES OF VACUUM-MELTED ZIRCALLOY-2*

Test temp., °F	Heat-treated condition	Yield strength, (0.2% offset) 1000 psi	Ultimate tensile strength, 1000 psi	Total elongation, %
Room temp.	1 hr at 1010°C, W.Q.	74.0	91.5	5.5
Room temp.	1 hr at 1010°C, F.C.	53.1	63.6	2.5
500	1 hr at 1010°C, W.Q.	42.0	57.1	11.0
500	1 hr at 1010°C, F.C.	23.0	32.4	17.5
700	1 hr at 1010°C, W.Q.	32.0	48.4	7.5
700	1 hr at 1010°C, F.C.	18.0	26.3	15.0

*Data from Bettis.

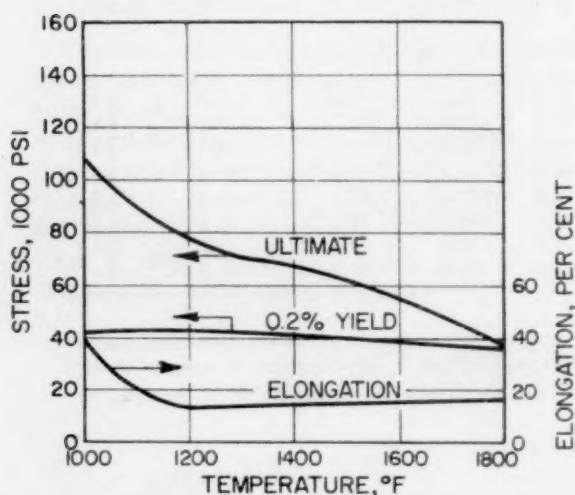


Figure 9—Short-time high-temperature tensile properties of solution-annealed Hastelloy B. Data taken from reference 49.

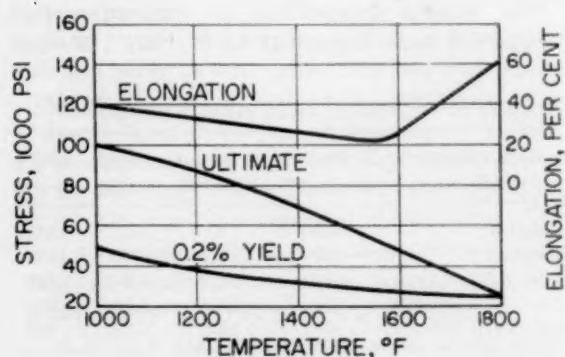


Figure 10—Short-time high-temperature tensile properties of solution-annealed Hastelloy W. Data taken from reference 49.

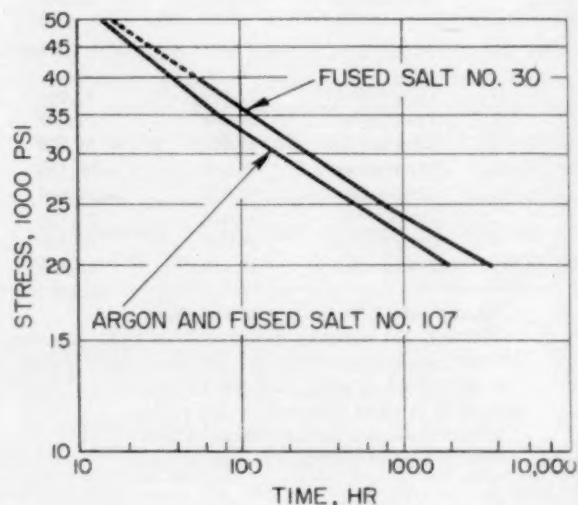


Figure 11—Stress-rupture curves of solution-annealed Hastelloy B sheet tested in various environments at 1300°F. Data taken from reference 49.

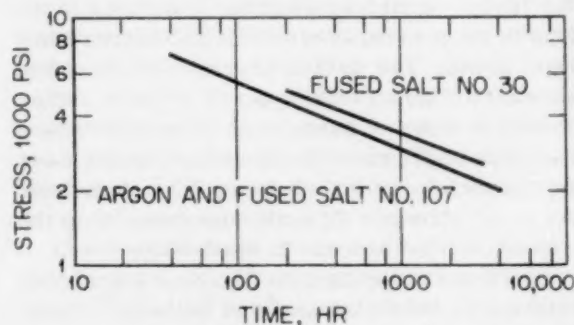


Figure 12—Stress-rupture curves of solution-annealed Hastelloy B sheet tested in various environments at 1800°F. Data taken from reference 49.

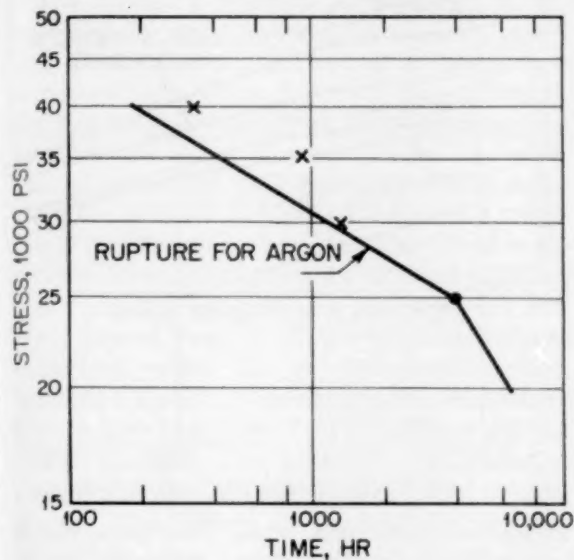


Figure 13—Stress-rupture plot of solution-annealed Hastelloy W sheet tested in various environments at 1300°F. x, tested in fused salt No. 30. •, tested in fused salt No. 107. Data taken from reference 49.

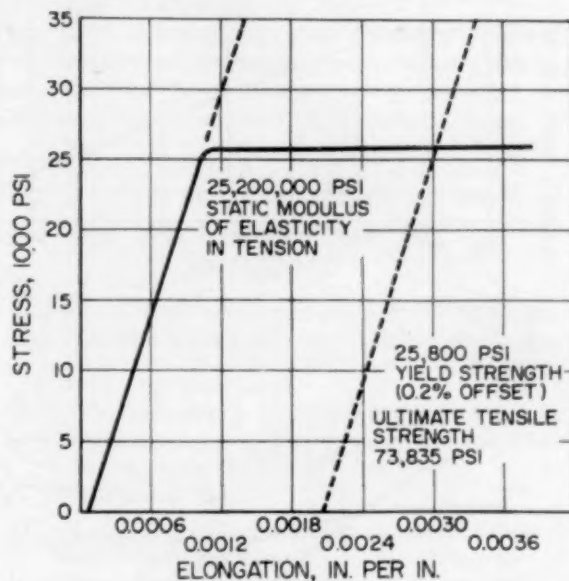


Figure 15—Stress-strain relationships for INOR-8 at 1200°F. Data taken from reference 21.

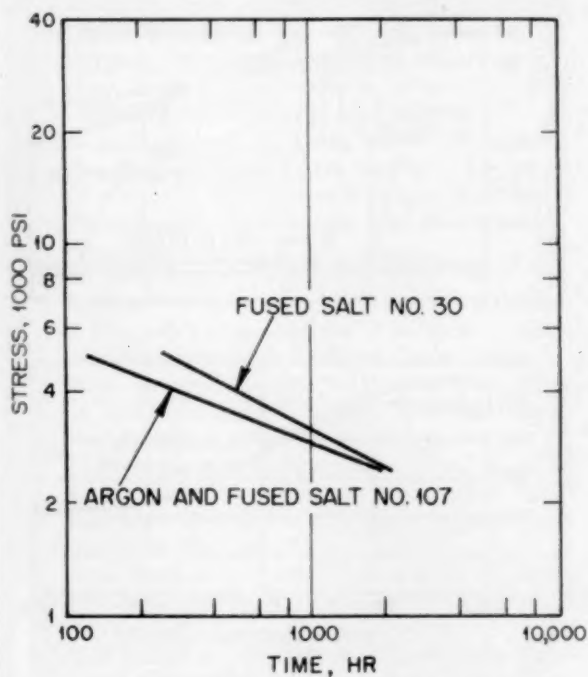


Figure 14—Stress-rupture curves of solution-annealed Hastelloy W sheet tested in various environments at 1800°F. Data taken from reference 49.

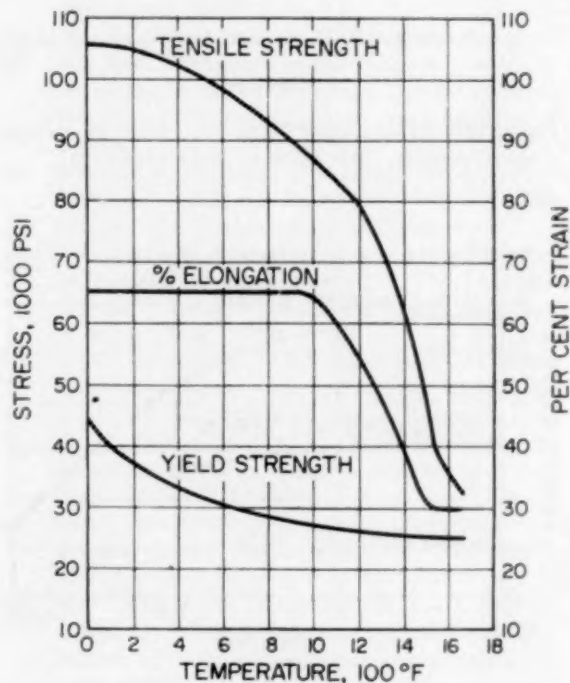


Figure 16—Tensile properties of INOR-8 as a function of temperature. Data taken from reference 21.

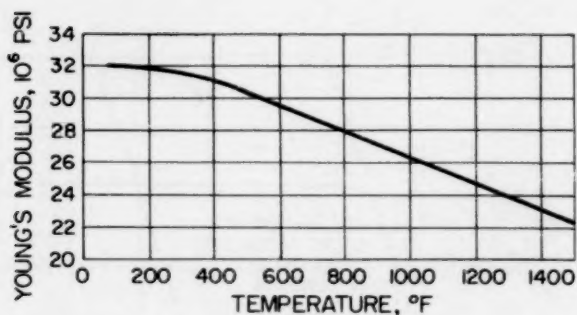


Figure 17—Young's modulus for INOR-8 as a function of temperature. Data taken from reference 21.

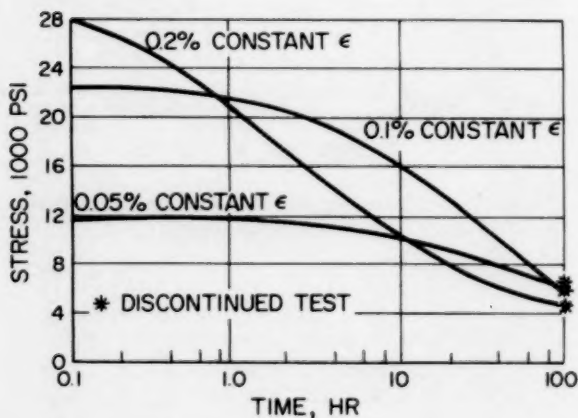


Figure 18—Relaxation of INOR-8 at 1300°F at various constant strains. Data taken from reference 21.

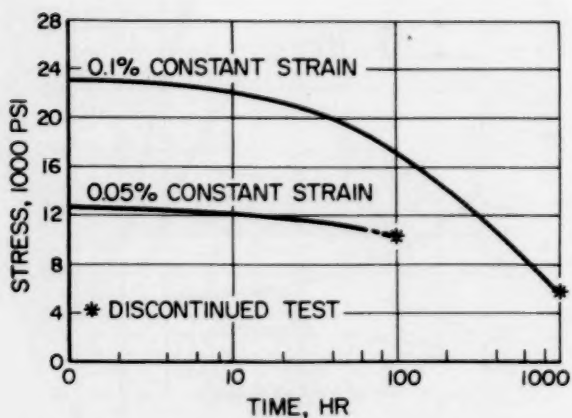


Figure 19—Relaxation of INOR-8 at 1200°F at various constant strains. Data taken from reference 21.

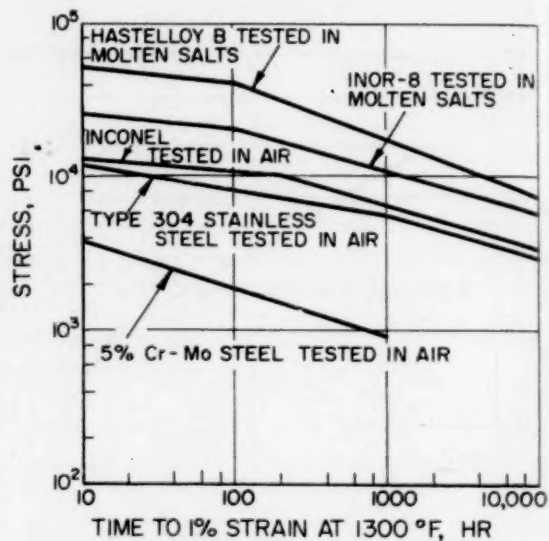


Figure 20—Comparison of the creep properties of several alloys. Data taken from reference 21.

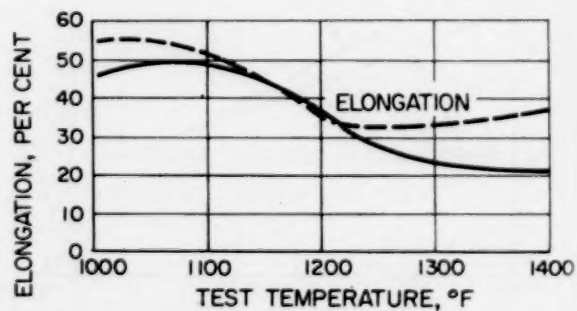
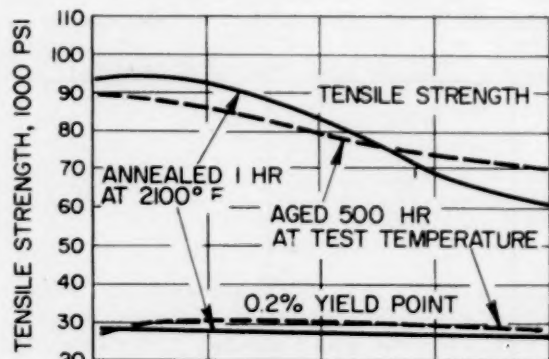


Figure 21—Effect of aging on high-temperature tensile properties of INOR-8. Data taken from reference 21.

Nickel-base Alloys

The creep properties of Hastelloy B and Hastelloy W were investigated by Oak Ridge.⁴⁹ The properties as determined in argon were compared with those in sodium, air, hydrogen, and two fused-salt solutions in the 1300 to 1800°F temperature range. The purpose of this study was to determine the suitability of these materials for use as structural members in a circulating fuel reactor. They were found to have excellent corrosion resistance in fused salts and good elevated-temperature strength, but suffered severe loss of ductility from phase changes occurring within the test temperature range. Figures 9 through 14 summarize the results from tensile and creep tests at elevated temperatures.

The mechanical properties of INOR-8, a nickel-molybdenum alloy, were also investigated.²¹ The effects of temperature on these properties are shown in Figs. 15 through 21.

(F. R. Shober)

References

1. Bettis Technical Review, WAPD-BT-10, October 1958. (Unclassified AEC report.)
2. Reactor Technology Quarterly Report No. 6, October 1958, KAPL-2000-3, October 20, 1958. (Unclassified AEC report.)
3. H. B. Probst, E. B. Evans, and W. M. Baldwin, Jr., An Investigation of the Scaling of Zirconium at Elevated Temperatures, Case Institute of Technology Report No. 24, Dec. 5, 1958. (Unclassified.)
- 4.* W. G. O'Driscoll, C. Tyzack, and T. Raine, The Oxidation of Groups IVA, VA, and VIA Elements in CO₂ and the Development of Oxidation Resistant Zirconium Alloy, A/CONF./15/P/1450.
5. R. G. Wheeler, The Effect of Reactor Atmosphere on Zirconium and Zirconium Alloys, HW-55958, May 6, 1958. (Unclassified AEC report.)
6. S. Kass, D. J. Fontanese, A. F. Oaks, and D. B. Scott, Pickling of Zircalloys Prior to Corrosion Exposure, WAPD-TM-141, Sept. 1, 1958. (Unclassified AEC report.)
7. A. B. Riedinger, Crevice Corrosion of Zircaloy, KAPL-M-ADR-5, Aug. 12, 1958. (Unclassified AEC report.)
- 8.* M. Coriou et al., Mechanism of Corrosion in High-temperature Water of Aluminum and Alloys Containing Iron and Nickel, A/CONF./15/P/1271.
9. Atomic Energy of Canada Limited, 1958. (Unpublished.)
- 10.* R. Caillat and R. Darros, Corrosion of Magnesium and Some Magnesium Alloys in Gas Cooled Reactors, A/CONF./15/P/1146.
11. Metallurgy Division Quarterly Report for July, August, and September, 1957, ANL-5797, October 1958. (Unclassified AEC report.)
12. A. B. McIntosh, Corrosion Problems in Nuclear Power Production, *Chemistry & Industry (London)* 22: 687-692 (1957).
13. J. C. Richmond and H. R. Thornton, Oxidation of Experimental Alloys, WADC-TR-58-164 (Part I), ASTIA 155688, June 1958. (Unclassified.)
14. W. Chubb et al., Constitution, Metallurgy, and Oxidation Resistance of Iron-Chromium-Aluminum Alloys, BMI-1298, Oct. 16, 1958. (Unclassified AEC report.)
15. E. C. Hirakis, Research for Coatings for Protection of Niobium Against Oxidation at Elevated Temperatures, WADC-TR-58-545, September 1958. (Unclassified.)
16. J. V. Cathcart, J. J. Campbell, and G. P. Smith, The Microtopography of Oxide Films on Niobium, *Journal of the Electrochemical Society*, 105(8): 442 (August 1958).
17. W. D. Klopp et al., Second Quarterly Progress Report on Investigation of the Properties of Tantalum and Its Alloys, Contract No. AF 33(616)-5668, Nov. 15, 1958. (Unclassified.)
18. D. E. Couch, H. Shapiro, and A. Brenner, The Use of Nickel-Aluminum Alloy Coatings for the Protection of Molybdenum from Oxidation, *Journal of the Electrochemical Society*, 105(8): 485 (August 1958).
19. W. C. Hayes and O. C. Shepard, Corrosion and Decarburization of the Ferritic Chromium-Molybdenum Steels in Sodium Coolant Systems, NAA-SR-2973, Dec. 1, 1958. (Unclassified AEC report.)
20. Nuclear Engineering Department Progress Report, for January 1-March 31, 1958, BNL-506, August 1958. (Unclassified AEC report.)
21. J. A. Lane, H. G. MacPherson, and Frank Maslan, Molten Salt Reactors, Part II, in "Fluid Fuel Reactors," Addison-Wesley Publishing Company, Reading, Mass., 1958, p. 563.
22. G. W. Horsley, Mass-transport and Corrosion of Iron-based Alloys in Liquid Metals, AEREM/R-2714, October 1958. (Unclassified British report.)
23. G. J. Dienes and A. C. Damask, Radiation-Enhanced Diffusion in Solids, *Journal of Applied Physics*, 29: 1713 (1958).
24. Solid State Division Annual Progress Report for Period Ending August 31, 1958, ORNL-2614, Nov. 30, 1958. (Unclassified AEC report.)
25. M. T. Simnad, R. Smoluchowski, and A. Spilner, Effect of Proton Irradiation upon Hydrogen Reduction of NiO, *Journal of Applied Physics*, 29: 1630 (1958).
- 26.* D. K. Holmes et al., On the Interpretation of Radiation Effects in Noble Metals, A/CONF./15/P/2385.
27. F. L. Vook, Length and Resistivity Changes in Germanium upon Low-temperature Deuteron Ir-

- radiation and Annealing, AECU-3808, May 1958. (Unclassified AEC report.)
28. F. E. Fujita and U. Ganser, Small Angle Scattering of X-Rays from Deuteron-Irradiated Germanium Crystals, *Journal of the Physical Society of Japan*, 13: 1068 (1958).
 29. P. J. Ring, J. G. O'Keefe, and P. J. Bray, Li^7 and F^{19} Nuclear Magnetic-Resonances in Neutron Irradiated LiF, *Physical Review Letters*, 1: 453 (1958).
 30. J. Spaepen, Density of Neutron Irradiated LiF Crystals, *Physical Review Letters*, 1: 281 (1958).
 31. D. L. Gray, Recovery of Lattice Expansion of Irradiated Molybdenum, HW-57903, Nov. 1, 1958. (Unclassified AEC report.)
 32. A. C. Damask, Hardness of Neutron-Irradiated Diamonds, *Journal of Applied Physics*, 29: 1590 (1958).
 33. W. Primak, Fast-Neutron-Induced Changes in Quartz and Vitreous Silica, *Physical Review*, 110, 1240 (1958).
 34. M. J. Makin and F. J. Minter, The Mechanical Properties of Irradiated Niobium, AERE-M/R-2649, August 1958. (Unclassified British report.)
 35. M. J. Makin, The Effect of Neutron Irradiation on the Mechanical Properties of Copper and Nickel, *Journal of the Institute of Metals*, 86: 449-455 (June 1958).
 36. H. T. Watanabe, Radiation Damage Studies Programs. ETR Loop Materials Progress Report III, IDO-16475, Sept. 15, 1958. (Unclassified AEC report.)
 - 37.* J. C. Wilson, Effects of Irradiation on the Structural Materials in Nuclear Power Reactors, A/CONF./15/P/1978.
 38. M. J. Makin, How Radiation Damages Metals, *Atoms and Nuclear Energy*, 9: 318-322 (September 1958).
 39. B. C. Allen, A. K. Wolff, A. R. Elsea, and P. D. Frost, The Effect of Nuclear Radiation on Structural Metals, REIC-5 (ASTIA AD-157170), The Radiations Effects Information Center, Battelle Memorial Institute, May 31, 1958.
 40. R. T. Begley, Development of Niobium-Base Alloys—Second Quarterly Progress Report, A-2551Z, Nov. 15, 1958. (Unclassified.)
 41. Semiannual Summary Research Report in Metallurgy for July–December 1957, ISC-977, Oct. 15, 1958. (Unclassified AEC report.)
 42. D. A. Douglas and J. R. Weir, The Recrystallization and Grain Growth of Inconel, ORNL-2406, Nov. 20, 1958. (Unclassified AEC report.)
 43. G. V. Samsonov and V. P. Latisheva, Investigation of the Diffusion of Boron and Carbon in Certain Metals of Transition Groups, AEC-tr-3321, 1956. (Unclassified AEC translation.)
 - 44.* Y. Adda and J. Philibert, Diffusion of Uranium with Various Transitional Metals, A/CONF./15/P/1160.
 45. L. R. Aronin and J. J. Pickett, Core-to-Clad Interdiffusion Studies on Zirconium-Clad Uranium-10 Wt. % Molybdenum Alloy Fuel Pins, NMI-4403, Jan. 10, 1958. (Unclassified AEC report.)
 46. Information Bibliography—Materials for Use in Nuclear Reactors, IGRL-IB/R-15 (2nd Ed.), Aug. 28, 1958. (Unclassified British report.)
 47. R. M. Evans (editor), Reactor Material Specifications, TID-7017, Oct. 29, 1958. (Unclassified AEC report.)
 48. R. W. Dayton and C. R. Tipton, Jr., Progress Relating to Civilian Applications During December, 1958, BMI-1307, January 1959. (Confidential AEC report.)
 49. C. R. Kennedy and D. A. Douglas, High-Temperature Mechanical Properties of Hastelloy B and Hastelloy W, ORNL-2402, Nov. 28, 1958. (Unclassified AEC report.)

*Second United Nations International Conference on the Peaceful Uses of Atomic Energy, Geneva, September 1958. (Individual papers available from the Office of Technical Services, Dept. of Commerce, Washington 25, D. C. Bound volumes of papers will be available from United Nations, Office of Public Information, New York.)

Melting, Casting, Heat-treatment, and Hot Working

At the recent Geneva Conference many noteworthy reports of activities relating to the melting, fabrication, and heat-treatment of reactor materials were presented. A compilation of information on the forming of unalloyed uranium was given by Fellows of Mallinckrodt.¹ The processing and qualities of Zircaloy were discussed by Richards, Harb, Friske, and Hurford of Bettis.²

The qualities of unalloyed uranium in reference to its hydrogen content have concerned the production reactor sites for some time. The particular quality that has received recent attention is the tendency exhibited by high-hydrogen uranium to cause porosity in the braze between the core and can in fuel elements. The hydrogen content of the core is the sum of that in the uranium after fabrication and that introduced during the heat-treatment. Since dingot uranium (primary reduction material) is fabricated directly to cores without a vacuum remelt operation, its hydrogen content is higher by the quantity picked up from heat-treatment. Therefore, canning porosity in cores made from dingot uranium is greater than that in other types.

If unalloyed uranium could be cast directly to near final shape and size a considerable improvement in material efficiencies could be realized. National Lead reports a program that produced solid and hollow slugs by a centrifugal casting technique for evaluation by the production reactors. It was established that heated molds (700 to 900°F) were necessary to produce the quality required. Various mold washes and glass mold liners were used.

A problem that has been the cause of considerable concern from time to time has been the occurrence and effects of stringers on the mechanical and corrosion properties of Zircaloy-2. As of now there is agreement that two types exist: (1) intermetallic stringers that occur in the grain boundaries of as-cast material and are elongated

during fabrication, and (2) gas-void stringers caused by ingot porosity that does not heal during fabrication. Studies relating to the occurrence of the gas-void type stringers (much more prevalent in Zircaloy melted in an atmosphere containing argon) have been in progress at Bettis.³ In part, it is concluded that (1) gas-void type stringers contain argon; (2) at temperatures up to 1000°C, no measurable permeation of argon through Zircaloy occurs; and (3) the gas-void type of stringer can be removed from Zircaloy by vacuum annealing above 1200°C.

Specific attempts to minimize or eliminate the stringers by changing fabrication procedures were made.⁴ From these studies it was concluded that (1) stringers and stringer type corrosion qualities of Zircaloy-2 were unchanged by a fabrication procedure in which the ingots were extruded to slabs at 1900°C and then hot rolled at 1475°F maximum, and (2) the fabrication procedure itself was a feasible process in that it was competitive in both yields and conversion costs with conventional blooming and forging techniques.

The occurrence of segregation in certain alloys of interest in reactor metallurgy is caused by properties of the phases present in the alloy systems (widely separated melting points, limited solubilities, and wide differences in the densities of the phases present). Alloys that have received considerable attention in this regard belong to the uranium-niobium, thorium-uranium, and aluminum-uranium systems. A proposed scheme to skirt these problems was to prepare the materials from prealloyed and possibly inhomogeneous starting materials by compacting macroscopic particles (shot or machine chips). Subsequent fabrication and heat-treatment would effect the densification required and produce the desired homogeneous bodies. Nuclear Metals has been engaged in activities relating to the preparation of alloys in this manner with varying degrees of success.

While the primary goal of alloy homogeneity was attained by this compacting technique, other

properties varied from those of materials prepared by melting and casting.

Improvements in both homogeneity and mechanical properties were observed for the aluminum-25 wt.% uranium alloy. In this instance, shot produced by pouring molten aluminum-uranium alloy on a spinning disk was compacted and then fabricated to the desired shape. It was demonstrated that, in the case of an aluminum-16 wt.% uranium alloy, a burnable poison (0.2 wt.% boron) could be homogeneously included with no impairment of the mechanical properties.

The alpha extrusion of uranium ingots directly to fuel slug size and the cost and qualities of the product have been studied in some detail through the cooperative efforts of Bridgeport Brass, National Lead, Mallinckrodt, and Hanford. The extrusion process for solid slugs as reported by Bridgeport Brass was revealed to be superior to fabrication by rolling. Costs were lower and material yields were significantly higher. Irradiation behavior based on very preliminary tests indicated that the extruded product was about equal to the roll product.

Other work at Bridgeport Brass indicates that the high alpha extrusion of hollow rods from cast hollow billets is more satisfactory than extrusion from pierced solid billets. This is particularly true for material yields and tool life.

Los Alamos has continued to be active in the development of particular fabrication processes.⁵ One is described in a recent report and pertains to the production of weld rod by alpha (1050°F) extrusion. Critical in the specific technique developed was the purity of the cast billet of unalloyed uranium. The maximum iron content was listed as 150 ppm. A typical analysis of uranium successfully fabricated was: carbon, 125 ppm; silicon, 70 ppm; iron, 90 ppm; all others, less than 15 ppm each.

A significant contribution to fabrication as a science stems from the Los Alamos development of a method for testing specimens in compression over a temperature range, at a constant temperature, and at constant and variable strain rates.⁶ It involves the use of a cam plastometer. For the material tested (depleted uranium), true stress and true strain curves were established at various temperatures and strain rates and an empirical equation fitted to these curves. Three parameters, two of which are temperature dependent, are contained in the equation. By a method described by Orowan,⁷ and with the true

stress-true strain relationships established experimentally as above, it is now possible to investigate mathematically the effects of work-roll diameter, temperature, coefficient of friction, and pass specifications. The programming of these normally laborious calculations for an electronic computer is described.

(E. L. Foster, Jr.)

Cladding

Cladding by Roll Bonding

In the consideration of various control-rod designs, the utilization of roll-clad titanium dispersions was considered in a study conducted at Bettis.⁴ Hafnium, titanium, and Zircaloy-2 were investigated as possible cladding materials. The roll-bonding characteristics of bimetal and trimetal composites of these materials were studied.

Rolling temperatures of 1550 to 1950°F and various reduction schedules were employed for roll bonding titanium to hafnium. All of the roll-bonding temperatures and reduction schedules resulted in well-bonded specimens. There was no appreciable difference in the bond properties with each change in the fabrication process, except for the increased amounts of diffusion with increasing temperatures. The hafnium to titanium bond exhibited limited ductility during bend testing.

Temperatures of 1600°F with reductions of 20 per cent per pass produced the best titanium to Zircaloy-2 bonds. These bonds were found to be quite ductile at a test temperature of 600°F.

Bonds between hafnium, titanium, and Zircaloy-2 were improved, after roll bonding at temperatures of 1550 to 1750°F, by an additional anneal. The as-roll-clad bonds of titanium to hafnium and Zircaloy to hafnium were weak and required an additional heat-treatment for strengthening. An annealing temperature of 2000°F was required to increase the amount of diffusion at the hafnium to Zircaloy bond.

(E. S. Hodge)

Pressure Bonding

The gas-pressure bonding process involves the use of relatively high gas pressures and temperatures to force components into intimate contact. The components for bonding are usually fabricated to approximately the de-

sired final dimensions and then assembled into a gas-tight container. Close dimensional control is achieved, as the deformation is limited to the amount necessary to bring the materials into intimate contact.

Battelle is investigating the use of the gas-pressure bonding technique for the simultaneous

than the niobium. Only partial bonding was obtained between molybdenum plates treated at 2300 to 2400°F for 3 hr at 10,000 psi of helium. Examination of the bonded plates revealed that excellent bonding was achieved in the areas where intimate contact was obtained.

(S. J. Paprocki)

Table V-1 DENSIFICATION OF URANIUM DIOXIDE CERMET FUEL MATERIALS BY GAS PRESSURE BONDING*

Specimen	Density		Bond conditions		
	Green pressed, % theoretical	Pressure bonded, % theoretical	Temp., °F	Pressure, psi	Time, hr
Type 302B stainless- 70 vol.% UO ₂	67	95	2300	10,000	3
Type 302B stainless- 80 vol.% UO ₂	68	94	2300	10,000	3
Molybdenum-70 vol.% UO ₂	69	93	2300	10,000	3

*Data taken from reference 8.

cladding and densification of uranium-bearing cermet fuel materials.⁸ Results of these studies are presented in Table V-1.

The gas-pressure bonding process is being applied to the preparation of Zircaloy-clad flat-plate uranium dioxide fuel elements.⁸⁻¹⁰ The uranium dioxide is separated by Zircaloy ribs bonded to the cladding for the purpose of compartmenting clad failures and also to add overall structural rigidity and strength to prevent deformation of the cladding by the release of fission gas. The fuel-element components are assembled, edge welded, evacuated, and sealed to form a gas-tight assembly. The Zircaloy compartmented frame is assembled from strip components which are forced into intimate contact and diffusion bonded into an integral unit during the bonding operation. The sealed fuel assemblies are bonded for 4 hr at 1550°F with a helium-gas pressure of 10,000 psi.

Studies are also being conducted to investigate the applicability of this process for the cladding and bonding of niobium and molybdenum fuel elements and assemblies.⁸⁻¹⁰ The initial studies have been concerned with determining the optimum conditions for the self-bonding of niobium and molybdenum. Niobium bonds possessing excellent strength have been obtained by bonding 3 hr at 2200°F with a gas pressure of 10,000 psi. The molybdenum apparently requires a higher combination of gas pressure and temperature

Diffusion Bonding

The method of fabricating compartmented, plate type UO₂-bearing fuel elements for the PWR Core 2 blanket by eutectic diffusion bonding of Zircaloy-2 cladding components is continuing at Bettis.⁴ This method involves the formation of a molten eutectic alloy film between the solid mating surfaces to be joined. The eutectic-alloy film is formed by diffusion of a thin preplaced layer of pure metal (nickel, copper, or iron), which serves as a bonding agent, onto the surfaces of the punched fuel receptacle plate during heating of the assembled components to the bonding temperature. Intimate contact is maintained between the cladding surfaces to be joined during the bonding operation by sealing the assembled fuel-element components by fusion welding along the outside periphery and applying a light, but positive, inert-gas pressure (15 to 60 psig) to the external cladding surfaces during the eutectic diffusion-bonding operation. A bonding temperature of about 1000°C and a bonding time of several minutes to several hours have produced strong bonds. Satisfactory heating and cooling rates, which have a significant effect on the results, have been achieved using an inert-gas-pressurized furnace incorporating a hot and cold zone.

Numerous plate type compartmented UO₂ fuel-element samples have been fabricated using the eutectic diffusion-bonding method. These sam-

Table V-2 INTERNAL INTEGRITY OF FUEL COMPARTMENTS AND BOND STRENGTH AS AFFECTED BY BONDING CONDITIONS*

Bonding agent	Bonding agent thickness, mils	Bonding conditions			Compartment integrity			Bond strength	
		Temp., °C	Time, hr	Pressure, psig	Samples tested	Compartments tested	Per cent compartments gas tight	Failure location†	Burst pressure, psi
Ni	0.09-0.17	1010	1/8-2	60	9			Bond	2400-2600
Ni	0.18-0.22	1010	2	60	23	155	100	Clad	2650-4500
Ni	0.21	1010	4	60	1	10	100	Clad	3600-3800
Cu	0.09-0.20	980-1054	1/4-3	15-30	21	165	100	Clad	2750-4300
Cu	0.13	925	1/4	15	1	10	100	Bond	
Cu	0.19	925	1/4	15	1	10	100	Bond	
Cu	0.25-0.39	980-1054	2-3-1/2	30-60	8	110	100	Clad	2880-3700
Cu	0.26	925	2	30	1	15	100	Bond	
Fe	0.12-0.22	980-1010	1/4-1/2	15-30	7	40	100	Clad	3300-3400
Fe	0.25	1025	2	30	1	10	100	Clad	3000-3780
Fe	0.25	980	3	30	1	10	100	Bond	

NOTE: Each fuel-element sample had over-all dimensions of 2.375 by 11.25 by 0.120 in. and contained 15 fuel compartments 0.25 by 3.0 by 0.080 in. separated by 0.080-in. wide ribs.

*Data taken from reference 4.

† Failure location determined using qualitative cladding tear test. All failures occurred through the cladding at compartment edges on internal-pressure burst tests.

Table V-3 BEHAVIOR OF INTENTIONALLY DEFECTED COMPARTMENTS IN WATER-LOGGING TESTS* (0.005-in.-diameter defect)

Bonding agent	Deposit thickness, mils	Maximum cladding deflection per water-logging cycle, mils									Total deflection, mils
		1	2	3	4	5	6	7	8	9	
Cu	0.16	0	0	0	0	0	5	0			
		0	0	0	0	0	0	0			
		0	0	0	0	0	0	0			
		0	0	0	0	7	16	0			
		0	0	0	0	0	0	0			
		0	0	0							
		0	0	0							
		13	0	0							
		0	0	0							
		0	0	0							
Ni	0.15	0	0	25	0	0	0	13	0	0	38
		0	0	0	0	0	0	14	8	36	58
		0	21	4	0	0	0	2	0	22†	49
		0	11	0	16	0	0	81	0	5	113
		0	0	0	0	5	0	0	0	0	5
		0	0	0	0	3	0	54	0	0	57
		0	0	0	0	0	0	13	0	7	20
		0	0	0	0	0	4	8	0	0	12
		0	0	0	0	0	6	8	9†		23
		0	0	0	0	0	17	7	0	12	36
Ni	0.20	0	0	0	0	0	6	26	0	0	32
		0	0	22	0	12	0	0	0	17	51
		0	0	0	0	2	0	13	0	7	22
		0	0	9	0	13	0	3	0	0	25
		0	0	10	0	33	0	5	0	0	48
		0	0	0	0	13	0	11	0	20	44

NOTE: All compartments are 0.25 by 3.0 by 0.080 in. and contain approximately 5 per cent void volume; cladding thickness is 0.025 in.

*Data taken from reference 4.

† Cladding fractured at compartment edge.

ples have been evaluated in out-of-pile tests by metallographic examination, internal pressurization, water-logging deflection, thermal cycling, and corrosion resistance. Metallographic examination has indicated that no layer of undiffused bonding agent or eutectic is present in the joints. The structure is essentially continuous except for the appearance of a composition gradient. However, some small isolated voids are present in the bond interface. They appear to be related to contamination of the mating Zircaloy-2 surfaces during the etching and plating operation. Interaction of fuel and cladding has been noted in bonded samples. This reaction of diffused oxygen from the UO_2 cores into the Zircaloy-2 cladding is eliminated by using a thin barrier layer of graphite which is sprayed on the fuel plates. Bond integrity was determined by internally pressurizing, to 700 psig of helium, intentionally defected compartments containing 0.040-in.-diameter holes and detecting the escape of helium through the leaks in the bonds of adjacent compartments. The results of this test are listed in Table V-2. Bond strength was determined by two destructive tests. The "peel" test gave a qualitative indication of the bond strength. The other test involved internal pressurization of the compartments until failure occurred. Table V-2 also gives the results of these two tests. The behavior of bonded samples in out-of-pile water-logging tests was determined by intentionally defecting them with 0.005-in.-diameter holes through the cladding subsequent to water logging them in 650°F water under 2200 psi pressure, followed by rapid immersion in a 650°F molten-lead bath. The amounts of compartment swelling are listed in Table V-3. Thermal cycling of individual fuel elements between 75 and 1100°F for as many as 200 cycles has not presented any distortion or dimensional-change problems. The corrosion-test results on bonded samples, listed in Table V-4, indicate that the exposed bonds do not display accelerated corrosion effects. Analyses of nickel, copper, and iron-bonded samples for hydrogen absorption during corrosion are given in Table V-5. These results indicate that the introduction of nickel into the cladding markedly accelerates hydrogen absorption but iron and copper do not.

Oxide plate fuel-element samples of high compartment integrity have been fabricated successfully using rectangular Zircaloy wire for forming the fuel compartments. Defected

compartments have shown complete integrity and normal type failures on internal-pressure burst tests.¹¹

(M. A. Gedwill, Jr.)

Coextrusion

The coextrudability of zirconium-5 wt.% molybdenum-2 wt.% tin and zirconium-5 wt.% niobium-2 wt.% tin with unalloyed uranium was investigated by Nuclear Metals.¹² Unalloyed uranium was clad with nominal cladding thicknesses of 0.010, 0.020, and 0.040 in., using both of these alloys. Extrusion was carried out in a 2.040-in. liner of a 300-ton press through a 0.450-in. die at a temperature of 1150°F. The thickest zirconium-molybdenum alloy cladding and the thinnest and medium zirconium-niobium alloy cladding were cracked after coextrusion. Samples taken from the sound rods were examined before and after thermal cycling 1100 times between room temperature and 1020°F. The bonds have good strength, and the indications are that these high-strength claddings do restrain the growth of uranium during thermal cycling.

The fabrication of zirconium-clad uranium-10 wt.% molybdenum alloy pins by the coextrusion process is being carried out.¹³ The assembled billet, which is contained in a steel jacket with a copper-nickel cutoff plug, is evacuated and sealed. It is heated to 1600°F and extruded using a 1.10-in. liner and a 0.250-in. die. The extrusion defects of approximately 3 in. at the front and 12 in. at the rear of the extrusion are cropped off. After being cold swaged to a 0.158-in. diameter (51 per cent) in three steps, the elements are cut to proper length, straightened, end cropped, and heat-treated.

Nuclear Metals¹⁴ undertook the development of a pair of nested aluminum-clad aluminum-12.5 wt.% uranium alloy cored tubes. The nominal dimensions were for a 10-ft 3-in. over-all length, with an 8-ft-core length. The outside diameters of the two tubes were 2.12 and 1.46 in., with core thicknesses of 0.06 and 0.07 in., respectively, and a cladding thickness of 0.03 in. for both. The components for the coextrusion billets were machined, cleaned, assembled, welded, degassed at 800°F to about 18 μ pressure, and sealed. The end seals at the front and rear of the core were aluminum-7.75 wt.% silicon alloy, whereas the outer cladding was 2S aluminum. The billet temperature for extrusion was 800°F. Inspection of the tubes after extru-

Table V-4 CORROSION OF EUTECTIC-DIFFUSION-BONDED FUEL ELEMENTS AFTER DEFECTING INDIVIDUAL COMPARTMENTS*

Bonding agent	Bonding conditions			Corrosion test conditions		Max compartment swelling, in.
	Deposit thickness, mils	Temp., °C	Time, hr	Pressure, psig	Environment	
Ni	0.20	1010	2	60	680°F degassed water	53
Ni	0.21	1010	2	60	680°F degassed water	53
Ni	0.21	1010	2	60	680°F degassed water	53
Ni	0.18	1010	2	60	680°F degassed water	46
Ni	0.21	1010	2	60	680°F degassed water	46
Ni	0.19	1010	2	60	680°F degassed water	46
Ni	0.26	1010	2	60	680°F degassed water	39
Ni	0.22	1010	2	60	680°F degassed water	36
Ni	0.26	1010	2	60	680°F degassed water	36
Cu	0.25	1010	2	60	680°F degassed water	36
Cu	0.25	1010	2	60	680°F degassed water	36
Cu	0.13	1010	1/4	15	680°F degassed water	17
Cu	0.18	980	1/2	30	680°F degassed water	28
Cu	0.18	980	2	30	680°F degassed water	28
Fe	0.12	1000	1/2	30	680°F degassed water	14
Cu	0.25	1010	2	60	680°F water + 300 psi H ₂	39
Cu	0.12	1010	1/4	15	680°F water + 300 psi H ₂	25
Cu	0.13	1010	1/4	15	680°F water + 300 psi H ₂	25
Cu	0.19	1010	1/4	15	680°F water + 300 psi H ₂	25
Cu	0.18	980	1/2	30	680°F water + 300 psi H ₂	7
Cu	0.18	980	2	30	680°F water + 300 psi H ₂	7
Fe	0.22	1000	1/2	30	680°F water + 300 psi H ₂	25
Fe	0.12	1000	1/2	30	680°F water + 300 psi H ₂	7
Ni	0.19	1010	2	60	750°F degassed steam	55
Ni	0.19	1010	2	60	750°F degassed steam	55
Ni	0.21	1010	2	60	750°F degassed steam	55
Ni	0.21	1010	2	60	750°F degassed steam	55
Ni	0.21	1010	2	60	750°F degassed steam	48
Cu	0.13	1010	1/4	15	750°F degassed steam	28
Cu	0.19	1010	1/4	15	750°F degassed steam	28
Fe	0.19	1010	1/4	15	750°F degassed steam	21

NOTE: Five compartments (0.25 by 3.0 by 0.08 in.) in each sample; all compartments were defected with a 0.040-in.-diameter hole through the cladding; no intercommunication of compartments was observed at 700 psi internal test pressure after corrosion testing.

*Data taken from reference 4.

Table V-5 HYDROGEN ABSORPTION DURING CORROSION TESTING OF SECTIONED EUTECTIC DIFFUSION-BONDED ELEMENTS*

Sample	Days	Environment	Hydrogen concentration, ppm	
			Weld area	Rib area
Beta-quenched Zircaloy-2	19	680°F degassed water		56
Beta-quenched Zircaloy-2	15	680°F degassed water with 300 psi H ₂ overpressure		81
Bonded with 0.20 mil Ni	11	680°F degassed water with 300 psi H ₂ overpressure	523	837
Bonded with 0.22 mil Fe	11	680°F degassed water with 300 psi H ₂ overpressure	91	112
Bonded with 0.13 mil Cu	11	680°F degassed water with 300 psi H ₂ overpressure	106	185
Bonded with 0.18 mil Ni	34	750°F degassed steam	285	434
Bonded with 0.26 mil Ni	27	750°F degassed steam	423	2150
Bonded with 0.22 mil Fe	14	750°F degassed steam	88	146
Bonded with 0.12 mil Cu	14	750°F degassed steam	67	70

NOTE: Original hydrogen concentration of cladding was in the range of 50 to 75 ppm.

*Data taken from reference 4.

sion and drawing revealed that bond strength, total U²³⁵ content in each core, and dimensional specifications, except for the core length in the outer tube, were all good. The core length of the outer tube was 2 in. short of the required length, but it was felt that this could be corrected by lengthening the billet core.

Zircaloy-2-clad uranium-2 wt.% zirconium alloy rods are being produced by coextrusion of composite billets.^{15,16} These rods are extruded with a nominal cladding thickness of 0.020 in. in long lengths to circumvent the end effects common to coextrusion. The long lengths are cut into appropriate lengths for incorporation into fuel rods and blanket rods. The two sizes of billets, 2 and 2³/₄ in. in diameter, are heated to 1200°F for extrusion through a plane circular die to 0.453-in.-diameter rod. The rods are extruded 0.010 in. oversize in diameter to provide stock for swaging.

The fabrication process for producing Zircaloy-2-clad 5 wt.% B₄C-Zircaloy-2 cermet

core strip is being developed by Knolls.¹⁷ The process utilizes small-scale hot coextrusion and cold-sizing techniques. The hot coextrusion of pressed compacts into Zircaloy-2 sleeves offers an attractive method of fabricating the strips directly, with little or no machining. Prior to extrusion, the powder, with end plugs inserted, is pressed into a machined Zircaloy-2 sleeve to a density of approximately 75 per cent of theoretical. The pressed compacts are canned in copper. The extrusion is being performed on a 100-ton press at temperatures of 1472, 1400, and 1337°F. The extruded rods are dejacketed, cold sized by drawing, X-rayed, and machined. Of eight extrusions analyzed, density measurements showed 93 per cent of theoretical for rods extruded at 1337°F and 96 per cent of theoretical for those extruded at 1472°F. The B₄C particles were stringered in the extrusion direction, and a large number of the particles were fractured. Full evaluation of the fabrication variables affecting the burnable-poison rod quality have not been completed.

The integral coextrusion process has been developed¹⁸ for producing a fuel element containing a thermocouple which is either completely or partially insulated from the fuel. The copper-constantan and the platinum-rhodium thermocouples were successfully extruded with glass insulation inside a Zircaloy-2-clad uranium-zirconium alloy elliptical rod. This process makes it possible to install a thermocouple of any length along the axial center line of the fuel element within the tolerance limits of the coextrusion process.

Hanford is developing an alternate end closure for coextruded Zircaloy-2-clad uranium fuel rods. The objective is to produce a bonded end closure that requires little or no machining, other than cutoff, and eliminates the etching procedures presently required. End caps were successfully slipped over the clad rods, welded to the Zircaloy-2 cladding, and swaged to the original rod diameter. The rods were autoclaved for 100 hr at 660°F in water. Micrographs prepared after autoclaving showed no uranium contamination in the weld.

(C. B. Boyer)

Extrusion Cladding

A series of experiments was conducted in extrusion cladding of cylindrical uranium fuel elements with aluminum.¹⁹ The extrusion tests were

conducted with a 1760-ton Schloemann opposed-ram cable-cladding press. Approximately 300 nickel-plated fuel elements, 1.34 in. O.D. by $\frac{1}{2}$ in. I.D. by 8.33 in. long, were clad in groups of six, each of which was oriented end to end and separated by $1\frac{1}{2}$ -in.-long aluminum spacers. The assembly of six was held together by a steel tie rod.

It was reported that these tests demonstrated the mechanical feasibility of extrusion cladding the external surface of cylindrical fuel elements with a 50 to 100-mil-thick wall of aluminum under a wide range of processing conditions and using several extrusion tool configurations. However, little or no bonding between the cladding and core was achieved in any of the tests. Separation of the cladding and element, when subjected to a bonding test, occurred both at the aluminum-nickel and nickel-uranium interfaces. However, it was stated that satisfactory bonding might have been achieved with feasible improvements in (1) the adhesion of the nickel plate to the uranium, and (2) the inertness of the preheating furnace atmosphere. This belief was based on the extrusion cladding experience developed at Savannah River Laboratories, Battelle, and Atomic Energy of Canada, Ltd.

Analyses of the test data indicated further to Hanford that the fuel-element preheat temperature was the major factor affecting extrusion speed, billet-container pressure, and operability. In general, higher preheat temperatures resulted in lower billet-container pressures, higher extrusion speeds, and smoother operation. On the other hand, varying the mandrel tip-to-die distance from one to two times the cladding thickness or changing from a shear to a "swage" die did not show any consistent change in extrusion pressure or operability. It was mentioned, however, that the broad variation in fuel preheat temperature may have masked the effects of tip-to-die spacing and die design. The swage die used in this work is the same as the shear die, except that the former has a 7-deg taper on the leading half of the land or bearing. The function of the taper is to increase the amount of radial pressure exerted on the fuel element by the extruding aluminum in order to improve the bond.

The cladding thickness was reported to have varied about ± 10 per cent of the nominal wall thickness for any given die size, under the wide range of experimental conditions tested. This suggested that much less variance might be

achieved when the proper extrusion conditions have been established and the process variables are under good control.

The surface smoothness of aluminum cladding was said to approach that of impact-extruded aluminum cans. (R. J. Fiorentino)

Canning

During the French-American Conference on Graphite Reactors,²⁰ it was brought out that uranium metal slugs which are to be coated with AlSi must be completely beta transformed prior to canning. All parts must be degreased and chemically cleaned to more than 4 hr prior to canning. The AlSi, which prevents penetration of the aluminum can by the uranium, contains 11.2 to 11.5 wt. % silicon and is held at 590 to 600°C during the coating process.

Some tests have been made on a standard fuel element, canned in an X-8001 jacket and AlSi bonded. A canned fuel element was heated for four months in 350°C water in an autoclave. Sections cut from the specimen showed that no metallurgical bond existed, although the can fit very closely to the core. Metallographically polished sections of the core-AlSi bond layer showed a fairly uniform 5-mil intrusion of an aluminum-uranium intermetallic compound, possibly UAl_3 , into the uranium.

Experimental work has been started to study the feasibility of injection casting future fuel elements into thin wall tubing. One casting was made in which aluminum was injection cast into a 78-in.-long, 0.560-in.-O.D., 0.008-in.-wall stainless-steel tube. Two lengths cut from this casting were thermal cycled for five cycles from room temperature to 450°C with no apparent separation. Injection casting into Zircaloy tubes has resulted in porosity in the core due to outgassing of the zirconium.

Zircaloy-2 cans were bright HF etched and assembled into graphite molds for direct casting of uranium. Three mold preheat temperatures were investigated while the uranium was cast at 1475°C. Small shrinkage was noted in both length and diameter. Argonne²¹ has worked out uranium-alloy casting temperatures and holding times for a number of zirconium and Zircaloy-2 mold designs.

Canning of graphite in Inconel X or type 316 stainless steel has not proved feasible, on the basis of work done at Battelle. The stainless steel carburized extensively and Inconel X cans

ruptured along the welds during prolonged thermal cycling between 480 and 1730°F. However, a silicon-coated type 316 stainless-steel-clad graphite specimen appeared to hold promise.

(P. H. Bonnell)

Nonelectrolytic Chemical-plating Techniques

A number of techniques for the protective coating of niobium were explored by Horizons, Inc.,²² including (1) disproportionation of chromium and titanium halides, (2) reaction with solutions of silicon in copper and aluminum in an attempt to form silicide coatings, (3) electrophoretic aluminum powder coatings, (4) sintering in powder packs of titanium and chromium, (5) flame spraying with alloy powders of various compositions, and (6) electroplating. Although some of the other techniques showed promise, flame spraying and electrodeposition were chosen for development as being the most straightforward. These are discussed further in the section on Corrosion of Niobium, p. 30.

At Bettis¹¹ the quality of chemical displacement coatings of nickel on Zircaloy-2 was greatly improved by agitation of the coating solution.

Uranium and uranium-zirconium alloys (0.5 to 4.0 wt.% zirconium) were coated with zirconium at Knolls²³ by thermal decomposition of zirconium iodide in vacuum at 1000°C. It was possible but difficult to avoid porosity in coatings on pure uranium. However, pore-free coatings could easily be obtained on the low-zirconium alloy, and lifetimes of 200 hr in 100°C water and 80 hr in 170°C water were considered to be attainable routinely by the technique.

An electroless plating method was explored⁸⁻¹⁰ for depositing thin coatings of molybdenum-rich MoO₂ on Croloy-2^{1/4}. However, attempts to deposit elemental molybdenum by electroless plating were unsuccessful. (J. M. Blocher, Jr.)

Ceramic Coatings

In a report by Sanderson and Porter, a review is presented of work being done by various laboratories on the development of coatings on graphite to protect it against high-temperature steam and to aid in the retention of fission products. SiC was reported as being promising, but the experimental results to date have been inconclusive. A coating developed by Minnesota Mining and Manufacturing Company, designated as 3M "Ceramic S," was thought to be a siliconized

SiC. This coating showed no loss in weight when specimens were exposed for 100 hr in steam at 900°C. Carbides of hafnium, molybdenum, titanium, or zirconium on graphite were reported to give good protection in air at 1000°C and to withstand cycling from 600 to 2800°C. No data were given regarding the effect of high-temperature steam on these coatings.

Argonne, in research on the injection molding of EBR-II type fuel elements, has been investigating mold-coating materials.²⁴ Some improvement in the uniformity of the castings has been obtained by spraying the molds with an alcohol suspension containing particles of ThO₂ less than 5 μ in diameter. Although such coatings produce some improvement, they are not considered entirely satisfactory.

Battelle is attempting to develop coatings of SiC on graphite by the thermal decomposition of a halide vapor.²⁵ The techniques involved were developed during previous research on preparation of NbC, TaC, and ZrC coatings on graphite. To produce satisfactory coatings, it is necessary to establish the ranges of vapor composition, pressure, and temperature in which SiC will form on the surface of the graphite. To date, the following limits have been established: vapor, SiI₄/SiBr₄ ratio of 1:1 to 3:1; pressure, 100 to 200 mm Hg; temperature, 1900 to 2000°C.

(B. W. King)

Welding and Brazing

A detailed summary of the development work conducted at Hanford on electron-beam welding was recently issued.²⁶ Most of the information has been covered in previous reviews in this series, but the above-mentioned report is notable because it covers, in one report, all Hanford experience with electron-beam welding.

Oak Ridge has resolved the weld-cracking problems encountered in some heats of INOR-8 nickel-molybdenum alloys.²⁷ High boron content was found to be the cause of cracking. A boron limit of 0.02 wt.% has been set to avoid this problem.

(R. E. Monroe)

Nondestructive Testing

Efforts to provide nondestructive testing methods suitable to meet the high standards of integrity demanded for nuclear components are being made on a wide front. Generally, these ef-

forts have resulted in improvements in standard ultrasonic, eddy current, and radiographic techniques as applied to the unique problems of testing core materials²⁸⁻³¹ and reactor components (references 27, 28, 31, and 32), rather than in new types of tests. A program has been initiated at Oak Ridge to develop ultrasonic inspection techniques for the nondestructive evaluation of weld quality in very intense radiation fields, such as would be encountered in remote reactor maintenance.

Although based on old principles, several interesting new instruments are being developed. An ultrasonic fluoroscope has been developed at Argonne.¹⁶ It consists in principle of a 60-segment mosaic of crystals, each electrically coupled to a mercury jet switch. The commutated signal is amplified and sent to a cathode-ray tube, the sweep circuit of which synchronized with the switch. Thus, the output of each segment is presented in position relative to its location in the mosaic, and the brilliance of each spot is proportional to the ultrasonic energy. The system is simple and practical. The resolution is below that of the usual scanning system but is sufficient to detect gross defects.

A transistorized model of a metals identification meter has been developed at Oak Ridge which utilizes induced eddy currents for identification by permeability and conductivity. The battery-powered instrument is portable and will identify all ferromagnetic and nonferromagnetic materials. Oak Ridge has also developed an eddy-current instrument to detect very small cracklike defects in $\frac{3}{4}$ in.-O.D. by 0.020-in.-wall type 304 stainless tubing. Scratches 1 to 2 mils deep by 10 mils wide by $\frac{1}{8}$ in. long can be detected. A nonlinear amplifier was developed to discriminate against signals produced by inconsequential variations in dimensions, conductivity, and permeability.

An X-ray sensitive Vidicon is used at Oak Ridge in a closed-circuit television system for remote reviewing of small intricate parts and assemblies. The advantages of this instrument are its inherent high resolution and magnification of images. (C. V. Weaver)

References

- 1.* John A. Fellows, Production Forming of Natural Uranium Metal, A/CONF./15/P/1433.
- 2.* E. L. Richards et al., The Melting and Fabrication of Zircaloy, A/CONF./15/P/1010.
3. Zirconium Highlights, WAPD-ZH-12, November 1958. (Unclassified AEC report.)
4. Bettis Technical Review, WAPD-BT-10, October 1958. (Unclassified AEC report.)
5. E. L. Brundige, G. S. Hanks, and J. M. Taule, Fabrication of Uranium Welding Rod, LA-2225, Sept. 9, 1958. (Unclassified AEC report.)
6. J. E. Hockett, The Roll Pressures of Uranium Sheet and Plate, LA-2233, Jan. 8, 1959. (Unclassified AEC report.)
7. E. Orowan, The Calculation of Roll Pressures in Hot and Cold Flat Rolling, *Proceedings of the Institute of Mechanical Engineers (London)*, 150: 140-167 (1943).
8. R. W. Dayton and C. R. Tipton, Jr., Progress Relating to Civilian Applications During December, 1958, BMI-1307, Jan. 1, 1959. (Confidential AEC report.)
9. R. W. Dayton and C. R. Tipton, Jr., Progress Relating to Civilian Applications During October 1958, BMI-1301, Nov. 1, 1958. (Unclassified AEC report.)
10. R. W. Dayton and C. R. Tipton, Jr., Progress Relating to Civilian Applications During November, 1958, BMI-1304, Dec. 1, 1958. (Unclassified AEC report.)
11. Technical Report—Pressurized Water Reactor (PWR) Project for the Period August 24, 1958, to October 23, 1958, WAPD-MRP-76. (Unclassified AEC report.)
12. S. R. Maloof, A Preliminary Study of High-Strength Zirconium-Base Alloys, NMI-1205, Aug. 1, 1958. (Unclassified AEC report.)
- 13.* W. N. McDaniel, O. E. Homeister, and D. O. Leaser, Development of Core Elements for the Enrico Fermi Power Reactor, A/CONF./15/P/792.
14. I. B. Roll, Aluminum-Clad, Uranium-Aluminum Core Tubes for NRU Reactor, NMI-4910, Mar. 17, 1958, Nuclear Metals, Inc., Cambridge, Mass.
- 15.* Robert A. Noland et al., The Manufacture of EBR-1, Mark III Fuel and Blanket Rods, A/CONF.15/P/791.
16. Metallurgy Division Quarterly Report for April, May, and June 1957, ANL-5790, July 1958. (Unclassified AEC report.)
17. R. F. Lupi and J. R. Demartino, Knolls Atomic Power Laboratory, 1958. (Unpublished.)
18. R. F. Lupi, Knolls Atomic Power Laboratory, July 1, 1958. (Unpublished.)
19. G. F. Jackey, Extrusion Cladding Uranium with Aluminum Using the Schloemann Cable-Cladding Press—Mechanical Aspects, HW-56801, July 21, 1958. (Unclassified AEC report.)
20. Proceedings of the French-American Conference on Graphite Reactors, 174-186, Nov. 12-15, 1957.
21. J. W. Frank and R. E. Macherey, Casting Uranium-5 Wt.% Zirconium-1.5 Wt.% Niobium Alloys into Zirconium and Zircaloy-2 Containers, ANL-5442, July 1958. (Unclassified AEC report.)

22. Emanuel C. Hirakis, Research for Protection of Niobium Against Oxidation at Elevated Temperatures, WADC-TR-58-545, September 1958. (Unclassified.)
23. W. L. Robb, Zirconium Coating of Uranium by the Iodide Process, *Journal of the Electrochemical Soc.*, 106: 126 (February 1959).
24. Metallurgy Division Quarterly Report for July, August, and September 1957, ANL-5797, October 1958. (Unclassified AEC report.)
- 25.* J. M. Blocher, Jr., and I. E. Campbell, Carbide Coatings for Graphite, A/CONF./15/P/1428.
26. W. L. Wyman and W. I. Steinkamp, Electron Beam Vacuum Welding—Development of Process, HW-55667, Apr. 8, 1958. (Unclassified AEC report.)
27. J. A. Lane, H. G. MacPherson, and Frank Maslan, Molten Salt Reactors, Part II, in "Fluid Fuel Reactors," Addison-Wesley Publishing Company, Reading, Mass., 1958, p. 563.
28. Technical Progress Report on Pressurized Water Reactor (PWR) Project for the Period October 24, 1958, to December 23, 1958, WAPD-MRP-77. (Unclassified AEC report.)
29. S. Priceman, Quantitative Determination of Ultrasonic Loading of Aluminum-Clad Fuel Plates by X-ray Densitometry, SCNC-277, October 1958. (Unclassified AEC report.)
30. Otto Nickel, Experiments in the Testing of Ingots with Gamma Radiation and Very Hard X-radiation (in German), *Zeitschrift Metallkunde*, 49: 368-375 (July 1958).
31. Symposium on Nondestructive Tests in the Field of Nuclear Energy, ASTM Special Technical Publication No. 223, 1958.
32. M. C. Lambert, Nondestructive Testing of MTR Type Fuel Plates by X-ray Absorption and Fluorescence Techniques, HW-57941, Oct. 28, 1958. (Unclassified AEC report.)

*Second United Nations International Conference on the Peaceful Uses of Atomic Energy, Geneva, September 1958. (Individual papers available from the Office of Technical Services, Dept. of Commerce, Washington 25, D. C. Bound volumes of papers will be available from United Nations, Office of Public Information, New York.)

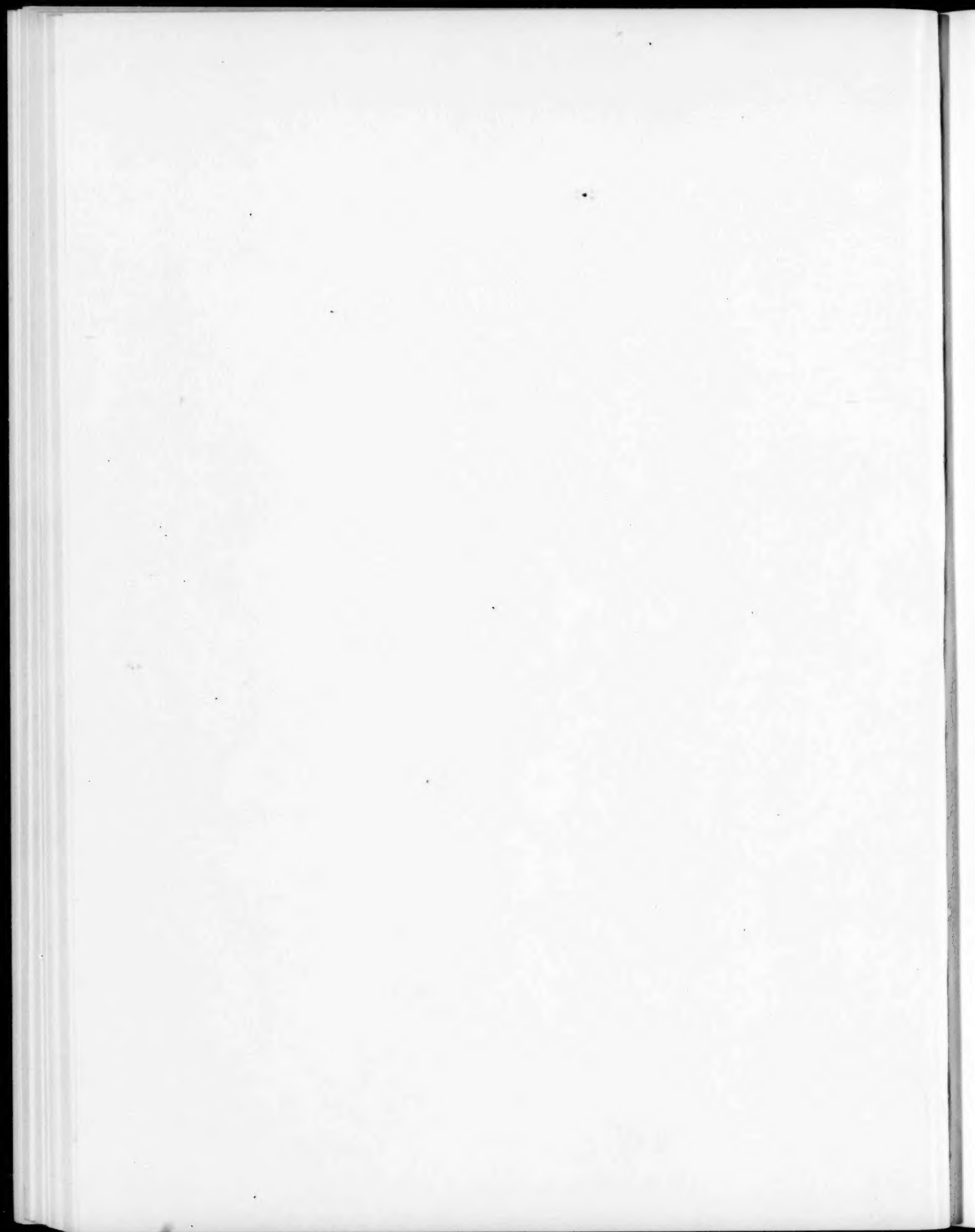
LEGAL NOTICE

This document was prepared under the sponsorship of the U. S. Atomic Energy Commission. Neither the United States, nor the Commission, nor any person acting on behalf of the Commission:

A. Makes any warranty or representation, expressed or implied, with respect to the accuracy, completeness, or usefulness of the information contained in this report, or that the use of any information, apparatus, method, or process disclosed in this report may not infringe privately owned rights; or

B. Assumes any liabilities with respect to the use of, or for damages resulting from the use of any information, apparatus, method, or process disclosed in this report.

As used in the above, "person acting on behalf of the Commission" includes any employee or contractor of the Commission, or employee of such contractor, to the extent that such employee or contractor of the Commission, or employee of such contractor prepares, disseminates, or provides access to, any information pursuant to his employment or contract with the Commission, or his employment with such contractor.



NUCLEAR SCIENCE ABSTRACTS

The U. S. Atomic Energy Commission, Technical Information Service, publishes *Nuclear Science Abstracts (NSA)*, a semimonthly journal containing abstracts of the literature of nuclear science and engineering.

NSA covers (1) research reports of the U. S. Atomic Energy Commission and its contractors; (2) research reports of government agencies, universities, and industrial research organizations on a world-wide basis; and (3) translations, patents, books, and articles appearing in technical and scientific journals.

Complete indexes covering subject, author, source, and report number are included in each issue. These are cumulated quarterly, semiannually, and annually providing a detailed and convenient key to the literature.

Availability of NSA

SALE NSA is available on subscription from the Superintendent of Documents, U. S. Government Printing Office, Washington 25, D. C., at \$18.00 per year for the semimonthly abstract issues and \$15.00 per year for the four cumulated-index issues. Subscriptions are postpaid within the United States, its Territories, Canada, Mexico, and all Central and South American countries, except Argentina, Brazil, British and French Guiana, Surinam, and British Honduras. Subscribers in these Central and South American countries, and in all other countries throughout the world, should remit \$22.50 per year for subscriptions to semimonthly abstract issues and \$17.50 per year for the four cumulated-index issues.

EXCHANGE NSA is also available on an exchange basis to universities, research institutions, industrial firms, and publishers of scientific information. Inquiries should be directed to the Technical Information Service Extension, U. S. Atomic Energy Commission, P. O. Box 62, Oak Ridge, Tennessee.